Evidence-Based Complementary and Alternative Medicine

Complementary and Alternative Therapies Targeting Inflammasomes for Human Diseases

Lead Guest Editor: Young-Su Yi
Guest Editors: Tae Jin Lee and Sehyun Kim

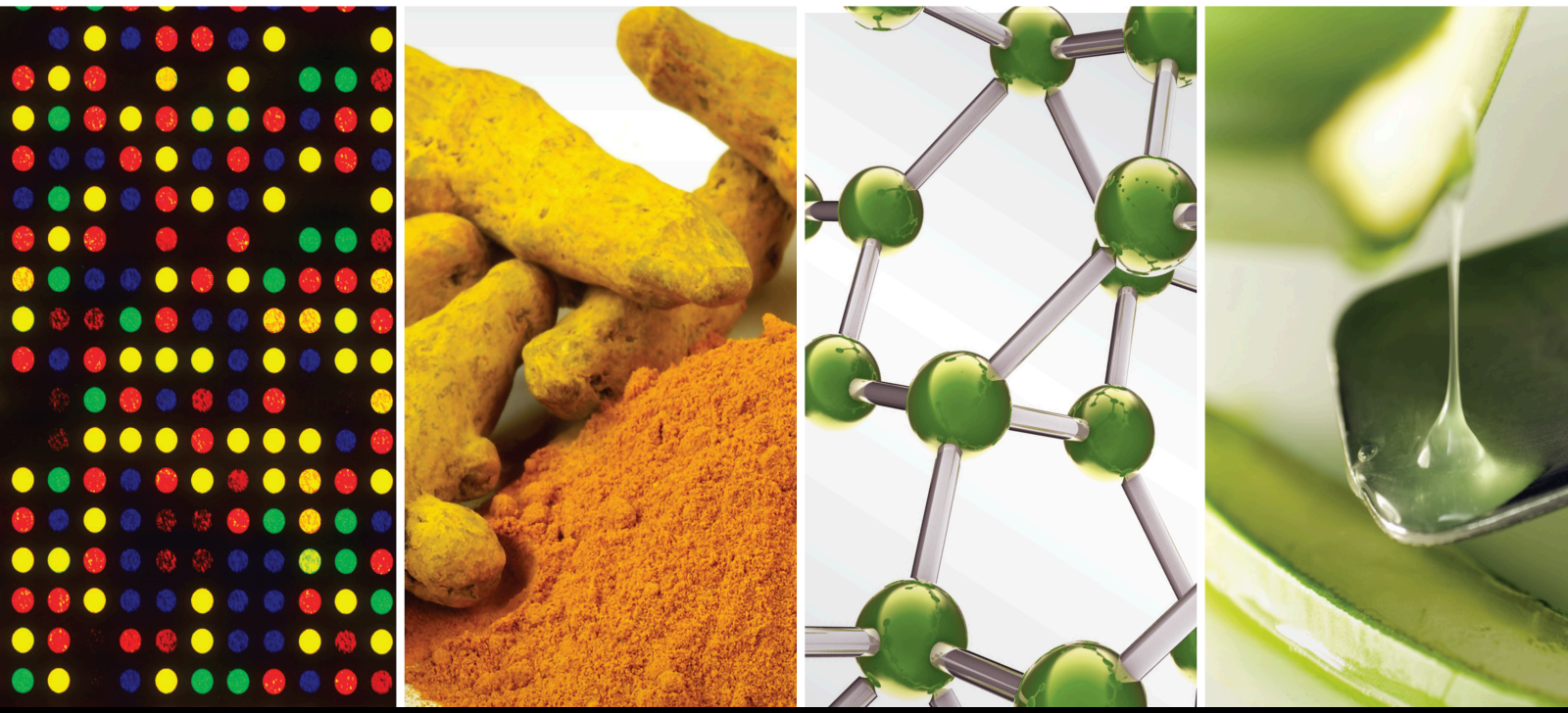

Complementary and Alternative Therapies Targeting Inflammasomes for Human Diseases

Evidence-Based Complementary and Alternative Medicine

Complementary and Alternative Therapies Targeting Inflammasomes for Human Diseases

Lead Guest Editor: Young-Su Yi
Guest Editors: Tae Jin Lee and Sehyun Kim

Editorial Board

Chris Zaslawski, Australia
Suzanna M. Zick, USA

Contents

Hindawi
Evidence-Based Complementary and Alternative Medicine
Volume 2020, Article ID 7949545, 2 pages
https://doi.org/10.1155/2020/7949545

Editorial

Complementary and Alternative Therapies Targeting Inflammasomes for Human Diseases

Young-Su Yi[1] **and Tae Jin Lee**[2]

[1]*Department of Life Sciences, Kyonggi University, Suwon 16227, Republic of Korea*
[2]*Department of Neurosurgery, University of Texas Health Science Center at Houston, Houston 77030, USA*

Correspondence should be addressed to Young-Su Yi; ysyi@kgu.ac.kr

Received 8 April 2020; Accepted 8 April 2020; Published 9 June 2020

Inflammation is an innate immunity protecting the body from invading pathogens and intracellular danger signals, whereas chronic inflammation, that is, slow, repeated, and long-term inflammation has been considered as a major risk factor to induce a variety of human diseases, such as inflammatory, autoimmune, metabolic diseases, and even cancers. An inflammatory response consists of two major consecutive steps: priming and triggering. Priming is the process that prepares for inflammatory response by upregulating the expression of inflammatory molecules, whereas triggering is the process that boosts the inflammatory response by activating the inflammatory molecules. Inflammasomes are intracellular protein complexes consisting of intracellular pattern recognition receptors (NLRP1, NLRP3, NLRC4, NLRP6, AIM2, and caspase-4/5/11), bipartite adaptor (ASC), and other inflammatory molecules, and inflammasome activation is the cardinal feature of triggering during inflammatory responses, which results in caspase-1 activation, gasdermin D-induced pyroptosis, an inflammatory form of cell death, and the secretion of proinflammatory cytokines, IL-1β, and IL-18.

Many efforts have been recently made on developing the efficacious and safe anti-inflammatory therapeutics treating various human diseases, and complementary and alternative medicines (CAMs) have been successfully proposed as the effective and safe anti-inflammatory agents that can overcome the serious adverse effects of conventional drugs, such as drug-failure patient groups, side effects, and toxicity. Despite these efforts, a large number of previous studies have mainly focused on the investigation of priming rather than triggering of inflammatory responses. Therefore, the studies focusing on the development of promising CAMs that can treat various human diseases by targeting inflammasomes are recently receiving high attention and required for further investigation. Given this limitation, not only basic studies of CAM-mediated anti-inflammatory actions by targeting inflammasomes but also development of novel CAMs that are selectively targeting inflammasomes, as well as being more efficacious and safer than conventional drugs, is highly demanded.

In this special issue, we invited investigators to contribute the latest original research and review articles investigating *in vitro*, *in vivo*, nonclinical, and clinical/translational studies focusing on the anti-inflammatory effects of CAMs by targeting inflammasomes and potential CAM therapeutics that will help in understanding the basic mechanisms as well as the development of promising CAMs targeting inflammasomes to prevent and treat various human diseases. In this special issue, six original and review articles were published regarding the complementary and alternative therapies targeting inflammasomes for human diseases.

The research article by S. Li et al. investigated whether exercise preconditioning (EP) ameliorates the rat cardiac dysfunction induced by exhaustive exercise by modulating NLRP3 inflammasome pathways and suggested that EP protects the heart from exhaustive exercise-induced injury via downregulation of TXNIP/TRX/NF-κBp65 and NLRP3 inflammatory signaling pathways. Additionally, this study

demonstrated that moderate intensity EP has the best protective effect.

The research article by Y. Geng et al. investigated the underlying anti-inflammatory mechanisms in Delta-opioid receptor (DOR) activation and electroacupuncture-mediated neuroprotection in cerebral ischemia/reperfusion (I/R) injury and suggested that the neuroprotective efficacy of electroacupuncture on cerebral I/R injury may be related to the inhibition of DOR-BDNF/TrkB inflammatory pathway and IL-1β secretion, an inflammasome-related proinflammatory cytokine.

The research article by T. Zheng et al. investigated the expression patterns and prognostic characteristics of inflammasome-related genes (IRGs) across cancer types and the development of a robust biomarker for the prognosis of kidney renal clear cell carcinoma (KIRC). This study suggested that the pan-cancer analysis provided a comprehensive landscape of IRGs across cancer types and identified a strong association between IRGs and the prognosis of KIRC. Moreover, this study also suggested that further IRGs signature not only represented a reliable prognostic predictor for KIRC but also verified the prognostic value of inflammasomes in KIRC, contributing to our understanding of therapies targeting inflammasomes for human cancers.

The review article by S. Li et al. classified alkaloids according to structural types and discussed the studies investigating the plant sources, applicable diseases, as well as anti-inflammatory mechanisms by inhibiting the production of IL-1β, an inflammasome-activated proinflammatory cytokine of 16 kinds of alkaloids commonly used in clinical treatment, such as berberine, tetrandrine, and stephanine, with the aim of providing a reference for drug research studies and clinical applications. This review provided the insight into the anti-inflammatory mechanisms of alkaloids in Chinese Materia Medicas through suppression of IL-1β production, in order to provide a reference for screening active ingredients with anti-inflammatory effects and finding new therapeutic targets.

Another review article by Y. Liu et al. discussed the studies investigating the potential benefits of drugs targeting the NLRP3 inflammasome in the therapy of atherosclerosis and concluded that using drugs targeting NLRP3 inflammasome for treating atherosclerosis is promising, but it also needs further pharmacological studies to verify the efficacy as well as further experimental epidemiological studies to ensure safety.

Finally, the review article by X. Yan et al. discussed the current knowledge on the involvement of cathepsins in the regulation of the innate and adaptive immune responses associated with the inflammatory molecules, IL-1β and caspase-1, during inflammasome activation in periodontitis. This review provided the insight given the roles of cathepsins in inflammatory responses that the regulation of cathepsins will be helpful for managing inflammatory responses via modulating the functions of IL-1β and caspase-1, inflammatory molecules activated in the inflammasome signaling pathway in patients with periodontitis, and thus beneficial to prevent and relax the systemic diseases as well as neurodegenerative diseases in the global aging society.

We hope that readers will be interested in understanding the mechanisms of CAM-mediated anti-inflammatory effect by inhibiting inflammasomes in inflammatory responses and developing novel promising anti-inflammatory CAM therapeutics that can target inflammasomes to prevent and treat various human diseases. We also hope this special issue attracts the interest of the scientific community, thereby contributing and improving further investigations leading to the discovery of new strategies, the unknown inflammasome targets, and the novel CAM therapeutics for the prevention and treatment of various human diseases.

Conflicts of Interest

The editors declare that there are no conflicts of interest regarding the publication of this special issue.

Acknowledgments

The editors thank all authors of the articles and all reviewers for their valuable contributions to this special issue. The editors also would like to express their thanks to Dr. Sehyun Kim for his contribution to this special issue.

Young-Su Yi
Tae Jin Lee

Hindawi
Evidence-Based Complementary and Alternative Medicine
Volume 2020, Article ID 5809298, 9 pages
https://doi.org/10.1155/2020/5809298

Research Article

Different Intensity Exercise Preconditions Affect Cardiac Function of Exhausted Rats through Regulating TXNIP/TRX/NF-κB$_{p65}$/NLRP3 Inflammatory Pathways

Yuemin Li,[1] Peng Xu,[1] Yang Wang,[2] Junshi Zhang,[1] Mei Yang,[1] Yumei Chang,[3] Ping Zheng,[1] Heling Huang,[4] and Xuebin Cao[1]

[1]*Department of Cardiology, The Hospital of the 82nd Group Army, Baoding 071000, Hebei, China*
[2]*Department of Clinical Pharmacy, The Hospital of the 82nd Group Army, Baoding 071000, Hebei, China*
[3]*Department of Central Laboratory, The Hospital of the 82nd Group Army, Baoding 071000, Hebei, China*
[4]*Department of Gynaecology, The Hospital of the 82nd Group Army, Baoding 071000, Hebei, China*

Correspondence should be addressed to Heling Huang; huangheling252@163.com and Xuebin Cao; caoxb252@163.com

Received 29 September 2019; Revised 14 February 2020; Accepted 6 March 2020; Published 9 June 2020

Guest Editor: Young-Su Yi

Objective. To investigate whether exercise preconditioning (EP) improves the rat cardiac dysfunction induced by exhaustive exercise (EE) through regulating NOD-like receptor protein 3 (NLRP3) inflammatory pathways and to confirm which intensity of EP is better. *Method*. Ninety healthy male Sprague Dawley rats were randomly divided into five groups: a control group (CON), exhaustive exercise group (EE), low-, middle-, and high-intensity exercise precondition and exhaustive exercise group (LEP + EE, MEP + EE, HEP + EE group). We established the experimental model by referring to Bedford's motion load standard to complete the experiment. Then, the pathological changes of the myocardium were observed under a light microscope. Biomarker of myocardial injury in serum and oxidative stress factor in myocardial tissue were evaluated by ELISAs. The cardiac function parameters were detected using a Millar pressure and volume catheter. The levels of thioredoxin-interacting protein (TXNIP), thioredoxin protein (TRX), nuclear transcription factor kappa B$_{p65}$ (NF-κB$_{p65}$), NLRP3, and cysteinaspartate specific proteinase 1 (Caspase-1) protein in rats' myocardium were detected by western blotting. *Results*. 1. The myocardial structures of three EP + EE groups were all improved compared with EE groups. 2. The levels of the creatine phosphating-enzyme MB (CK-MB), reactive oxygen species (ROS), interleukin-6 (IL-6), C-reactive protein (CRP), and tumor necrosis factor alpha (TNF-α) in three EP + EE groups were all increased compared with CON but decreased compared with the EE group ($P < 0.05$). 3. Compared with the CON group, slope of end-systolic pressure volume relationship (ESPVR), ejection fraction (EF), and peak rate of the increase in pressure (dP/dt_{max}) all dropped to the lowest level in the EE group ($P < 0.05$), while the values of cardiac output (CO), stroke volume (SV), end-systolic volume (Ves), end-diastolic volume (Ved), and relaxation time constant (Tau) increased in the EE group ($P < 0.05$). 4. Compared with the CON group, the expression levels of TXNIP, NF-κB$_{p65}$, NLRP3, and Caspase-1 all increased obviously in the other groups ($P < 0.05$); meanwhile, they were all decreased in three EP + EE groups compared with the EE group ($P < 0.05$). 5. NLRP3 was positively correlated with heart rate, IL-6, and ROS, but negatively correlated with EF ($P < 0.01$). *Conclusion*. EP protects the heart from EE-induced injury through downregulating TXNIP/TRX/NF-κB$_{p65}$/NLRP3 inflammatory signaling pathways. Moderate intensity EP has the best protective effect.

1. Introduction

Exhaustive exercise (EE) refers to the continuous exercise in the overload state of the body. People who often engage in high-intensity exercise, such as athletes and soldiers, will be going to be EE. EE can cause a series of adverse reactions, including oxidative stress and myocardial inflammation [1]. It also can lead to oxidative stress and increase the production of reactive oxygen species (ROS) [2]. ROS is important for cellular homeostasis, in that it intervenes as cell

signaling body in diverse pathways [3]. ROS raises thioredoxin interactions protein (thioredoxin-interacting protein, TXNIP) [4]. As a negative regulator of the thioredoxin protein (TRX) antioxidant system, TXNIP interacts with TRX in dormant cells and keeps it in an inactive state to maintain the balance of oxidation [5, 6]. Reactive oxygen species-thioredoxin-interacting protein (ROS-TXNIP) can form ROS-TXNIP inflammatory body axis, which can activate a nuclear transcription factor kappa B_{p65} (NF-κB_{p65}) and regulate inflammation [7, 8]. NF-κB_{p65} is a powerful proinflammatory transcription factor that can trigger the activation of intracellular signal transduction [9]. The activated NF-κB_{p65} combines with the two binding sites of NOD-like receptor protein 3 (NLRP3) promoter region and activates the NLRP3 inflammatory corpuscle [10]. The activation of NLRP3 inflammasome accelerates the release of cysteinaspartate specific proteinase 1 (Caspase-1) and promotes the increase of downstream inflammatory factors [11]. Another study has reported that the inhibition of NLRP3-inflammasome could decrease the incidence of myocardial infarction and improve myocardial function in animal myocardial infarction models [12]. EE-induced inflammatory mediators can induce myocardial cell apoptosis and cardiac dysfunction [13, 14]. The inflammatory cytokines including tumor necrosis factor alpha (TNF-α), interleukin-6 (IL-6), interleukin 1 beta (IL-1β), and c-reactive protein (CRP) could directly or indirectly induce left ventricular dysfunction [15].

While exercise precondition (EP) can reduce the cardiac injury through tolerance training, it is one of the interventions to improve cardiac function [16–18]. Meng et al. have confirmed that EP could reduce the apoptosis of cardiac cells by inhibiting the TNF-α mediated apoptosis signaling pathway, and long-term EP had better effects than short-term EP. The EP anti-inflammatory strategy may be effective in improving cardiac dysfunction and heart failure after myocardial infarction [19]. Jiao et al. have proved that EP could regulate NLRP3 inflammation, reduce downstream inflammatory factors such as IL-1β and CRP, and play a protective role on the heart.

However, the effect of EE on the TXNIP/TRX/NF-κB_{p65}/NLRP3 signaling pathway and the association of the inflammatory signaling pathway activated by EP and its cardiac protecting resist to the injury of EE all remain unclear. We hypothesize that EP can protect the heart from the cardiac injury induced by EE, and the protection is possibly triggered by the TXNIP/TRX/NF-κB_{p65}/NLRP3 signaling pathway.

Meanwhile, there is also a controversy on which level of EP has a better protective effect on cardiac function [20]. It is still unclear which intensity or type of EP has the most significant protective effect on heart [21]. Therefore, we aimed to solve the above problem in this experiment.

2. Materials and Methods

2.1. Drugs and Main Instruments. The main reagents used in the present study are listed below. ROS kits were provided by Nanjings Mr Ng biological technology Co., Ltd. The CK-MB kit was provided by Wuhan huamei biological engineering Co., Ltd. IL-6, CRP, and TNF-α kits were purchased from the Wuhan optimal, born trade Co., Ltd. TXNIP, TRX, NF-κB_{p65}, NLRP3, and Caspase-1 antibody were obtained from Abcam Trading (Shanghai) Company Ltd. β-Actin antibody was supplied by Beijing zhongshan jinqiao biotechnology Co., Ltd.

The following main instruments were used in the present study: a PowerLab signal acquisition and analysis system, a MultiscanGO enzyme standard instrument (Thermo, United States), a Sigma 3k15 high-speed refrigerated centrifuge (SIGMA, Germany), a pressure volume catheter (SPR-838, Millar company, USA), a PowerLab data acquisition and analysis system (AD Instruments, Australia), vertical electrophoresis system (BIO-TEK, USA), transfer electrophoresis system (BIO-TEK, USA), a gel imaging system (Bio Spectrum), an image analysis system (Image-Pro Plus 4.1), a PowerLab data acquisition and analysis system (AD Instruments, Australia), a bioelectric amplifier (AD Instruments, Australia), and a needle electrode (AD Instruments, Australia).

2.2. Establishment and Grouping of Animal Models. Ninety male Sprague Dawley rats (200 ± 30 g) were provided by the Academy of Military Medical Sciences; License number: SCXK (Beijing)-2012-004. All experiments were conducted in compliance with the guide for the Care and Use of Laboratory Animals and approved by the Ethics Committee for the Use of Experimental Animals at the Hospital of the 82nd Group Army. Standard rodent dry feed was provided ad libitum, the indoor temperature was maintained at 18 to 22°C, and the relative humidity was maintained at 40 to 55%. SD rats were adaptive fed for 1 week and then randomly divided into 5 groups ($n = 18$): the control group (CON), exhaustive exercise group (EE), low-intensity exercise preconditioning + exhaustive exercise group (LEP + EE), middle-intensity exercise preconditioning + exhaustive exercise group (MEP + EE), and intense exercise preconditioning + exhaustive exercise group (HEP + EE group), following the standards of Bedford exercise load to establish the animal sport models [22]. In the LEP + EE group, the run slope was 3° and the speed was 30 m/min, equivalent to 40%~50% VO_{2max}. In the MEP + EE group, the run slope was risen to 6° and speed was risen to 32 m/min, equivalent to 65%~75% VO_{2max}. In the HEP + EE group, the run slope was also 6° and the speed was 36 m/min, equivalent to 90%~95% VO_{2max}. Exercise was followed for 8 weeks. Then, the EE, LEP + EE, MEP + EE, and HEP + EE groups run with the slope of 6° and the speed of 36 m/min until exhaustion. Criteria for judging exhaustion: the rats were left behind the runway more than 10 times in a row, and the photoelectric acoustic stimulation was invalid. Ten of the 18 animals in each group were used for the pressure volume catheter detection of cardiac function, which was an invasive experiment. These animals were euthanized after the experiment. Serum, electrocardiogram and myocardial specimens were collected from the remaining animals ($n = 8$ animals per group). There are two mice lost, respectively, in the EE group, LEP + EE group, and MEP + EE group. Also,

the CON group and HEP + EE group have no lost mice (CON, HEP + EE $n = 10$; EE, LEP + EE, MEP + EE $n = 8$).

2.3. Collection and Preparation of Serum and Myocardial Samples. Rats were subjected to abdominal anesthesia with pentobarbital sodium (40 mg/kg), the chest was opened, and the blood was collected from the inferior thoracic vena cava. The blood was centrifuged at 3000 r/min for 20 minutes; the supernatant was collected and stored in a −80°C freezer until the detection of serum indicators.

Then, the hearts were quickly removed and washed with cold saline. Tissues were stored individually in a refrigerator at −80°C until western blot detection.

2.4. The Structure of the Myocardium Was Observed by Using an Optical Microscope. All rats were anesthetized with pentobarbital sodium (40 mg/kg, intraperitoneal injection). The hearts were quickly removed and washed with cold saline. Myocardial tissue of the left ventricle was collected for light microscopy analysis. The tissue was fixed with 10% formaldehyde, paraffin-embedded, sectioned, dehydrated with different concentration gradients of alcohol, stained with HE, and observed by the light microscopy.

2.5. Enzyme-Linked Immunoassays for ROS, TNF-α, IL-6, CRP, and CK-MB in Rat Serum. The serum was removed from the −80°C freezer and thawed. Enzyme-linked immunosorbent assays were performed according to the instructions included in the kits. The OD value of each sample was measured at 450 nm. The OD value for the standard was measured, and a standard curve was constructed with the OD value on the y-axis and the concentration on the x-axis. The concentration of the indicated marker in each sample was obtained from the standard curve.

2.6. Determination of Cardiac Function Parameters with a Pressure Volume Catheter. Rats were anesthetized with pentobarbital sodium (40 mg·kg^{-1}, i.p.), and the closed-chest approach was chosen for catheter insertion [23]. The animal was fixed in the supine position on the operating table. The skin of the neck was disinfected prior to a midline neck incision, and the trachea was separated and intubated. The right carotid artery was separated from the common carotid artery. Two 4-0 silk threads were sewn through the common carotid artery, and one of the silk threads was used to ligate the proximal end of the carotid artery. A cut was made at the end of the heart to complete the knot. The pressure volume catheter was inserted through the incision into the left chamber along the inverse blood flow of the carotid artery and calibrated with MPVS control software. The left ventricular pressure volume waveform of the anesthetized rats was recorded with Chart 7 software in real-time. Vessels and catheters were fixed with another silk thread. The baseline data was recorded for 15 minutes. The abdominal skin was disinfected, a median incision was made, the inferior vena cava was occluded, and changes in the waveform were recorded. A 20 μl solution of 30% NaCl was rapidly injected into the anterior jugular vein, and pressure-volume waveform changes were recorded. The first 4 holes of a calibration cuvette with known diameters (provided by the manufacturer) were quickly filled, and the catheter tip was submerged in fresh heparinized warm blood. The conductance changes in the volume channel were recorded, and the volume was then calculated.

The cardiac output (CO), heart rate (HR), end-systolic pressure (Pes), end-systolic volume (Ves), end-diastolic volume (Ved), stroke volume (SV), left ventricular development pressure (Pdev), ejection fraction (EF), peak rate of pressure rise (dP/dt_{max}), peak rate of pressure decline ($-dP/dt_{min}$), slope of the end-systolic pressure volume relationship (ESPVR), and relaxation time constant (Tau) were detected. The pressure volume loop (PV Loop) was drawn with pressure on the Y-axis and volume on the X-axis.

2.7. Western Blot Analysis of TXNIP, TRX, NF-κB$_{p65}$, NLRP3, and Caspase-1 Levels in the Left Ventricular Myocardium. The heart was removed from the −80°C freezer, and the left ventricular myocardial tissue was sheared on ice, minced with fine scissors, and 50 mg was removed and mixed with lysis buffer containing protease inhibitors and a phosphatase inhibitor. The solution was intermittently homogenized with an electric homogenate machine for 1 minute, incubated on ice for 30 minutes, and centrifuged at 12,000 r/min for 20 minutes at 4°C. The supernatant was then placed in a 0.5 ml centrifuge tube. The nucleoproteins were extracted according to the manufacturer's instructions. The protein concentrations were determined by the bicinchoninic acid (BCA) method with bovine serum albumin used as the standard. Then, the protein samples were diluted to the same volume and heated at 100°C for 5 minutes after the addition of an equal volume of loading buffer. The denatured protein samples were separated by SDS/polyacrylamide gel electrophoresis (SDS-PAGE) at 100 V for 2 h and transferred to polyvinylidene fluoride (PVDF) membranes. Membranes were blocked with blocking buffer containing 5% skim milk at room temperature for 1 hour and then incubated with primary antibodies overnight at 4°C. After the membranes were washed with Tris-buffered saline (TBS) containing Tween three times, they were incubated with secondary goat anti-mouse IgG antibodies conjugated to horseradish peroxidase for 1 h at room temperature and then exposed to enhanced chemiluminescence (ECL) for 1 to 2 min to detect the bands. A gel imaging system was used to capture images for the quantitative analysis, and grayscale values were determined.

2.8. Statistical Analysis. The data are presented as means ± SD. SPSS20.0 statistical software was used to analyze all experimental data. Single factor analysis of variance was used for comparisons of multiple means after a one-way ANOVA and a homogeneity test were first performed. Comparisons of mean values between two groups were performed using the LSD test if the variance was equal or Dunnett's T3 method if the variance was unequal. Correlation analysis was performed by calculating Pearson's

correlation coefficients. Also, the single factor regression analysis was performed. $P < 0.05$ was considered to indicate a significant difference in all statistical methods.

3. Results

3.1. The Microstructure of Myocardial Tissue in Rats with Different Intensity EP. In the Con group, myocardial fibers arranged neatly and the cardiomyocyte membranes showed integrity. The interstitial was not edema, muscle membrane was not damaged, and there was no myocardial cell swelling or inflammatory cell infiltration (Figure 1(a)). EE Group: the myocardial staining was not uniform obviously, and a large number of myocardial fiber structures were broken and multiple myocardial fibers were disordered (Figure 1(b) A). Also, a large number of myocardial cells had edema and necrosis and were infiltrated by inflammatory cell (Figure 1(b) B). Meanwhile, mesenchymal fibers had moderate hyperplasia and edema (Figure 1(b) C). The results of LEP + EE, MEP + EE, and HEP + EE groups were all better than those of EE groups (Figures 1(c)–1(e)), and the improvement in the MEP + EE group was the most significant (Figure 1(c)).

3.2. The Effect of Different Intensity EP on Serum ROS, TNF-α, IL-6, CRP, and CK-MB Levels of Exhausted Rats. Compared with the CON group, the serum levels of ROS, TNF-α, IL-6, CRP, and CK-MB in the EE, LEP + EE, MEP + EE, and HEP + EE groups were all increased with statistical significance ($P < 0.05$). Compared with the EE group, the contents of ROS, TNF-α, IL-6, CRP, and CK-MB in the LEP + EE, MEP + EE, and HEP + EE groups were all decreased significantly ($P < 0.05$). Compared with LEP + EE group, the ROS, TNF-α, IL-6, and CRP in MEP + EE and HEP + EE groups all decreased prominently ($P < 0.05$). Compared with MEP + EE group, the CK-MB and IL-6 significantly increased in HEP + EE groups ($P < 0.05$) (Figure 2).

The data are presented as means ± SD, $n = 8$ per group. ROS: reactive oxygen species; TNF-α: tumor necrosis factor alpha; IL-6: interleukin-6; CRP: C-reactive protein; CK-MB: creatine phosphating-enzyme MB. CON: the control group, EE: the exhaustive exercise group, LEP + EE: the low-intensity exercise preconditioning + exhaustive exercise group, MEP + EE: the middle-intensity exercise preconditioning + exhaustive exercise group, and HEP + EE: the group intense exercise preconditioning + exhaustive exercise group. $^{*}P < 0.05$, compared with the CON group; $^{\#}P < 0.05$, compared with the EE group; $^{\Delta}P < 0.05$, compared with the LEP + EE group; $^{\star}P < 0.05$, compared with the MEP + EE group.

3.3. The Effect of Different Intensity EP on the Cardiac Function Parameters of Exhausted Rats. Compared with the CON group, ESPVR, EF, and dP/dt_{max} all dropped to the lowest level in the EE group with statistically significant difference ($P < 0.05$), while the levels of CO, SV, Ves, Ved, and Tau increased significantly ($P < 0.05$). SV, Ves, Ved, and ESPVR in the LEP + EE, MEP + EE, and HEP + EE groups were all significantly different from those in the EE group ($P < 0.05$), and CO in the MEP + EE group was obviously lower than that in the HEP + EE group ($P < 0.05$). CO, SV, Ves, Ved, and Tau of the MEP + EE group were all the lowest among EP groups (Table 1).

3.4. The Effect of EP on the Expression of TXNIP, TRX, NF-κBp65, NLRP3, and Caspase-1 in the Myocardium. Compared with CON group, the TXNIP, NF-κB_{p65}, NLRP3, and Caspase-1 all increased obviously, but TRX reduced significantly in EE, LEP + EE, and HEP + EE groups ($P < 0.05$). The expression level of TXNIP, NF-κB_{p65}, NLRP3, and Caspase-1 in LEP + EE, MEP + EE, and HEP + EE groups was all higher than that of the EE group, while the level of TRX was lower than that of the EE group ($P < 0.05$). Compared with the LEP + EE group, the TXNIP and Caspase-1 increased in MEP + EE and HEP + EE groups ($P < 0.05$). In addition, the level of NF-κB_{p65} and NLRP3 in the MEP + EE group was lower than that of LEP + EE group ($P < 0.05$, Figure 3).

3.5. Analysis of the Correlations between ROS, Myocardial Protein NLRP3, Inflammatory Factors, and Cardiac Function Parameters in Rats with Different Intensity EP. By Pearson linear correlation analysis, NLRP3 was positively correlated with ROS in the CON group ($r = 0.87$, $P < 0.01$). In the MEP + EE group, NLRP3 was positively correlated with HR, ($r = 0.75$, $P < 0.01$) and negatively correlated with EF, ($r = -0.89$, $P < 0.01$). In the HEP + EE group, NLRP3 was positively correlated with IL-6, ($r = 0.87$, $P < 0.01$) and negatively correlated with EF, ($r = -0.84$, $P < 0.01$) (Table 2).

4. Discussion

In this experiment, we studied the effects of different intensity EP on improving the structure of myocardium, reducing myocardial injury, and improving cardiac function in the exhausted rats. We found that the mechanism was EP could inhibit oxidative stress and regulate TXNIP/TRX/NF-κB_{p65}/NLRP3 inflammatory pathways to improve inflammatory state. Furthermore, the moderate intensity EP has the best effect on cardiac protection.

Sports medicine studies have shown that certain decompensated changes occurred in myocardial morphological structure and functional metabolism after repeated high-intensity exercise training. The rupture of myocardial fibers caused the release of CK-MB from cardiomyocyte to peripheral blood. Studies have shown that the serum level of CK-MB increased significantly after exhaustive swimming. Wang has confirmed that the content of CK-MB could reflect the degree of cardiac injury [24]. In this study, EP improved the severe damage and inflammatory infiltration in myocardial fiber structure and decreased the serum level of CK-MB in exhausted rats.

The increased ventricular wall pressure which is led by exhaustion can result in fatigue, and cardiac remodeling may occur [25, 26]. Under the overload pressure, the left

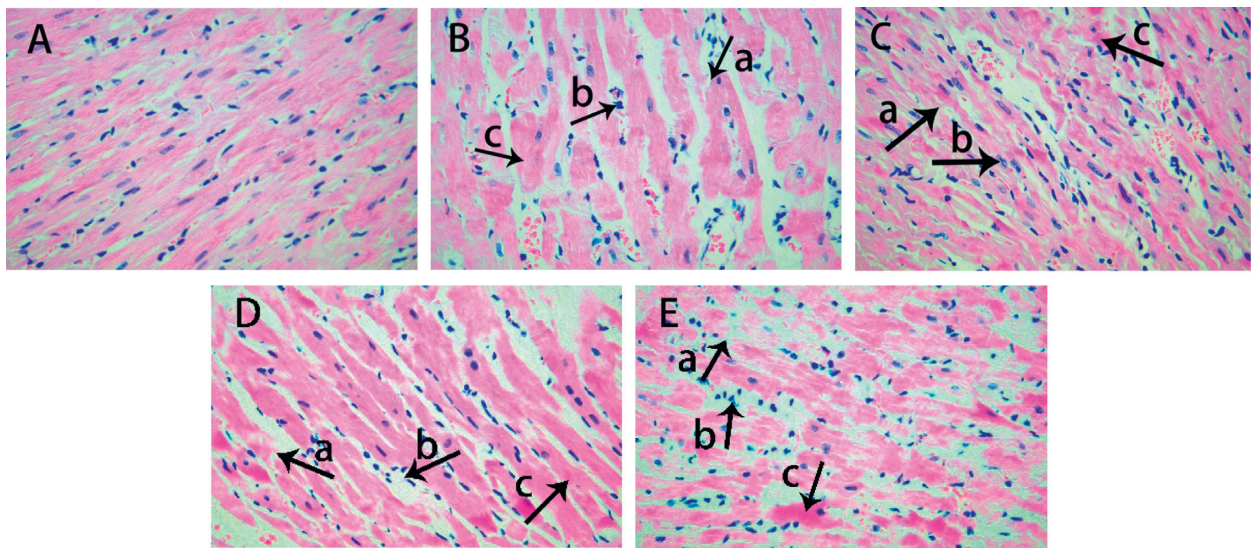

Figure 1: Microstructure of the myocardium using an optical microscope in each group of rats (HE ×400). (a) The control group, (b) the exhaustive exercise group, (c) the low-intensity exercise preconditioning + exhaustive exercise group, (d) the middle-intensity exercise preconditioning + exhaustive exercise group, and (e) the intense exercise preconditioning + exhaustive exercise group. n = 8 per group. (A) The arrow shows myocardial rupture. (B) The arrow shows myocardial cell edema and inflammatory infiltration. (C) The arrow shows myocardial hyperplasia and edema.

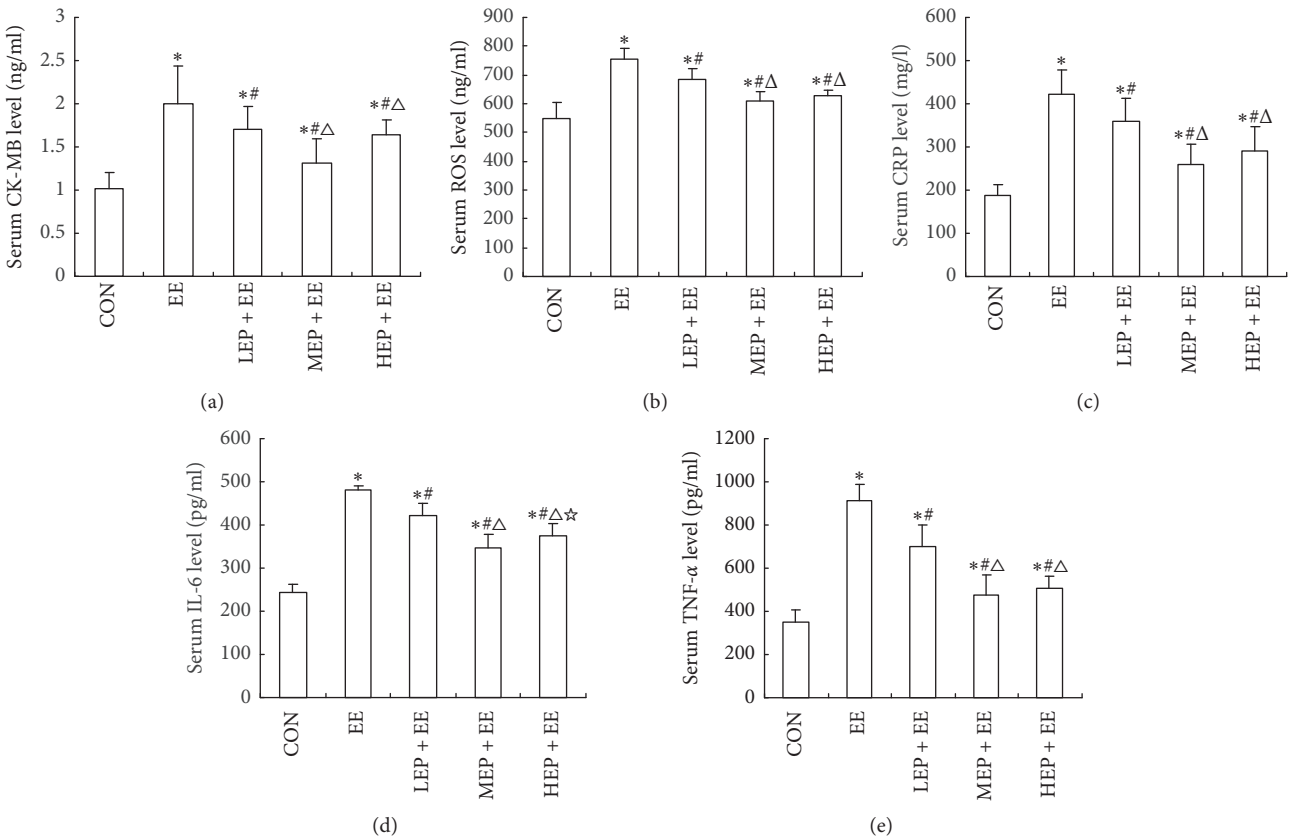

Figure 2: The effect of EP with different intensities on the serum (a) CK-MB, (b) ROS, (c) CRP, (d) IL-6, and (e) TNF-α levels in exhausted rats.

Table 1: The effect of EP with different intensity on cardiac function parameters in exhausted rats ($\overline{x} \pm s$, CON and HEP + EE, $n = 10$; EE, LEP + EE, and MEP + EE, $n = 8$).

	CON	EE	LEP + EE	MEP + EE	HEP + EE
Parameter					
CO (ml/min)	31.33 ± 6.89	62.78 ± 9.60*	44.78 ± 6.87$^{*\#}$	38.09 ± 9.54$^{*\#}$	61.01 ± 12.78$^{*\blacktriangle\star}$
SV (μL)	96.69 ± 15.73	188.34 ± 39.33*	105.97 ± 25.16$^{\#}$	99.17 ± 19.96$^{\#}$	117.17 ± 17.43$^{\#}$
Ves (μL)	152.29 ± 23.86	235.97 ± 65.06*	147.59 ± 69.20$^{\#}$	107.79 ± 35.70$^{\#}$	152.23 ± 28.17$^{\#}$
Ved (μL)	220.48 ± 31.69	430.26 ± 88.97*	236.35 ± 65.06$^{\#}$	226.61 ± 32.06$^{\#}$	262.66 ± 35.37$^{\#}$
Pes (mmHg)	111.79 ± 18.47	115.43 ± 27.70	109.72 ± 21.43	137.79 ± 18.62$^{*\#\blacktriangle}$	133.38 ± 20.69$^{*\blacktriangle}$
Pdev (mmHg)	111.03 ± 18.73	96.44 ± 20.59	111.99 ± 19.13	139.81 ± 20.24$^{*\#\blacktriangle}$	135.41 ± 16.53$^{*\#\blacktriangle}$
HR (bpm)	320.41 ± 28.94	298.28 ± 58.59	344.33 ± 83.40	396.24 ± 12.65$^{*\#\blacktriangle}$	397.67 ± 23.54$^{*\#\blacktriangle}$
Systolic indices					
EF (%)	44.24 ± 8.80	40.07 ± 8.12*	56.74 ± 15.98$^{*\#}$	61.25 ± 8.74$^{*\#}$	58.15 ± 7.33$^{*\#}$
dP/dt_{max} (mmHg/s)	11025 ± 4472	7894 ± 2803*	9518 ± 3299	13935 ± 2696$^{\#\blacktriangle}$	13171 ± 2350$^{\#\blacktriangle}$
ESPVR	0.81 ± 0.39	0.28 ± 0.12*	0.73 ± 0.31$^{\#}$	0.78 ± 0.29$^{\#}$	1.03 ± 0.22$^{\#\blacktriangle}$
Diastolic indices					
$-dP/dt_{min}$ (mmHg/s)	−10718 ± 5866	−8346 ± 3093	−8985 ± 3987	−14068 ± 3221$^{\#\blacktriangle}$	−11589 ± 2889
Tau (ms)	4.76 ± 5.10	11.03 ± 2.46*	11.47 ± 3.37*	8.34 ± 1.07*	9.71 ± 1.85*

CON: the control group ($n = 10$), EE: the exhaustive exercise group ($n = 8$), LEP + EE: the low-intensity exercise Epreconditioning + exhaustive exercise group ($n = 8$), MEP + EE: the middle-intensity exercise preconditioning + exhaustive exercise group ($n = 8$), HEP + EE: the group intense exercise preconditioning + exhaustive exercise group ($n = 10$). CO: cardiac output; SV: stroke volume; Ves: end-systolic volume; Ved: end-diastolic volume; Pes: end-systolic pressure; Pdev: left ventricular development pressure; HR: heart rate; EF: ejection fraction; dP/dt_{max}: peak rate of the increase in pressure; ESPVR: slope of end-systolic pressure volume relationship; $-dP/dt_{min}$: peak rate of the decrease in pressure; Tau: relaxation time constant; $^{*}P < 0.05$, compared with the CON group; $^{\#}P < 0.05$, compared with the EE group; $^{\blacktriangle}P < 0.05$, compared with the LEP + EE group; $^{\star}P < 0.05$, compared with the MEP + EE group.

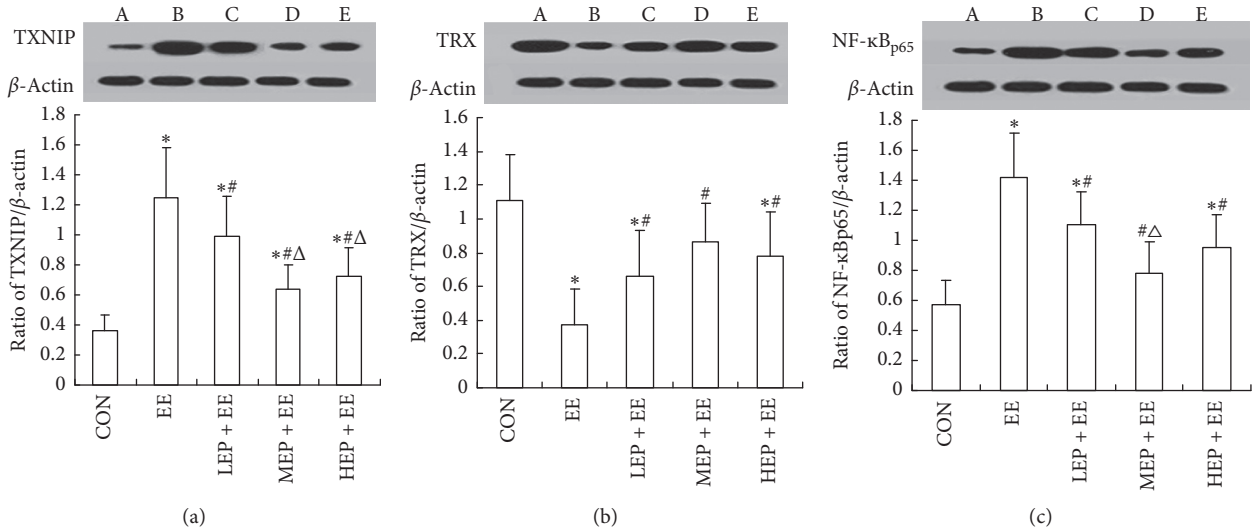

Figure 3: Continued.

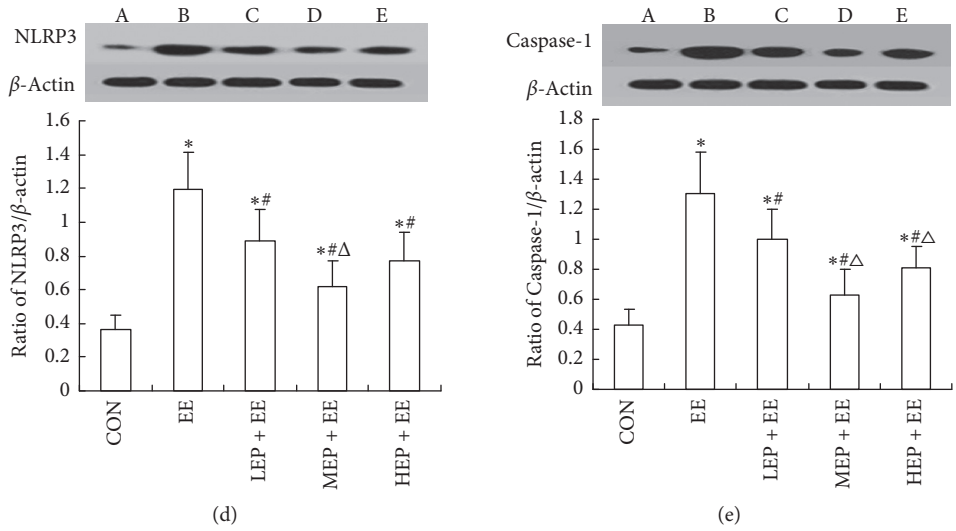

Figure 3: The comparisons with the relative expressions of myocardial protein TXNIP, TRX, NF-κB$_{p65}$, NLRP3, and Caspase-1 in each group rats ($n = 8$, $\overline{x} \pm s$). (a) Ratio of TXNIP/β-actin in rats' myocardium; (b) ratio of TRX/β-actin in rats' myocardium; (c) ratio of NF-κB$_{p65}$/β-actin in rats' myocardium; (d) ratio of NLRP3/β-actin in rats' myocardium; and (e) ratio of Caspase-1/β-actin in rats' myocardium. β-Actin: protein internal reference; TXNIP: thioredoxin-interacting protein; TRX: thioredoxin protein; NF-κB$_{p65:}$ nuclear transcription factor kappa B$_{p65}$; NLRP3; NLRP3 inflammatory; and Caspase-1: cysteinaspartate specific proteinase 1. A: the control group, B: the exhaustive exercise group, C: the low-intensity exercise preconditioning + exhaustive exercise group, D: the middle-intensity exercise preconditioning + exhaustive exercise group, and E: the group intense exercise preconditioning + exhaustive exercise group.$^{*}P < 0.05$, compared with the CON group; $^{\#}P < 0.05$, compared with the EE group; $^{\Delta}P < 0.05$, compared with the LEP + EE group.

Table 2: Pearson's correlation analysis of NLRP3, HR, EF, IL-6, and ROS in rats with preadaptive exercise of different intensity (r, $n = 8$).

Group	HR (bpm)	EF (%)	IL-6 (pg/ml)	ROS
CON	0.25	−0.02	0.14	0.87**
EE	0.08	−0.12	0.46	0.11
LEP + EE	0.03	−0.32	0.66	0.24
MEP + EE	0.75*	−0.89**	0.39	0.08
HEP + EE	0.56	−0.84**	0.87**	0.03

The data show Pearson's correlation coefficient (r), $n = 8$ animals per group. NLRP3: NLRP3 inflammatory; HR: heart Rate; EF: ejection fraction; IL-6: interleukin-6; ROS: reactive oxygen species. For groups, see the footnote to Table 1. $^{*}P < 0.05$, $^{**}P < 0.01$.

ventricular diastolic function and contractile function were impaired in rats. The dP/dt_{max} dropped to the lowest level in the EE group. The level of CO is one of the key factors that determine the ability of exercise [27]. In case of impaired cardiac function, the body can maintain a relatively normal level of cardiac function in a short term through the Frank–Starling compensation mechanism [28]. The results of our experiment showed that CO, SV, Ves, and Ved all increased in exhausted rats. The increase of SV after strenuous exercise added cardiac pump blood volume to meet the metabolic needs of all important organs in the whole body, and it was consistent with previous research conclusions. ESPVR and EF were significantly decreased, which indicated that myocardial systolic function decreased. In addition, the experimental results were consistent with previous results that the parameter Tau value was a representative indicator of the left ventricular diastolic function, and it was inversely proportional to the active diastolic function of the left ventricle. Our results indicated that EP had a protective effect on ventricular systolic and diastolic functions, and the effect of moderate intensity EP was better.

In recent years, oxidative stress and the activation of inflammatory pathways have been considered to play important roles in the transformation of cardiac remodeling and heart failure [29]. Murry and colleagues found that EP could substantially reduce infarct size. They also reported that many authors reproduced the infarct-sparing effect of EP in several mammalians after this original observation in dogs, such as rat, mice, rabbit, swine, and goat. Furthermore, it has been demonstrated that EP could protect the heart against the damage caused by ischemia-reperfusion and improve vascular and coronary reactivity [30]. Recent studies have attempted to reduce the damage of cardiovascular disease by eliminating reactive oxygen species or modulating inflammation [31]. The inhibiting of oxidative stress and ROS plays a cardioprotective role [5]. At a molecular level, exercise modulates the NF-κB signaling axis and contributes to prevent cardiac hypertrophy and right ventricle diastolic dysfunction. EP provides a cardio protection through a shift of the NF-κB signaling. In addition, proinflammatory cytokines such as TNF-α may depress cardiac contractility by promoting hypertrophy, apoptosis, and fibrosis [6]. EP can alleviate patcardiac remodeling and cardiac dysfunction through inhibiting the activation of NF-κB$_{p65}$ pathways [9, 32]. Our study showed that EP could protect cardiac function through reducing the expression of TXNIP, NLRP3, NF-κB$_{p65}$, caspase-1, and the downstream inflammatory cytokines such as TNF-α, IL-6, and CRP.

EE causes damage to cardiac function [33]. Feriani et al. found significant improvement in inflammatory parameters and cardiac function indicators in exhausted rats after aerobic exercise training. In order to control the harmful effects of inflammation on cardiac function, we need to pay more attention to the regulation of inflammatory pathways and strictly control inflammatory pathways and their activators [34, 35]. This experiment showed that ROS was positively correlated with NLRP3, that was to say, oxidative stress was related to the inflammatory pathway of NLRP3. NLRP3 was positively correlated with IL-6, and this suggested that NLRP3 inflammation activation could increase the release of downstream inflammatory factors. NLRP3 was positively correlated with HR and negatively correlated with EF, and these indicated that NLRP3 affected cardiac function likely.

In summary, EP can be used as a prevention and treatment for improving the exercise-induced heart injury. EP with different intensity, especially the moderate intensity EP, had a better effect on regulating inflammatory pathways and protecting cardiac function; these provided a new research theory for exercise physiology and exercise cardiology, but whether high-intensity EP has local damage to the myocardium and cardiac function still needs to be further studied. In addition, how to translate these experimental theoretical knowledge into clinical application may be an important field of translational medicine research in the future.

Data Availability

All datasets analyzed to support the findings of the current study are available from the corresponding author upon reasonable request.

Disclosure

Xuebin Cao and Heling Huang are co-corresponding authors.

Conflicts of Interest

The authors declare that there are no conflicts of interest.

Authors' Contributions

Xuebin Cao contributed to the conception of the study. Yuemin Li and Peng Xu performed the experiments, drafted the manuscript, and contributed significantly to analysis. Yang Wang wrote the manuscript and revised the manuscript. Junshi Zhang performed the part of experiments. Mei Yang played a role in interpreting the results. Yumei Chang provided materials. Zheng Ping analyzed the data. Heling Huang helped to perform the analysis with constructive discussions.

Acknowledgments

This study was supported by grants from the Medical Science Research Program of the Chinese Army (CWS12J064), the Medical Technology Project of the Chinese Army (BWS11J058), and the Logistical Science Research Project of the Chinese Army (CBJ13J002).

References

[1] C. Chen, X. Ma, C. Yang et al., "Hypoxia potentiates LPS-induced inflammatory response and increases cell death by promoting NLRP3 inflammasome activation in pancreatic β cells," *Biochemical & Biophysical Research Communications*, vol. 495, no. 4, pp. 2512–2518, 2017.

[2] D. Camiletti-Moirón, V. A. Aparicio, P. Aranda, and Z. Radak, "Does exercise reduce brain oxidative stress? A systematic review," *Scandinavian Journal of Medicine & Science in Sports*, vol. 23, no. 4, pp. e202–e212, 2013.

[3] V.-M. Nancy, M.-G. Ángel, M.-S. Eduardo Osiris et al., "Antioxidant and adaptative response mediated by Nrf2 during physical exercise," *Antioxidants (Basel)*, vol. 8, no. 6, p. 196, 2019.

[4] J.-Y. Choe and S.-K. Kim, "Quercetin and ascorbic acid suppress fructose-induced NLRP3 inflammasome activation by blocking intracellular shuttling of TXNIP in human macrophage cell lines," *Inflammation*, vol. 40, no. 3, pp. 980–994, 2017.

[5] S. K. Powers, A. J. Smuder, A. N. Kavazis, and J. C. Quindry, "Mechanisms of exercise-induced cardioprotection," *Physiology*, vol. 29, no. 1, pp. 27–38, 2014.

[6] R. Nogueira-Ferreira, D. Moreira-Gonçalves, A. F. Silva et al., "Exercise preconditioning prevents MCT-induced right ventricle remodeling through the regulation of TNF superfamily cytokines," *International Journal of Cardiology*, vol. 203, pp. 858–866, 2016.

[7] Q. Bi, J. Hou, P. Qi et al., "TXNIP/TRX/NF-κB and MAPK/NF-κB pathways involved in the cardiotoxicity induced by Venenum Bufonis in rats," *Scientific Reports*, vol. 6, p. 22759, 2016.

[8] K. K. V. Haack and I. H. Zucker, "Central mechanisms for exercise training-induced reduction in sympatho-excitation in chronic heart failure," *Autonomic Neuroscience*, vol. 188, no. 4, pp. 44–50, 2015.

[9] O. N. Van, G. H. Van, M. Verdonckt et al., "Caspase-1 engagement and TLR-induced c-FLIP expression suppress ASC/Caspase-8-dependent apoptosis by inflammasome sensors NLRP1b and NLRC4," *Cell Reports*, vol. 21, no. 12, p. 3427, 2017.

[10] Y. Yin, F. Chen, W. Wang et al., "Resolvin D1 inhibits inflammatory response in STZ-induced diabetic retinopathy rats: possible involvement of NLRP3 inflammasome and NF-κB signaling pathway," *Molecular Vision*, vol. 23, pp. 242–250, 2017.

[11] M. Meng, "Digitoflavone (DG) attenuates LPS-induced acute lung injury through reducing oxidative stress and inflammatory response dependent on the suppression of TXNIP/NLRP3 and NF-κB," *Biomedicine & Pharmacotherapy*, vol. 94, pp. 712–725, 2017.

[12] R.-C. Yue, S.-Z. Lu, Y. Luo et al., "Calpain silencing alleviates myocardial ischemia-reperfusion injury through the NLRP3/ASC/Caspase-1 axis in mice," *Life Sciences*, vol. 233, Article ID 116631, 2019.

[13] R. Dra, M. J. Gomes, C. M. Rosa et al., "N-acetylcysteine influence on oxidative stress and cardiac remodeling in rats during transition from compensated left ventricular hypertrophy to heart failure," *Cellular Physiology & Biochemistry International Journal of Experimental Cellular Physiology*

Biochemistry & Pharmacology, vol. 44, no. 6, pp. 2310–2321, 2017.

[14] I. Gregersen, E. T. Askevold, E. L. Sagen et al., "Interleukin 27 is increased in carotid atherosclerosis and promotes NLRP3 inflammasome activation," *PLoS One*, vol. 12, no. 11, Article ID e0188387, 2017.

[15] H. Li, W. Miao, J. Ma et al., "Acute exercise-induced mitochondrial stress triggers an inflammatory response in the myocardium via NLRP3 inflammasome activation with mitophagy," *Oxidative Medicine and Cellular Longevity*, vol. 2016, Article ID 1987149, 11 pages, 2016.

[16] J. L. Macnicol, M. I. Lindinger, and W. Pearson, "A time course evaluation of inflammatory and oxidative markers following high intensity exercise in horses: a pilot study," *Journal of Applied Physiology*, vol. 124, no. 4, pp. 860–865, 2017.

[17] S.-Q. Du, X.-R. Wang, W. Zhu et al., "Acupuncture inhibits TXNIP-associated oxidative stress and inflammation to attenuate cognitive impairment in vascular dementia rats," *CNS Neuroscience & Therapeutics*, vol. 24, no. 1, pp. 39–46, 2018.

[18] I. Bonadei, E. Sciatti, E. Vizzardi et al., "Effects of ivabradine on endothelial function, aortic properties and ventricular-arterial coupling in chronic systolic heart failure patients," *Cardiovascular Therapeutics*, vol. 36, no. 3, Article ID e12323, 2018.

[19] K. Fujisue, K. Sugamura, H. Kurokawa et al., "Colchicine improves survival, left ventricular remodeling, and chronic cardiac function after acute myocardial infarction," *Circulation Journal Official Journal of the Japanese Circulation Society*, vol. 81, no. 8, 2017.

[20] G. A. Paz, E. Iglesiassoler, J. M. Willardson et al., "Postexercise hypotension and heart rate variability responses subsequent to traditional, paired set, and superset training methods," *Journal of Strength & Conditioning Research*, vol. 33, no. 9, p. 1, 2017.

[21] R. Maral, R. Hamid, R. Fatemeh et al., "The greater effect of high-intensity interval training versus moderate-intensity continuous training on cardioprotection against ischemia-reperfusion injury through Klotho levels and attenuate of myocardial TRPC6 expression," *BMC Cardiovascular Disorders*, vol. 19, p. 118, 2019.

[22] T. G. Bedford, C. M. Tipton, N. C. Wilson, R. A. Oppliger, and C. V. Gisolfi, "Maximum oxygen consumption of rats and its changes with various experimental procedures," *Journal of Applied Physiology*, vol. 47, no. 6, pp. 1278–1283, 1979.

[23] P. Pacher, T. Nagayama, P. Bátkai, and D. A. Kass, "Measurement of cardiac function using pressure-volume conductance catheter technique in mice and rats," *Nature Protocols*, vol. 3, no. 9, pp. 1422–1434, 2008.

[24] X. W. Wang, X. B. Cao, C. C. Hou et al., "A clinical study of exhaustive cardiac injury in a combat zone," *Chinese Journal of Integrated Traditional Chinese and Western Medicine First Aid*, vol. 20, no. 5, pp. 270–274, 2013.

[25] C. R. Frasier, R. L. Moore, and D. A. Brown, "Exercise-induced cardiac preconditioning: how exercise protects your achy-breaky heart," *Journal of Applied Physiology*, vol. 111, no. 3, pp. 905–915, 2011.

[26] W. J. Paulus and C. Tschöpe, "A novel paradigm for heart failure with preserved ejection fraction," *Journal of the American College of Cardiology*, vol. 62, no. 4, pp. 263–271, 2013.

[27] D. Laroche, C. Joussain, C. Espagnac et al., "Is it possible to individualize intensity of eccentric cycling exercise from perceived exertion on concentric test?" *Archives of Physical Medicine and Rehabilitation*, vol. 94, no. 8, pp. 1621–1627, 2013.

[28] A. Crisafulli, "The impact of cardiovascular diseases on the cardiovascular regulation during exercise in humans: studies on the metaboreflex elicited by the post-exercise muscle ischemia method," *Current Cardiology Reviews*, vol. 13, no. 4, 2017.

[29] Y. Zhang, J. Huang, X. Yang et al., "Altered Expression of TXNIP in the peripheral leukocytes of patients with coronary atherosclerotic heart disease," *Medicine*, vol. 96, no. 49, p. e9108, 2017.

[30] K. T. Lamont, S. Somers, L. Lacerda et al., "Is red wine a SAFE sip away from cardioprotection? Mechanisms involved in resveratrol- and melatonin-induced cardioprotection," *Journal of Pineal Research*, vol. 50, no. 4, pp. 374–380, 2011.

[31] M. Narasimhan and N. S. Rajasekaran, "Cardiac Aging-benefits of exercise, Nrf2 activation and antioxidant signaling, exercise for cardiovascular disease prevention and treatment," *Advances in Experimental Medicine and Biology*, Springer, Berlin, Germany, pp. 231–255, 2017.

[32] T. Xu, B. Zhang, F. Yang et al., "HSF1 and NF-κB p65 participate in the process of exercise preconditioning attenuating pressure overload-induced pathological cardiac hypertrophy," *Biochemical and Biophysical Research Communications*, vol. 460, no. 3, pp. 622–627, 2015.

[33] B. T. Smenes, F. H. Bækkerud, K. H. Slagsvold et al., "Acute exercise is not cardioprotective and may induce apoptotic signalling in heart surgery: a randomized controlled trial," *Interactive Cardiovascular & Thoracic Surgery*, vol. 27, no. 1, pp. 95–101, 2018.

[34] K. Ellwanger, E. Becker, I. Kienes et al., "The NLR family pyrin domain containing 11 protein contributes to the regulation of inflammatory signalling," *Journal of Biological Chemistry*, vol. 293, no. 8, pp. 2701–2710, 2018.

[35] A. G. La, D. J. Rakhit, and G. Claessen, "Exercise and the right ventricle: a potential achilles' heel," *Cardiovascular Research*, vol. 113, no. 12, pp. 1499–1508, 2017.

Hindawi
Evidence-Based Complementary and Alternative Medicine
Volume 2020, Article ID 3259795, 13 pages
https://doi.org/10.1155/2020/3259795

Research Article

Prognostic Inflammasome-Related Signature Construction in Kidney Renal Clear Cell Carcinoma Based on a Pan-Cancer Landscape

Tianyu Zheng,[1] **Xindong Wang**,[2] **Peipei Yue**,[3] **Tongtong Han**,[1] **Yue Hu**,[1] **Biyao Wang**,[1] **Baohong Zhao**,[4] **Xinwen Zhang**,[4] **and Xu Yan**[1]

[1]*The VIP Department, School and Hospital of Stomatology, Liaoning Provincial Key Laboratory of Oral Diseases, China Medical University, Shenyang 110002, China*
[2]*Department of Orthopedics, The First Hospital of China Medical University, Shenyang 110001, China*
[3]*Department of Biochemistry and Molecular Biology, China Medical University, Shenyang 110001, China*
[4]*Center of Implant Dentistry, School and Hospital of Stomatology, Liaoning Provincial Key Laboratory of Oral Diseases, China Medical University, Shenyang 110002, China*

Correspondence should be addressed to Xinwen Zhang; zhangxinwen@cmu.edu.cn and Xu Yan; kqyx2003@126.com

Received 9 January 2020; Revised 20 February 2020; Accepted 6 March 2020; Published 3 April 2020

Guest Editor: Young-Su Yi

Objective. To investigate the expression patterns and prognostic characteristics of inflammasome-related genes (IRGs) across cancer types and develop a robust biomarker for the prognosis of KIRC. *Methods*. The differentially expressed IRGs and prognostic genes among 10 cancers were analyzed based on The Cancer Genome Atlas (TCGA) dataset. Subsequently, an IRGs risk signature was developed in KIRC. Its prognostic accuracy was evaluated by receiver operating characteristic (ROC) analysis. The independent predictive capacity was identified by stratification survival and multivariate Cox analyses. The gene ontology (GO) analysis and principal component analysis (PCA) were performed to explore biological functions of the IRGs signature in KIRC. *Results*. The expression patterns and prognostic association of IRGs varied from different cancers, while KIRC showed the most abundant survival-related dysregulated IRGs. The IRG signature for KIRC was able to independently predict survival, and the signature genes were mainly involved inimmune-related processes. *Conclusions*. The pan-cancer analysis provided a comprehensive landscape of IRGs across cancer types and identified a strong association between IRGs and the prognosis of KIRC. Further IRGs signature represented a reliable prognostic predictor for KIRC and verified the prognostic value of inflammasomes in KIRC, contributing to our understanding of therapies targeting inflammasomes for human cancers.

1. Introduction

Inflammasomes are a kind of intracellular innate immune multiprotein complexes, the concept of which was introduced by Martinon in 2002 [1]. Inflammasomes consist of three components: sensor protein, apoptosis-associated speck-like protein containing a caspase recruitment domain (ASC)/PYCARD, and pro-caspase-1. Inflammasomes can be activated by recognizing pathogen-associated and damage-associated molecular patterns (PAMPs and DAMPs) via their sensor protein, inducing the activation of pro-caspase-1. Activated caspase-1 (CASP1) will promote the release of inflammatory cytokines interleukin (IL)-1β and IL-18 which subsequently participate in immune and inflammatory response [2]. Studies have shown that inflammasomes play essential roles in regulating the physiological and pathological processes and correlate with various human diseases such as type 2 diabetes [3], immune-related diseases [4], and tumor [5].

In tumor, inflammasomes prove to be double-edged. On the one hand, inflammasomes are involved in regulating

antitumor immunity. Inflammasomes downstream effectors IL-18 and IL-1β can inhibit the killing against cancer cells by certain immune cells, which is detrimental to the control of tumor growth and metastasis [6, 7]. On the other hand, inflammasomes are critical in the regulation of multiple cell death modes such as apoptosis and pyroptosis. NOD-like receptor (NLR) containing a pyrin domain 3 (NLRP3) inflammasome and absent in melanoma 2 (AIM2) inflammasome can induce apoptosis by recruiting and activating caspase-8 via ASC [8]. In addition, inflammasome-mediated activated CASP1 can cleave gasdermin D (GSDMD) and expose N-terminus of pore-forming activity, leading to cell membrane nanopores and cell swelling, and finally to cell pyroptosis [9, 10]. Pyroptosis is a kind of programmed cell death marked by inflammatory cytokines release [11]. These inflammasome-mediated cell death pathways are undoubtedly beneficial to tumor inhibition.

Recent studies have demonstrated that the functions of inflammasomes in tumor, to a certain extent, are determined by the different types of cells and tissues [12–14]. However, there is still no systematic molecular profile of inflammasome-related genes (IRGs) across diverse human cancers until now. The accessibility of high-throughput expression datasets offers the opportunity to investigate the roles of inflammasomes in various cancers. In this study, we identified dysregulated IRGs and prognostic IRGs among 10 cancer types using transcriptome data from The Cancer Genome Atlas (TCGA) [15]. Kidney renal clear cell carcinoma (KIRC) was observed to have most significant IRGs dysregulation and association with tumor prognosis, but few studies have focused on the relationship between inflammasomes and KIRC.

KIRC, the most frequent type of renal cell carcinoma (RCC) [16], have high risk of metastasis and mortality [17]. Currently, the primary treatment for localized RCC remains surgery. However, occurrences of recurrence or distant metastasis in postoperative patients with KIRC account for approximately 30% [18]. Therefore, reliable prognostic models are urgently required to predict the risk of progression for patients with KIRC. From the perspective of pan-cancer analysis, the relationship between inflammasomes and KIRC might be quite close. Thus, an IRGs signature was further constructed to predict patient survival and detect the prognostic value of inflammasomes in KIRC. Broadly speaking, the pan-cancer analysis will help us better understand the molecular mechanism of inflammasomes in the progression of human cancers. Moreover, our robust prognostic indicator confirms the vital role of inflammasomes in KIRC and provides novel therapeutic strategies for KIRC.

2. Materials and Methods

2.1. Selection of IRGs. A total of 40 genes were included in the inflammasome-related gene set: 20 of them were retrieved from the gene set (REACTOME_INFLAMMASOMES, M1072) in the Molecular Signatures Database v7.0 [19, 20], while the added genes were described as the components of inflammasome complexes or being involved in the inflammasome-related pathways according to the published literature.

2.2. Samples of Databases. The RNA sequencing (RNA-Seq) cohorts and clinical information involved in the pan-cancer analysis were obtained from TCGA. To ensure the stability of differential analysis and survival analysis, we only selected 10 types of cancer containing more than 20 normal samples and 20 dead samples. The cancer types included colon adenocarcinoma (COAD), liver hepatocellular carcinoma (LIHC), breast invasive carcinoma (BRCA), head and neck squamous cell carcinoma (HNSC), lung squamous cell carcinoma (LUSC), lung adenocarcinoma (LUAD), kidney renal papillary cell carcinoma (KIRP), KIRC, stomach adenocarcinoma (STAD), and uterine corpus endometrial carcinoma (UCEC). For the TCGA cohorts, we downloaded counts as well as FPKM values of the mRNA expression data. The counts data were used for gene differential expression analysis, whereas FPKM data for prognostic genes identification.

For establishing the risk model in KIRC, 526 patients with complete survival information in TCGA_KIRC dataset were used as a discovery set. The FPKM values of the KIRC RNA-Seq were log-transformed by $\log_2$(FPKM+1) before being applied to the model. To test the prognostic reliability of the model, these 526 KIRC samples were randomized to internal validation set-1 ($n = 132$) or internal validation set-2 ($n = 394$). The TCGA database also included 72 normal samples, of which 71 had matched KIRC samples. Furthermore, three datasets (GSE40435, GSE53757, and GSE73731) were selected from the Gene Expression Omnibus (GEO) database as external validation cohorts for their larger sample sizes. In detail, GSE40435 contained 101 pairs of KIRC and the corresponding normal samples [21]; GSE53757 had 72 KIRC and 72 unpaired normal samples [22], whereas GSE73731 included 265 tumor samples only [23]. The expression matrixes of the GEO datasets were obtained and normalized by the limma package of R [24]. Above KIRC datasets and corresponding clinical features of patients are shown in Table 1.

2.3. Bioinformatic Analysis. The R package "edgeR" was performed to identify the differentially expressed IRGs between tumor and normal samples [25], with a filter condition of adjusted p value < 0.05 and absolute log fold-change (FC) > 1. Also, "edgeR" package was used to analyze differential expression between the high- and low-risk groups. The heatmap and principal component analysis (PCA) were carried out with R packages. The Search Tool for the Retrieval of Interacting Genes database (version 11.0) was used for accessing protein-protein interaction (PPI) [26] and Cytoscape software (version 3.7.2) for visualization [27]. To investigate the functional roles of the IRGs signature in KIRC, gene ontology (GO) analysis was conducted on g: Profiler database [28].

2.4. Statistical Analysis. Univariate Cox regression model was applied to obtain prognostic characteristics of IRGs. For constructing the IRGs signature in KIRC, least absolute shrinkage and selection operator (LASSO) Cox regression analysis was performed to select the most optimal prognostic

Table 1: Clinical characteristics of the KIRC patients.

Id	No. of KIRC samples	No. of normal renal tissue samples	KIRC samples				
			Death events	Mean age (years)	Gender (female/male)	Stage (I/II/III/IV)	Grade (1/2/3/4)
TCGA	526	72	170	60.42	183/343	261/57/123/82	13/226/205/74
GSE40435	101	101	NA	64.12	42/59	—	22/47/24/8
GSE53757	72	72	NA	NA	—	24/19/14/15	—
GSE73731	265	—	NA	NA	102/160	41/12/28/44	22/90/95/49

genes by R package "glmnet" [29]. The packages "survival" and "survminer" of R were used for conducting Kaplan–Meier survival analysis and log-rank test to evaluate the survival difference. The "survivalROC" package was used to perform a time-dependent receiver operating characteristic (ROC) analysis, and the area under the curve (AUC) value was calculated to measure the prognostic accuracy of the risk signature. Additionally, univariate and multivariate Cox regression analyses were conducted to determine whether the risk signature was an independent prognostic factor for KIRC. The expression levels of unpaired samples and risk score distribution were evaluated by independent samples t-test, while the expression levels of paired samples were analyzed by paired t-test. All the statistical analyses were performed on GraphPad Prism 7 software (GraphPad Software Inc., La Jolla, CA) and R software (R.3.6.0). A two-tailed p value less than 0.05 was considered to be statistically significant.

3. Results

3.1. The Pan-Cancer Expression Patterns and Prognostic Characteristics of IRGs. The flow chart of this study is shown in Figure 1. To explore the expression patterns and prognostic association of IRGs across human cancers, we identified differentially expressed IRGs between cancer and normal samples as well as survival-related IRGs among 10 cancers. Generally, 33 (82.5%) of the IRGs were dysregulated in one or more cancer types (Figure 2(a)), while 35 (87.5%) were significantly associated with overall survival (OS) of patients (Figure 2(c)). We observed AIM2 overexpression in 8 cancers and its association with poor prognosis in two kidney carcinomas (KIRC and KIRP). Thioredoxin-interacting protein (TXNIP) expression was consistently suppressed in 7 cancers and positively correlated with patient OS in 2 cancers (KIRC and HNSC) of the 7. The PPI network of all of the IRGs is displayed in Supplementary Figure 1. Furthermore, the expression patterns and prognostic characteristics of IRGs varied from different cancer types, and the numbers of dysregulated and survival-related IRGs for each type were calculated (Figures 2(b) and 2(d)). Abnormally expressed IRGs were most in LUSC and KIRC ($n = 16$, resp.) and least in STAD ($n = 6$). The unsupervised clustering showed that expression patterns of the homologous tissues LUAD and LUSC were relatively close (Figure 2(a)). Besides, survival-related IRGs were most in KIRC ($n = 19$) and least in LUSC as well as COAD ($n = 1$, resp.).

It is worth mentioning that prognostic and dysregulated IRGs were most abundant in KIRC, but rarely reported. Similarly, KIRC showed the largest number ($n = 8$) of dysregulated IRGs related to OS (Figure 2(e)). Furthermore, among the eight genes, the risky genes (PSTPIP1, IFI16, NLRC5, AIM2, and PYCARD) were consistently upregulated, whereas the protective genes (IL1RL1, TXNIP, and APP) were consistently downregulated in KIRC in comparison to normal tissues (Table 2). Due to most survival-related dysregulated IRGs and less studies of inflammasomes in KIRC, the prognostic value of inflammasomes in KIRC was worth investigating. Thus, we further developed an IRGs signature in KIRC to predict patient survival.

3.2. Construction of an IRGs Signature for Predicting OS of KIRC Patients. Based on the pan-cancer analysis, eight dysregulated genes associated with OS of KIRC patients were obtained from TCGA_KIRC dataset (Table 2). Then, a total of five prognostic genes were selected by LASSO Cox regression (Supplementary Figures 2(a) and 2(b)); interferon gamma-inducible protein 16 (IFI16) and AIM2 were identified as risky factors (HR > 1), whereas IL-1 receptor-like 1 (IL1RL1), TXNIP, and amyloid precursor protein (APP) were protective factors (HR < 1).

The five-gene differential expression in KIRC tissues was tested using paired KIRC samples from TCGA and GSE40435, as well as unpaired KIRC samples from GSE53757. As shown in Figure 3, RNA-Seq data from all these validated cohorts confirmed a significant dysregulation of IFI16, IL1RL1, and AIM2 in KIRC tissues. In addition, downregulation of TXNIP and APP was assured by two cohorts, respectively. Overall, compared with normal kidney tissues, the five genes were significantly dysregulated in KIRC. Subsequently, a risk signature was established based on the five IRGs' LASSO Cox regression coefficients (Table 2) and expression levels:

$$\begin{aligned}\text{Risk score} = {} & (0.5409 \times \text{IFI16 expression}) \\ & + (0.1449 \times \text{AIM2 expression}) \\ & + (-0.0698 \times \text{IL1RL1 expression}) \\ & + (-0.3261 \times \text{TXNIP expression}) \\ & + (-0.5283 \times \text{APP expression}).\end{aligned} \quad (1)$$

The risk score for each patient was calculated by our IRGs signature. In the discovery set, patients were divided into high-risk and low-risk groups according to the median

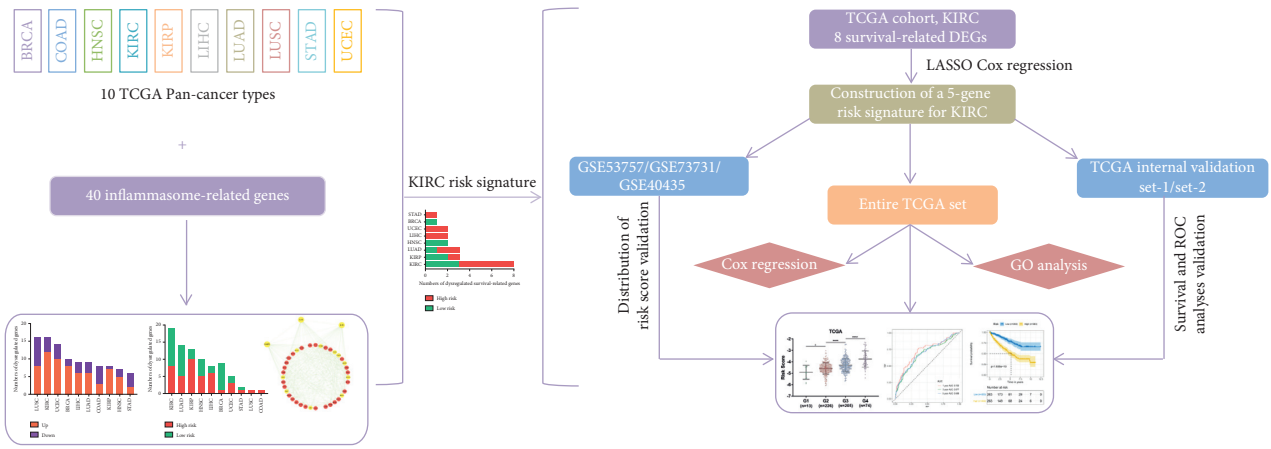

Figure 1: Flow chart of the analysis procedure: data acquisition, signature construction, and validation in KIRC.

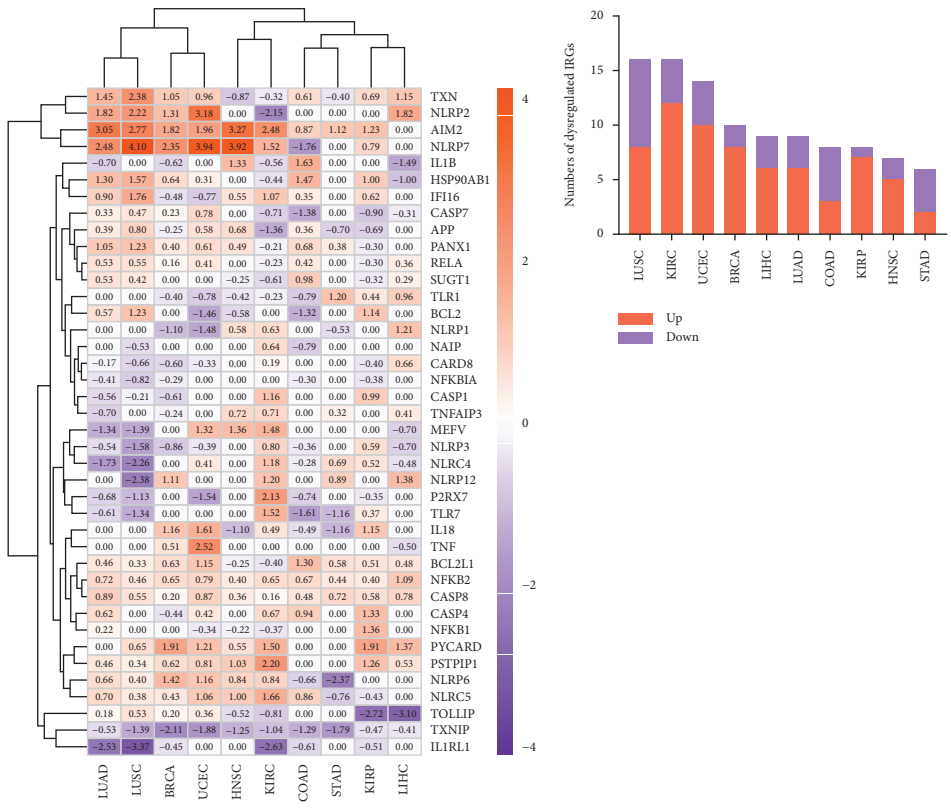

(a) (b)

Figure 2: Continued.

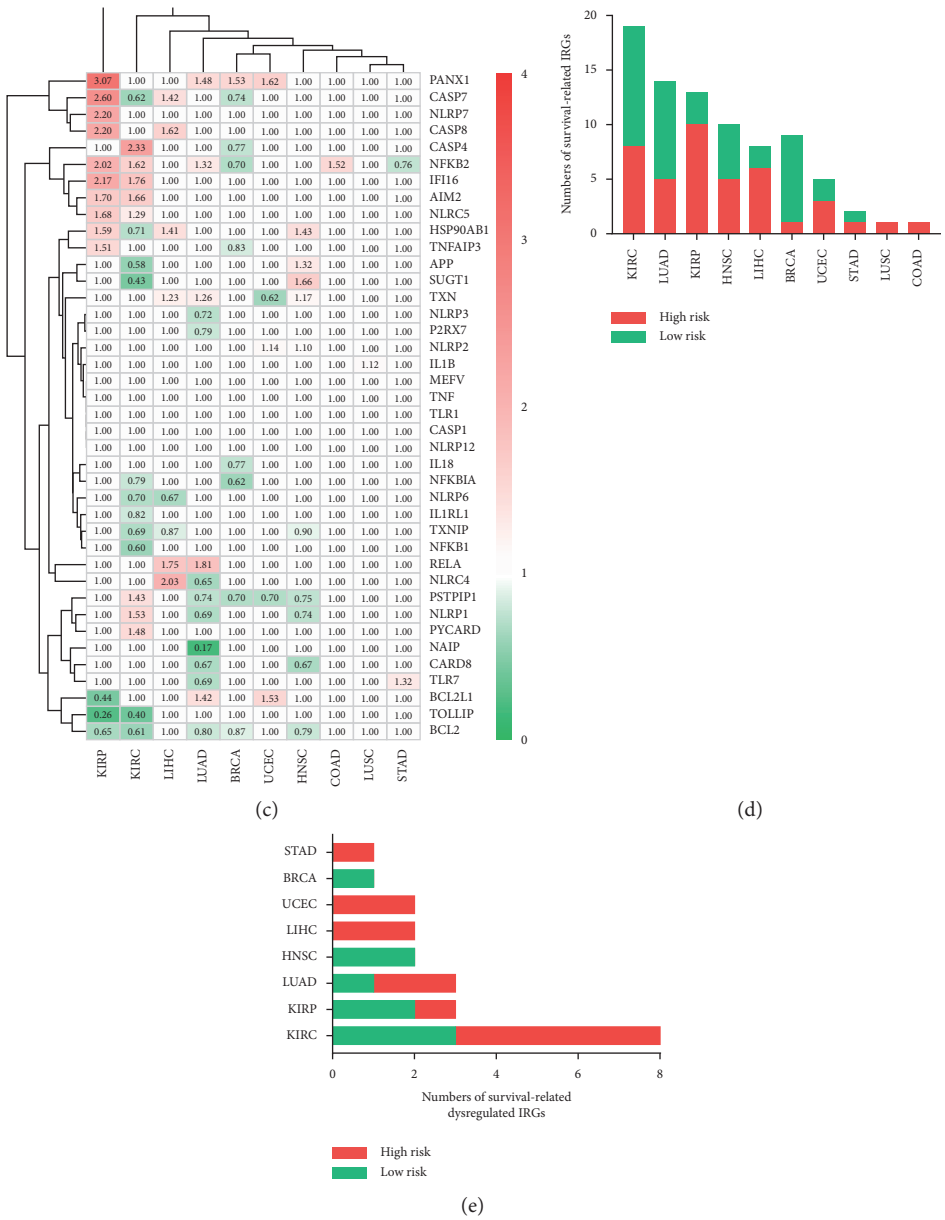

Figure 2: (a) The expression patterns of IRGs across cancers on transcriptome level. Numerical value reflects log FC. (b) The numbers of dysregulated IRGs among 10 cancers. (c) The association between IRGs and prognosis of cancers. Numerical value indicates hazard ratio (HR). (d) The numbers of prognostic IRGs among 10 cancers. (e) The numbers of dysregulated IRGs associated with survival among 8 cancers.

risk score of −4.427 as a cutoff value. The risk score, survival status, and the five-gene expression of each patient are displayed in Supplementary Figures 2(c)-2(e). As expected, the high-risk group had higher expression levels of the risky genes and lower expression levels of the protective genes (Supplementary Figure 2(e)). Further, Kaplan–Meier analysis and ROC analysis were conducted in the discovery set (entire TCGA set), and high-risk group had significantly shorter OS time in comparison to the low-risk group (Figure 4(a)). ROC curves showed that the 1-year, 3-year, and 5-year predictive accuracy of the risk model were 0.722, 0.677, and 0.688, respectively (Figure 4(a)).

3.3. The IRGs Signature Associated with Poor Clinicopathologic Characteristics of KIRC Patients. Since the IRGs signature was negatively correlated to patient OS, we investigated its correlation with multiple clinicopathologic factors of KIRC patients based on the TCGA dataset. We compared distribution of the risk score among different tumor (T) stages, node (N) stages, metastasis (M) stages, TNM stages, and histologic grades. It was noteworthy that higher risk indicated more advanced grades of all these clinicopathologic parameters (Figure 5(a)–5(e)), suggesting the relationship between the IRGs signature and the progression of KIRC.

Table 2: Univariate and LASSO regression analyses of 8 IRGs in the entire TCGA set.

Symbol	Univariate regression		LASSO coefficient
	HR	p value	
PSTPIP1	1.4301	0.0004	—
IFI16	1.7617	0.0001	0.5409
NLRC5	1.2888	0.0165	—
IL1RL1	0.8195	0.0378	−0.0698
AIM2	1.6595	0.0001	0.1449
TXNIP	0.6896	0.0001	−0.3261
PYCARD	1.4824	0.0001	—
APP	0.5769	0.0001	−0.5283

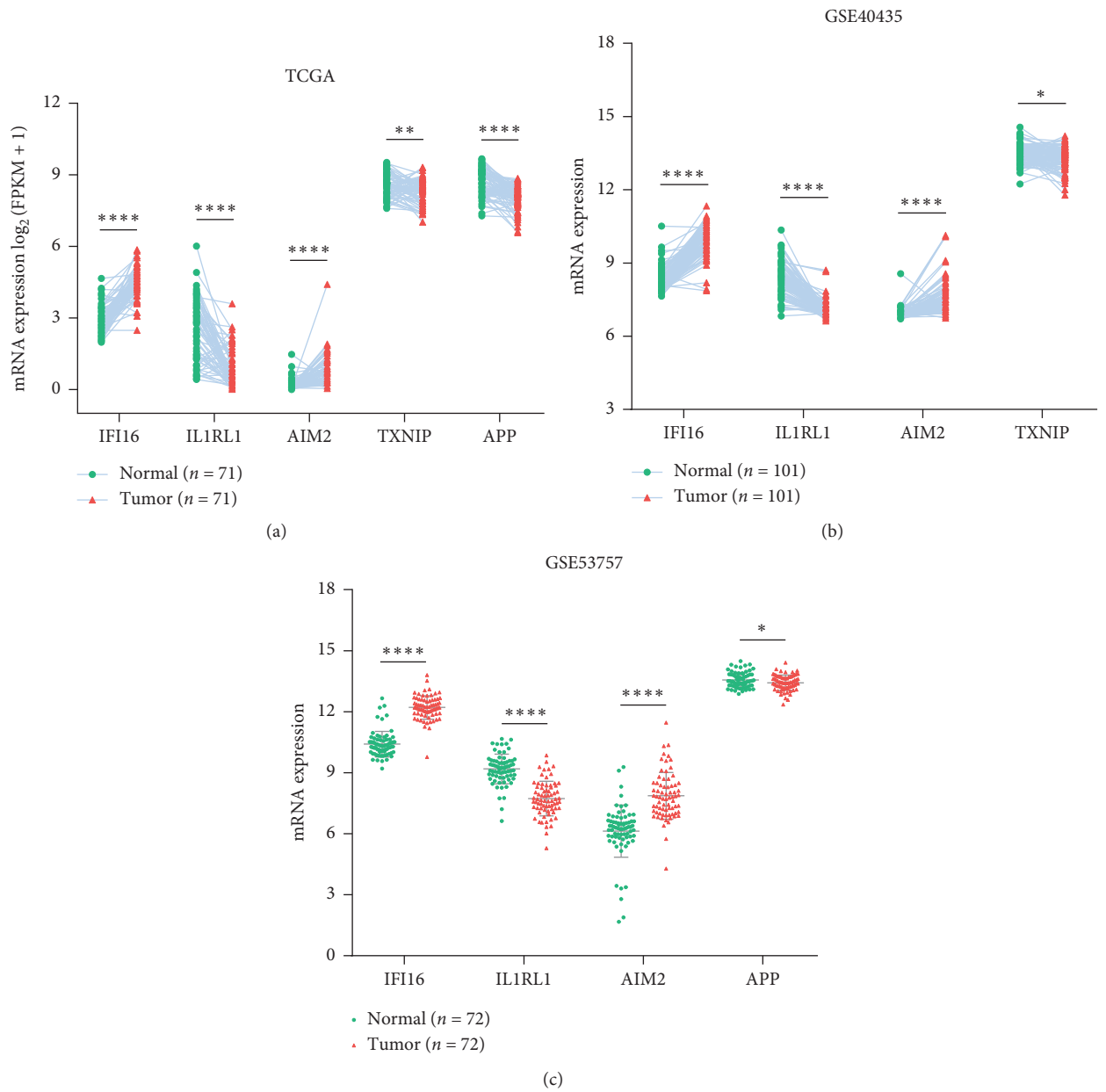

Figure 3: The mRNA levels of signature genes in paired KIRC samples (a-b) and unpaired KIRC samples (c). * $p < 0.05$, ** $p < 0.01$, *** $p < 0.001$, and **** $p < 0.0001$.

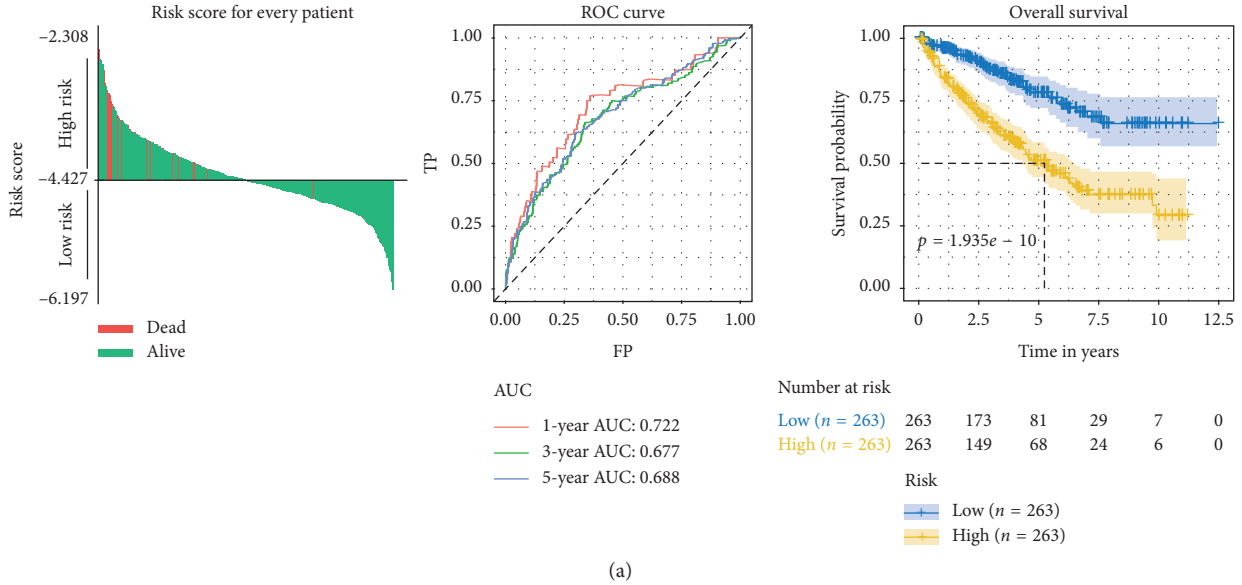

(a)

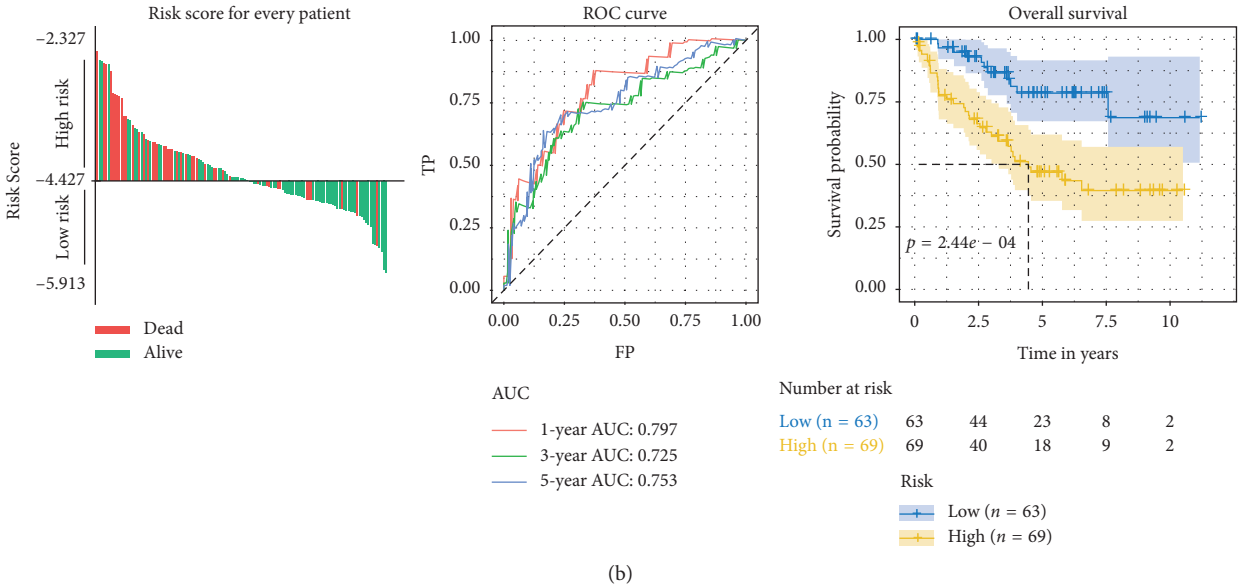

(b)

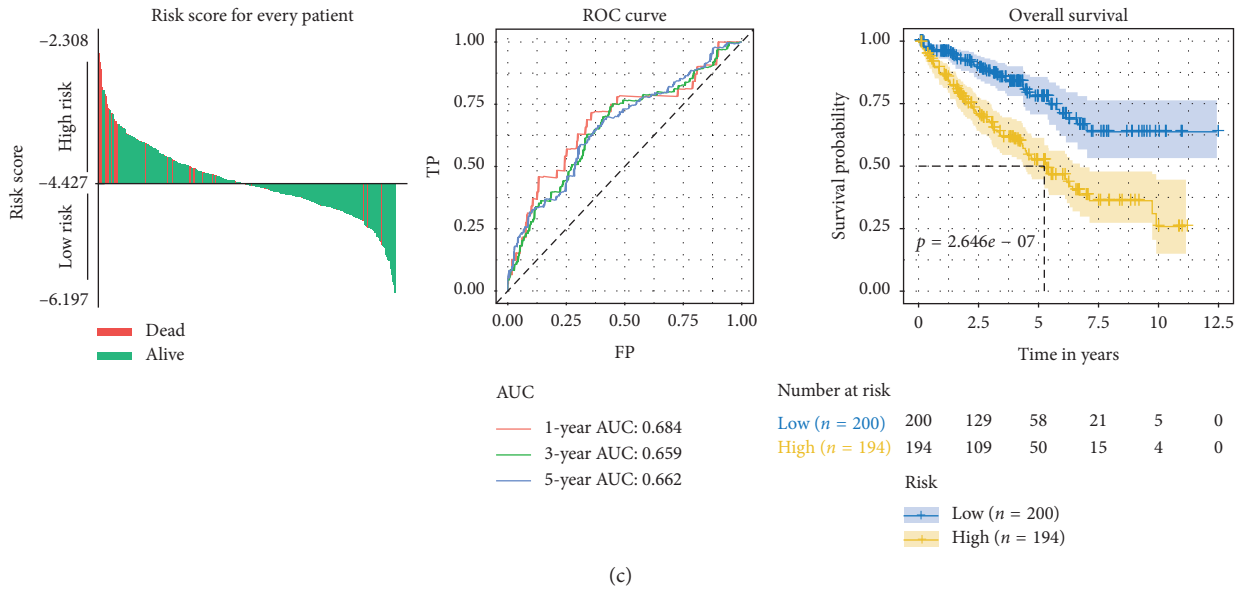

(c)

Figure 4: (a–c) Risk score for each patient, ROC curves (1-year, 3-year, and 5-year), and Kaplan–Meier survival curves in the entire TCGA set (a), internal validation set-1 (b), and internal validation set-2 (c).

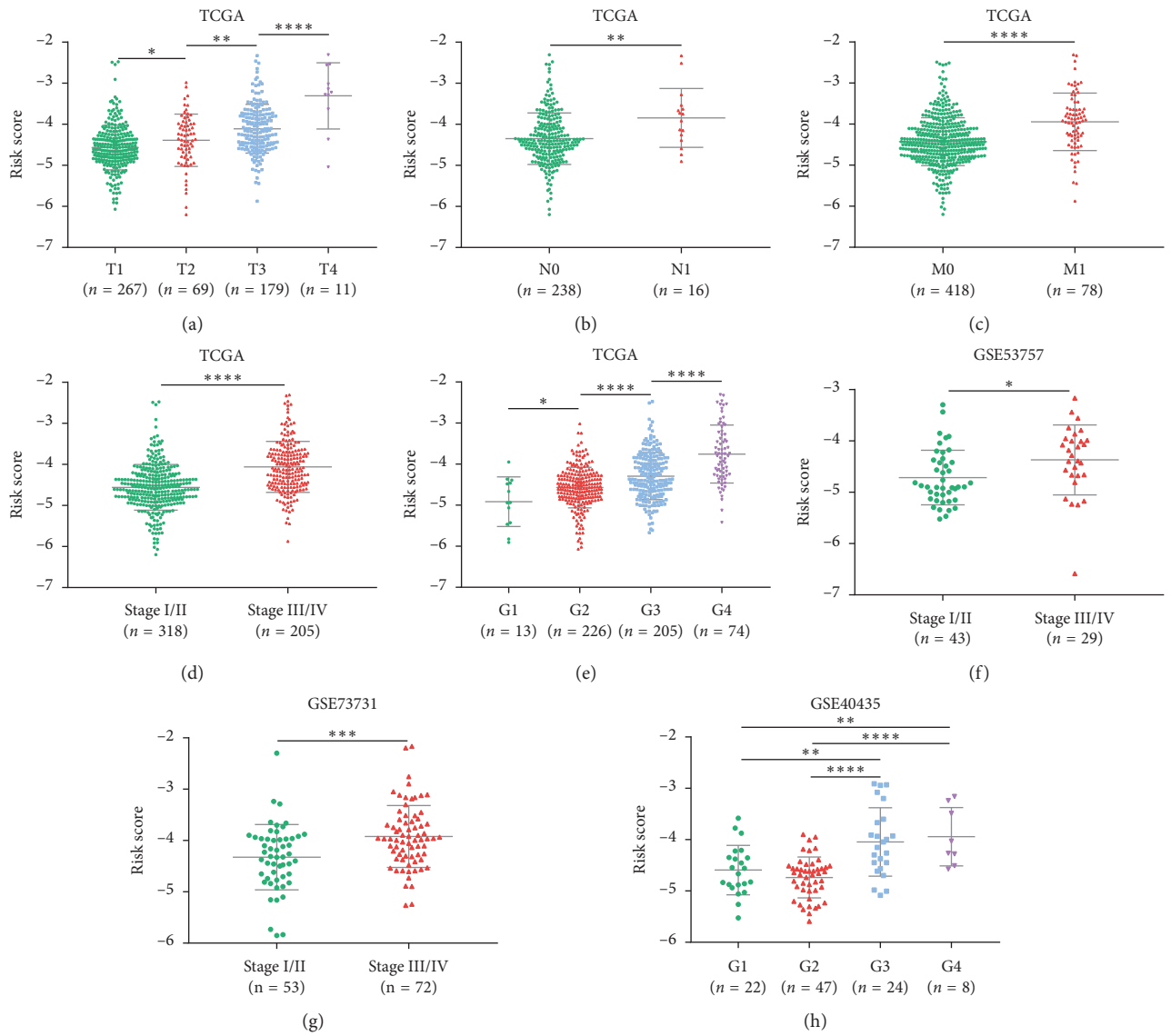

Figure 5: (a–e) Risk score distribution in the entire TCGA set by different T stages (a), N stages (b), M stages (c), TNM stages (d), and grades (e). Risk score distribution in the external validation sets by different stages (f-g) and grades (h).

3.4. Validation of the IRGs Signature. To verify the reliability of our IRGs signature, two internal validation sets and three external validation sets (GSE40435, GSE53757, and GSE73731) were used to test above results. The same hazards model was applied to all the validation cohorts to obtain the risk score for each patient. In the internal validation set-1/set-2, the same cutoff value for grouping was utilized, and the prognostic association and predictive accuracy of the IRGs signature were assured (Figures 4(b)-4(c)). Besides, the findings that risk score related to stage and grade of KIRC were confirmed by the external validation cohorts (Figures 5(f)–5(h)).

3.5. Prognostic value of the IRGs Signature. To detect the prognostic performance of the IRGs signature in stratified cohorts, patients were classified based on age, gender, tumor stage, lymph node status, and distant metastasis status. Due to the small sample size of patients at N1 stage ($n = 16$), we carried out stratification analysis on patients at N0 stage. In all cohorts, the high-risk groups were observed to have worse survival than the low-risk ones (Figure 6). Thus, the IRGs signature was able to distinguish patients with poor survival outcomes without considering traditional clinical factors. Additionally, univariate and multivariate Cox regression analyses were conducted in the entire TCGA set to explore whether the IRGs signature could independently predict OS for KIRC patients. As shown in Table 3, the IRGs signature remained significantly correlated with OS even adjusted by age, T staging, N staging, M staging, and grade, suggesting that the IRGs signature represent an independent prognostic predictor for KIRC.

3.6. Different Immune Response Patterns between High- and Low-Risk Groups. To unearth the biological characteristics

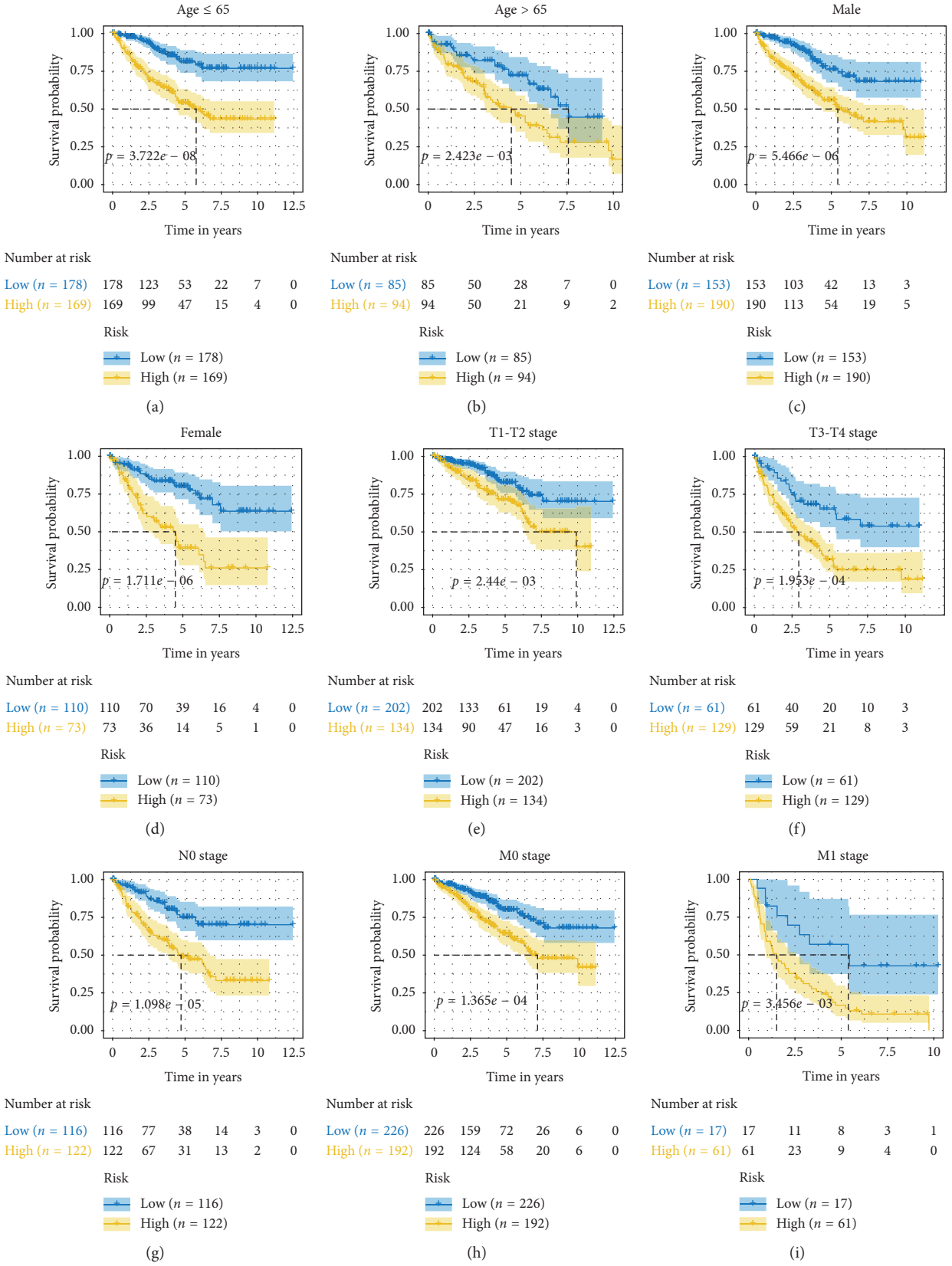

Figure 6: (a–i) Survival analyses of the IRGs signature in the TCGA cohorts stratified by age (a-b), gender (c-d), T stage (e-f), N stage (g), and M stage (h–i).

Table 3: Univariate and multivariate Cox regression analyses of the IRGs signature in the entire TCGA set.

Variable		Univariate regression		Multivariate regression	
		HR	p value	HR	p value
Age (years)	≤65 vs. > 65	0.6065	0.0012	0.7141	0.1131
Gender	Female vs. male	1.0415	0.7990	—	—
T stage	T1-T2 vs. T3-T4	0.3067	0.0001	0.5932	0.0346
N stage	N0 vs. N1	0.3168	0.0007	0.8144	0.5783
M stage	M0 vs. M1	0.2210	0.0001	0.3555	0.0001
Grade	G1-G2 vs. G3-G4	0.3611	0.0001	0.5847	0.0412
Risk	High vs. low	2.8241	0.0001	2.0438	0.0041

of the IRGs signature in KIRC, we analyzed the differentially expressed genes between high-risk group and low-risk group using the entire TCGA dataset. Then, the significantly upregulated genes in the high-risk group (log FC > 2, adjusted p value < 0.05) were involved in the GO analysis. It was shown that immune-related pathways were enriched in the high-risk group (Figure 7(a)). We further conducted PCA of immune-related genes in the two groups, with the gene sets acquired from "Immune Process" and "Immune Response" GO terms. As a result, the high- and low-risk groups generally presented distinct directions of immune-related gene distribution, indicating different immune states of the two groups (Figure 7(b)). Above results indicated the five IRGs mainly involved in immune-related processes.

4. Discussion

Accumulating evidence has revealed that inflammasomes are involved in the pathological processes of different tumors [14, 30, 31], but the specific molecular mechanisms remained incompletely elucidated. In this study, we identified different expression patterns and prognostic characteristics of IRGs among 10 cancers. Remarkably, dysregulation and prognostic correlation of IRGs were most significant in KIRC. Meanwhile, KIRC had the most abundant dysregulated genes associated with patient survival. All of these suggested that inflammasomes might contribute to the progression of KIRC. Considering the potential essential roles of inflammasomes in KIRC and lack of relevant studies, we further focused the analysis on KIRC and established a risk signature for KIRC in order to guide the diagnosis and treatment of KIRC.

KIRC is an aggressive tumor that requires effective predictive biomarkers, but the prognostic models are currently limited. Based on the study value of inflammasomes in KIRC, we produced an IRGs signature to predict the prognosis of patients with KIRC. The signature gene dysregulation in KIRC was confirmed in both paired and unpaired tissues from TCGA and external validation cohorts, indicating the reliability of our differential analyses. Moreover, the fact that the five genes were consistently dysregulated in KIRC indicated the stability of our signature.

Survival analysis suggested that the IRGs signature was closely related to poor prognosis in KIRC. The ROC analysis showed that our signature had an accurate prognostic performance. Additionally, compared with several existing signatures for the TCGA discovery cohorts, our IRGs signature was demonstrated to have a superior predictive accuracy for 5-year survival (AUC = 0.688 vs. 0.637 [32]/0.649 [33]/0.660 [34]). We also performed Kaplan–Meier analysis in stratified cohorts and found its ability to identify patients with worse survival regardless of other clinical variables. Moreover, the five-gene signature was an independent prognostic indicator for KIRC according to the results of univariate and multivariate Cox analyses. Collectively, the IRGs signature can act as a reliable prognostic predictor for KIRC. The prognostic value of our IRGs signature verified the crucial roles inflammasomes played in KIRC, indicating IRGs as potential prognostic biomarkers for KIRC. Moreover, the five-gene signature was positively correlated with advanced stages of the clinicopathologic parameters, suggesting that the signature genes might impact the proliferation, metastasis, and differentiation of KIRC; nevertheless, previous studies have concentrated more on their functions in other cancers than KIRC; hence, further studies are needed for KIRC.

Among the five genes, both AIM2 and IFI16, as the PYHIN family members and innate immune DNA sensors [35, 36], were observed to be risky factors for KIRC. Interestingly, studies have previously reported the tumor-suppressive activity of AIM2 [37, 38] and IFI16 [39, 40]. However, increasing studies have also suggested their tumor-promoting property, corresponding to our findings. For instance, AIM2 improved proliferation of non-small-cell lung cancer (NSCLC) cells via inflammasome-dependent pathway [41]. Knockdown of either AIM2 or IFI16 in oral squamous cell carcinoma cells reduced cell growth [42]. As for the protective factors (IL1RL1, TXNIP, and APP), IL1RL1 was similarly identified to function as a tumor suppressor in mammary tumor [43]. TXNIP was commonly silenced in cancer cells due to genetic or epigenetic events [44]. In addition, a recent study revealed that downregulation of TXNIP could predict worse survival in KIRC, which is in good accordance with our results [45]. Regarding APP, current studies have demonstrated its overexpression and characteristic of oncogenes in some malignancies such as breast cancer [46], pancreatic cancer [47], and NSCLC [48]. In contrast, we observed its decreased expression to be associated with worse prognosis in KIRC. Accordingly, APP may play dual roles in tumor progression and act as an antioncogene in KIRC.

To investigate the biological functions of the five-gene signature in KIRC, GO analysis and PCA were performed, demonstrating that the combined signature was able to distinguish different immune states, and the signature genes were mainly involved in immune-related processes; besides,

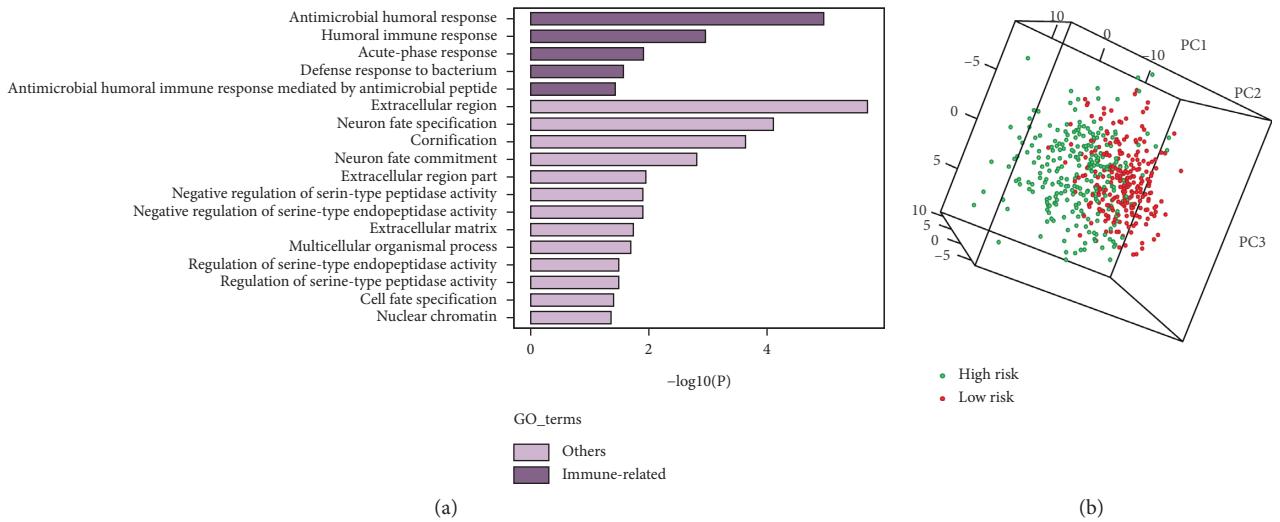

(a) (b)

Figure 7: (a) GO analysis based on the upregulated genes (log FC > 2) in the high-risk group. (b) PCA analysis of the low- and high-risk groups based on immune-related genes in the entire TCGA cohort.

immune response might serve as an underlying mechanism of the signature genes impacting KIRC progression. For treating patients with metastatic RCC, targeted therapies and immunotherapies such as high-dose IL-2 and immune checkpoint inhibitors (ICIs) have been introduced [49, 50]. Nevertheless, many patients fail to benefit from the therapy strategies [50, 51]. Given the association between the signature genes and immune states, these genes might be related to immune therapeutic response of KIRC. Scholars have combined preclinical RNA-Seq data with clinical gene expression profile to establish predictive signatures of prognosis and therapeutic response for gliomas [52, 53]. Inspired by their work, we would further use single-cell RNA-Seq data to explore the roles of the signature genes in immunotherapy.

5. Conclusions

In general, we performed a pan-cancer analysis of abnormally expressed and survival-related IRGs across 10 cancer types, indicating a strong correlation between IRGs and the prognosis of KIRC. We further established an IRGs signature that could independently predict survival for patients with KIRC, which confirmed the prognostic value of inflammasomes in KIRC. Moreover, the signature might influence the progression of KIRC. Further exploration on biological functions of the IRGs signature suggested that the signature genes are mostly involved in immune-related pathways and provided novel perspectives for therapy of KIRC. Thus, our study not only presented a systematic landscape of IRGs across human cancers but also developed a robust prognostic predictor for KIRC from the perspective of pan-cancer analysis.

Data Availability

All raw data included in this study can be acquired from the two public repositories: The Cancer Genome Atlas (TCGA) database and Gene Expression Omnibus (GEO) database. And, the data used to support our findings are available from the corresponding author upon request.

Conflicts of Interest

The authors declare that they have no conflicts of interest regarding the publication of this paper.

Acknowledgments

This work was financially supported by grants from the National Natural Science Foundation of China (No. 81700977 and 81500858) and Technology Project Program of Liaoning Province of China (No. 20170541059) from the Natural Sciences Foundation of Liaoning Province of China.

Supplementary Materials

The PPI network of the 40 IRGs is shown in Supplementary Figure 1. Supplementary Figure 2 presents the construction of LASSO Cox regression model, and each patient's risk score, survival status, and the five-gene expression. (*Supplementary Materials*)

References

[1] F. Martinon, K. Burns, and J. Tschopp, "The inflammasome," *Molecular Cell*, vol. 10, no. 2, pp. 417–426, 2002.

[2] J. von Moltke, J. S. Ayres, E. M. Kofoed, J. Chavarría-Smith, and R. E. Vance, "Recognition of bacteria by inflammasomes," *Annual Review of Immunology*, vol. 31, no. 1, pp. 73–106, 2013.

[3] B. Vandanmagsar, Y.-H. Youm, A. Ravussin et al., "The NLRP3 inflammasome instigates obesity-induced inflammation and insulin resistance," *Nature Medicine*, vol. 17, no. 2, pp. 179–188, 2011.

[4] J. M. Kahlenberg and I. Kang, *Clinicopathologic Significance of Inflammasome Activation in Autoimmune Diseases*, Arthritis & rheumatology, Hoboken, NJ, USA), 2019.

[5] N. Ershaid, Y. Sharon, H. Doron et al., "NLRP3 inflammasome in fibroblasts links tissue damage with inflammation in breast cancer progression and metastasis," *Nature Communications*, vol. 10, no. 1, p. 4375, 2019.

[6] M. Terme, E. Ullrich, L. Aymeric et al., "IL-18 induces PD-1-dependent immunosuppression in cancer," *Cancer Research*, vol. 71, no. 16, pp. 5393–5399, 2011.

[7] M. T. Chow, J. Sceneay, C. Paget et al., "NLRP3 suppresses NK cell-mediated responses to carcinogen-induced tumors and metastases," *Cancer Research*, vol. 72, no. 22, pp. 5721–5732, 2012.

[8] V. Sagulenko, S. J. Thygesen, D. P. Sester et al., "AIM2 and NLRP3 inflammasomes activate both apoptotic and pyroptotic death pathways via ASC," *Cell Death & Differentiation*, vol. 20, no. 9, pp. 1149–1160, 2013.

[9] L. Sborgi, S. Rühl, E. Mulvihill et al., "GSDMD membrane pore formation constitutes the mechanism of pyroptotic cell death," *The EMBO Journal*, vol. 35, no. 16, pp. 1766–1778, 2016.

[10] J. Shi, Y. Zhao, K. Wang et al., "Cleavage of GSDMD by inflammatory caspases determines pyroptotic cell death," *Nature*, vol. 526, no. 7575, pp. 660–665, 2015.

[11] T. Strowig, J. Henao-Mejia, E. Elinav, and R. Flavell, "Inflammasomes in health and disease," *Nature*, vol. 481, no. 7381, pp. 278–286, 2012.

[12] S. K. Drexler, L. Bonsignore, M. Masin et al., "Tissue-specific opposing functions of the inflammasome adaptor ASC in the regulation of epithelial skin carcinogenesis," *Proceedings of the National Academy of Sciences*, vol. 109, no. 45, pp. 18384–18389, 2012.

[13] Q. Deng, Y. Geng, L. Zhao et al., "NLRP3 inflammasomes in macrophages drive colorectal cancer metastasis to the liver," *Cancer Letters*, vol. 442, pp. 21–30, 2019.

[14] R. Kolb, P. Kluz, Z. W. Tan et al., "Obesity-associated inflammation promotes angiogenesis and breast cancer via angiopoietin-like 4," *Oncogene*, vol. 38, no. 13, pp. 2351–2363, 2019.

[15] J. N. Weinstein, E. A. Lingua, E. A. Collisson et al., "The Cancer Genome Atlas Pan-Cancer analysis project," *Nature Genetics*, vol. 45, no. 10, pp. 1113–1120, 2013.

[16] B. Shuch, A. Amin, A. J. Armstrong et al., "Understanding pathologic variants of renal cell carcinoma: distilling therapeutic opportunities from biologic complexity," *European Urology*, vol. 67, no. 1, pp. 85–97, 2015.

[17] Y.-W. Lin, L.-M. Lee, W.-J. Lee et al., "Melatonin inhibits MMP-9 transactivation and renal cell carcinoma metastasis by suppressing Akt-MAPKs pathway and NF-κB DNA-binding activity," *Journal of Pineal Research*, vol. 60, no. 3, pp. 277–290, 2016.

[18] S. MacLennan, M. Imamura, M. C. Lapitan et al., "Systematic review of perioperative and quality-of-life outcomes following surgical management of localised renal cancer," *European Urology*, vol. 62, no. 6, pp. 1097–1117, 2012.

[19] A. Subramanian, P. Tamayo, V. K. Mootha et al., "Gene set enrichment analysis: a knowledge-based approach for interpreting genome-wide expression profiles," *Proceedings of the National Academy of Sciences*, vol. 102, no. 43, pp. 15545–15550, 2005.

[20] A. Liberzon, C. Birger, H. Thorvaldsdóttir, M. Ghandi, J. P. Mesirov, and P. Tamayo, "The molecular signatures database hallmark gene set collection," *Cell Systems*, vol. 1, no. 6, pp. 417–425, 2015.

[21] M. B. Wozniak, F. Le Calvez-Kelm, B. Abedi-Ardekani et al., "Integrative genome-wide gene expression profiling of clear cell renal cell carcinoma in Czech Republic and in the United States," *PLoS One*, vol. 8, no. 3, Article ID e57886, 2013.

[22] C. A. von Roemeling, D. C. Radisky, L. A. Marlow et al., "Neuronal pentraxin 2 supports clear cell renal cell carcinoma by activating the AMPA-selective glutamate receptor-4," *Cancer Research*, vol. 74, no. 17, pp. 4796–4810, 2014.

[23] X. Wei, Y. Choudhury, W. K. Lim et al., "Recognizing the continuous nature of expression heterogeneity and clinical outcomes in clear cell renal cell carcinoma," *Scientific Reports*, vol. 7, no. 1, p. 7342, 2017.

[24] M. E. Ritchie, B. Phipson, Di Wu et al., "Limma powers differential expression analyses for RNA-sequencing and microarray studies," *Nucleic Acids Research*, vol. 43, no. 7, p. e47, 2015.

[25] D. J. McCarthy, Y. Chen, and G. K. Smyth, "Differential expression analysis of multifactor RNA-Seq experiments with respect to biological variation," *Nucleic Acids Research*, vol. 40, no. 10, pp. 4288–4297, 2012.

[26] D. Szklarczyk, A. L. Gable, D. Lyon et al., "STRING v11: protein-protein association networks with increased coverage, supporting functional discovery in genome-wide experimental datasets," *Nucleic Acids Research*, vol. 47, no. D1, pp. D607–D613, 2019.

[27] P. Shannon, A. Markiel, O. Ozier et al., "Cytoscape: a software environment for integrated models of biomolecular interaction networks," *Genome Research*, vol. 13, no. 11, pp. 2498–2504, 2003.

[28] U. Raudvere, L. Kolberg, I. Kuzmin et al., "g:Profiler: a web server for functional enrichment analysis and conversions of gene lists (2019 update)," *Nucleic Acids Research*, vol. 47, no. W1, pp. W191–W198, 2019.

[29] J. Friedman, T. Hastie, and R. Tibshirani, "Regularization paths for generalized linear models via coordinate descent," *Journal of Statistical Software*, vol. 33, no. 1, pp. 1–22, 2010.

[30] M. Gao, P. Zhang, L. Huang et al., "Is NLRP3 or NLRP6 inflammasome activation associated with inflammation-related lung tumorigenesis induced by benzo(a)pyrene and lipopolysaccharide?" *Ecotoxicology and Environmental Safety*, vol. 185, p. 109687, 2019.

[31] B. Flood, J. Manils, C. Nulty et al., "Caspase-11 regulates the tumour suppressor function of STAT1 in a murine model of colitis-associated carcinogenesis," *Oncogene*, vol. 38, no. 14, pp. 2658–2674, 2019.

[32] X. Hua, J. Chen, Y. Su et al., "Identification of an immune-related risk signature for predicting prognosis in clear cell renal cell carcinoma," *Aging*, vol. 12, 2020.

[33] J.-H. Zeng, W. Lu, L. Liang et al., "Prognosis of clear cell renal cell carcinoma (ccRCC) based on a six-lncRNA-based risk score: an investigation based on RNA-sequencing data," *Journal of Translational Medicine*, vol. 17, no. 1, p. 281, 2019.

[34] L. Chen, Y. Luo, G. Wang et al., "Prognostic value of a gene signature in clear cell renal cell carcinoma," *Journal of Cellular Physiology*, vol. 234, no. 7, pp. 10324–10335, 2019.

[35] V. Hornung, A. Ablasser, M. Charrel-Dennis et al., "AIM2 recognizes cytosolic dsDNA and forms a caspase-1-activating inflammasome with ASC," *Nature*, vol. 458, no. 7237, pp. 514–518, 2009.

[36] L. Unterholzner, S. E. Keating, M. Baran et al., "IFI16 is an innate immune sensor for intracellular DNA," *Nature Immunology*, vol. 11, no. 11, pp. 997–1004, 2010.

[37] K. L. DeYoung, M. E. Ray, Y. A. Su et al., "Cloning a novel member of the human interferon-inducible gene family associated with control of tumorigenicity in a model of human melanoma," *Oncogene*, vol. 15, no. 4, pp. 453–457, 1997.

[38] S. M. Man, Q. Zhu, L. Zhu et al., "Critical role for the DNA sensor AIM2 in stem cell proliferation and cancer," *Cell*, vol. 162, no. 1, pp. 45–58, 2015.
[39] N. Fujiuchi, J. A. Aglipay, T. Ohtsuka et al., "Requirement of IFI16 for the maximal activation of p53 induced by ionizing radiation," *Journal of Biological Chemistry*, vol. 279, no. 19, pp. 20339–20344, 2004.
[40] W. Lin, Z. Zhao, Z. Ni et al., "IFI16 restoration in hepatocellular carcinoma induces tumour inhibition via activation of p53 signals and inflammasome," *Cell Proliferation*, vol. 50, no. 6, 2017.
[41] M. Zhang, C. Jin, Y. Yang et al., "AIM2 promotes non-small-cell lung cancer cell growth through inflammasome-dependent pathway," *Journal of Cellular Physiology*, vol. 234, no. 11, pp. 20161–20173, 2019.
[42] Y. Kondo, K. Nagai, S. Nakahata et al., "Overexpression of the DNA sensor proteins, absent in melanoma 2 and interferon-inducible 16, contributes to tumorigenesis of oral squamous cell carcinoma with p53 inactivation," *Cancer Science*, vol. 103, no. 4, pp. 782–790, 2012.
[43] C. T. R. Viana, L. A. A. Orellano, L. X. Pereira et al., "Cytokine production is differentially modulated in malignant and non-malignant tissues in ST2-receptor deficient mice," *Inflammation*, vol. 41, no. 6, pp. 2041–2051, 2018.
[44] K. Nagaraj, L. Lapkina-Gendler, R. Sarfstein et al., "Identification of thioredoxin-interacting protein (TXNIP) as a downstream target for IGF1 action," *Proceedings of the National Academy of Sciences*, vol. 115, no. 5, pp. 1045–1050, 2018.
[45] Y. Gao, J.-C. Qi, X. Li et al., "Decreased expression of TXNIP predicts poor prognosis in patients with clear cell renal cell carcinoma," *Oncology Letters*, vol. 19, no. 1, pp. 763–770, 2020.
[46] J. Y. S. Tsang, M. A. Lee, T.-H. Chan et al., "Proteolytic cleavage of amyloid precursor protein by ADAM10 mediates proliferation and migration in breast cancer," *EBioMedicine*, vol. 38, pp. 89–99, 2018.
[47] D. E. Hansel, A. Rahman, S. Wehner et al., "Increased expression and processing of the Alzheimer amyloid precursor protein in pancreatic cancer may influence cellular proliferation," *Cancer Research*, vol. 63, no. 21, pp. 7032–7037, 2003.
[48] A. Sobol, P. Galluzzo, M. J. Weber, S. Alani, and M. Bocchetta, "Depletion of amyloid precursor protein (APP) causes G0 arrest in non-small cell lung cancer (NSCLC) cells," *Journal of Cellular Physiology*, vol. 230, no. 6, pp. 1332–1341, 2015.
[49] R. Garje, J. An, A. Greco et al., "The future of immunotherapy-based combination therapy in metastatic renal cell carcinoma," *Cancers*, vol. 12, no. 1, 2020.
[50] R. Flippot, B. Escudier, and L. Albiges, "Immune checkpoint inhibitors: toward new paradigms in renal cell carcinoma," *Drugs*, vol. 78, no. 14, pp. 1443–1457, 2018.
[51] B. I. Rini, D. F. McDermott, H. Hammers et al., "Society for immunotherapy of cancer consensus statement on immunotherapy for the treatment of renal cell carcinoma," *Journal for Immunotherapy of Cancer*, vol. 4, p. 81, 2016.
[52] J. Zhang, M. Guan, Q. Wang et al., "Single-cell transcriptome-based multilayer network biomarker for predicting prognosis and therapeutic response of gliomas," *Briefings in Bioinformatics*, 2019.
[53] X. Sun, X. Liu, M. Xia et al., "Multicellular gene network analysis identifies a macrophage-related gene signature predictive of therapeutic response and prognosis of gliomas," *Journal of Translational Medicine*, vol. 17, no. 1, p. 159, 2019.

Hindawi
Evidence-Based Complementary and Alternative Medicine
Volume 2020, Article ID 1561342, 15 pages
https://doi.org/10.1155/2020/1561342

Review Article

NLRP3 Inflammasome: A Potential Alternative Therapy Target for Atherosclerosis

Yang Liu,[1,2] Chao Li,[1] Honglin Yin,[1] Xinrong Zhang,[1] and Yunlun Li[1,2]

[1]*Experimental Center, Shandong University of Traditional Chinese Medicine, 250355 Ji-nan, China*
[2]*Affiliated Hospital of Shandong University of Traditional Chinese Medicine, 250000 Ji-nan, China*

Correspondence should be addressed to Yunlun Li; yunlun.lee@hotmail.com

Received 8 January 2020; Revised 21 February 2020; Accepted 4 March 2020; Published 31 March 2020

Guest Editor: Young-Su Yi

Atherosclerosis (AS) is a complex and chronic inflammatory disease that occurs in multiple systems of the human body. It is an important pathological basis for a variety of diseases and a serious threat to human health. So far, many theories have been formed to explain the pathogenesis of atherosclerosis, among which "inflammation theory" has gradually become a research focus. This theory presents that inflammatory response runs through the whole progress of AS, inflammatory cells play as the main executors of AS, and inflammatory mediators are the key molecules of AS. In the inflammatory process of atherosclerosis, the role of NLRP3 in the atherosclerosis has gradually got the attention of researchers. NLRP3 is a kind of signal-transductional pattern recognition receptors (PRRs). After recognizing and binding to the damage factors, NLRP3 inflammasome will be assembled to activate IL-1β and caspase-1 pathways, resulting in promoting the inflammation process of AS, reducing the stability of the plaques, and finally increasing the incidence of adverse cardiovascular events. Taken above, the article will review the potential benefits of drugs targeting the NLRP3 inflammasome in the therapy of AS.

1. Introduction

Atherosclerosis (AS) is a chronic disease caused by many factors, which often causes some important adverse cardiovascular and cerebrovascular events, including coronary artery, carotid artery, cerebral artery-related diseases, and peripheral artery diseases. The prevalence of atherosclerosis is increasing year by year all over the world, which continues to threaten human health and make our society carry great burden [1].

The injury of the arterial intima and formation of lipid stripe are considered as the initial manifestation of atherosclerosis. Excessive low-density lipoprotein (LDL) accumulates and deposits in vascular subcutaneous tissue, which activates the immune stress of arterial endothelial cells and causes a series of inflammatory reactions [2]. LDLs are modified to oxidized LDLs (ox-LDLs), which stimulate endothelial cells to generate a large number of chemokines and recruit T cells and monocytes [3, 4]. Monocytes begin to bind with E-selectin and P-selectin at the activated endothelium and migrate to the intima. Vascular endothelial cells (VECs) secrete a variety of cytokines and chemokines to promote the migration of monocytes. The vascular endothelial monocytes are transformed into macrophages. Macrophages engulf lipids and form foam cells, which in turn promotes the occurrence and development of AS. With the development of atherosclerosis, lipid stripes gradually mature into fibrous plaques covered with the fibrous cap. During the formation of fibrous cap, due to the common influence of a variety of cytokines and chemokines, vascular smooth muscle cells (VSMCs) change from static and contractile state to active and synthetic state, and then move to the artery intima [5].

Inflammatory factors run through the whole process of atherosclerosis. In 1999, Ross proposed the hypothesis of inflammatory response to atherosclerosis [6]. Since then, more and more research has proved that inflammatory factors and inflammasomes play a critical role in the inflammatory response of atherosclerosis. Among them, the NLRP3 inflammasome which is a representative is paid

much attention. NLRP3 inflammasome is related to many diseases involved in multiple systems, such as chronic obstructive pulmonary disease [7, 8], asthma [7], gout [9, 10], Crohn disease [11], heart failure [12], and myocardial infarction [13, 14]. Recently, the results of the CANTOS test [15] showed that the anti-inflammatory treatment aiming at the interleukin-1β (IL-1β) pathway significantly reduced the recurrence rate of cardiovascular events, which had nothing to do with lipid level. It directly confirms the theory of inflammation in atherosclerosis and provides a theoretical basis for the clinical anti-inflammatory treatment of atherosclerosis [15]. This review focuses on the role and regulatory mechanism of the NLRP3 inflammasome in atherosclerosis, and the NLRP3 inflammasome could be considered as a potential therapeutic target for AS.

2. NLRP3 Inflammasome

2.1. Structure of NLRP3. The NOD-like receptors (NLRs), as signal-transductional PRRs, are distributed in the cytoplasm and are important receptors in the signaling pathway against intracellular pathogens and injury factors. So far, 23 NLRs have been found in humans and 34 in mice.

NLR consists of three domains, with leucine-rich repeats (LRR) at the C-terminal, responsible for the identification and binding of specific PAMP and DAMP [16]. Nucleotide-binding oligomerization domain (NOD) in the middle is the characteristic of NLR, also known as the NACHT domain, named by the first letter of four known NLR family members [17].The function of NOD prompts NLR molecular aggregation to change its configuration [17]. The N-terminal is the effector domain, mainly composed of caspase recruitment domain (CARD), pyrin domain (PYD), or baculovirus inhibitor of apoptosis protein repeat domain (BIR), which mediates the homologous protein interaction to transmit signals downstream [18]. According to the structural characteristics of the effect domain, several subfamilies can be further divided, including NLRA, NLRB, NLRC, and NLRP [19].

NLRP is the largest subfamily of NLR. Currently, 14 kinds of NLRP have been discovered, and NLRP3 has gradually become a "molecule star" (Figure 1) [20]. The structure of NLRP3 was analyzed by Cryo-EM, and the map revealed an earring shape characteristic of NLRs, containing a curved LRR domain and a compact NACHT comprising NBD, HD1, WHD, and HD2 (as shown in Figure 2) [21]. The N-terminus of NLRP3 contains PYD and is mainly expressed in macrophages and peripheral blood leukocytes [22]. NLRP3 can identify and combine with PAMP, such as the MDP, bacterial mRNA, *Listeria monocytogenes*, and *Staphylococcus aureus* [22]. The above events resulted in the conformational change of NLRP3, which exposed it to NOD and promoted oligomerization. Through PYD-PYD interaction, it will recruit apoptosis-related card-like protein (ASC) [23]. Then, NLRP3, ASC, and caspase-1 comprise the NLRP3 inflammasome [24]. ASC recruits procaspase-1 via CARD-CARD interaction, resulting in a conformational change to produce active caspase-1, and cleaving pro-IL-1β and pro-IL-18 to the inflammatory cytokines IL-1β and IL-18 [24].

2.2. Activation of NLRP3. Production of the NLRP3 inflammasome includes two processes: priming and activation (as shown in Figure 3) [25]. The response is initiated by the TLR, which recognizes and binds the corresponding signals to activate NF-κB at the transcriptional level, facilitating the synthesis of NLRP3 and various inflammatory precursors, such as IL-1β and IL-18 precursors, in preparation for the next inflammatory response [26]. NLRP3 is activated by related ligands and then recruits ASC and procaspase-1 to assemble into the NLRP3 inflammasome [27]. NLRP3 inflammasome which includes mature caspase-1 can promote the activation of proinflammatory mediators such as IL-1β and IL-18 and promote the occurrence of inflammatory response [27]. The activation mechanism of NLRP3 in the second stage is the focus of the current research, and a variety of mature hypotheses have been formed and supplemented to explain the activation process of NLRP3.

2.2.1. The First Hypothesis: Ion Flow Hypothesis. When cells are damaged or necrotic, ATP generated inside the cell is released to outside of the cell to activate the P2X7 ion channel controlled by ATP on the membrane, causing ion transmembrane migration [28]. Under the continuous stimulation of ATP, P2X7 receptors lead to a large amount of Ca^{2+} and Na^{+} inflow, resulting in the efflux of K^{+} [29]. P2X7R channel opening breaks the intracellular ion balance and makes pannexin-1 as the half channel protein to form pores on the cell membrane. Extracellular ligands (e.g., ATP and LPS) enter the cell, activate NLRP3 inflammatory cells, and promote the secretion and release of IL-1β [30]. It has been reported that inflammasomes can be triggered to assemble and recruit procaspase-1, when the intracellular concentration of K^{+} is less than 90 mmol·l^{-1} ($[K^{+}] < 90$ mmol·l^{-1}) [31]. Therefore, intracellular low concentration of K^{+} is recognized as a common mechanism to induce activation of the NLRP3 inflammasome [32].

P2X7 receptor activation also promotes calcium influx, and Ca^{2+} mobilization in the NLRP3 inflammasome activation is prevalent but ambiguous [33]. Chu et al. showed that the BAPTA-AM, a Ca^{2+} chelator, inhibits IL-1 formation, suggesting the involvement of Ca^{2+} mobilization in NLRP3 inflammasome activation [34]. The increase in intracellular Ca^{2+} from varieties of Ca^{2+} pool plays a critical role in activation of the NLRP3 inflammasome [35]. The inhibitor of IP3R prevents Ca^{2+} flux and also hinders the NLRP3 activation [36]. Additionally, the entry of Ca^{2+} through Ca^{2+} channels on the plasma membrane is an indispensable approach to the increase in Ca^{2+} in the cytosol, such as P2X7R, TRPM2, and TRPM7 [37]. Beyond the above, the lysosome has ability to release Ca^{2+} in the process of NLRP3 inflammasome activation [38]. The inhibition of the ER or plasma membrane Ca^{2+} channels will abate caspase-1 activation and IL-1β secretion in response to NLRP3 stimuli [38]. In spite of abundant studies on Ca^{2+} in NLRP3 activation, the accurate mechanism has not been revealed. It was successfully

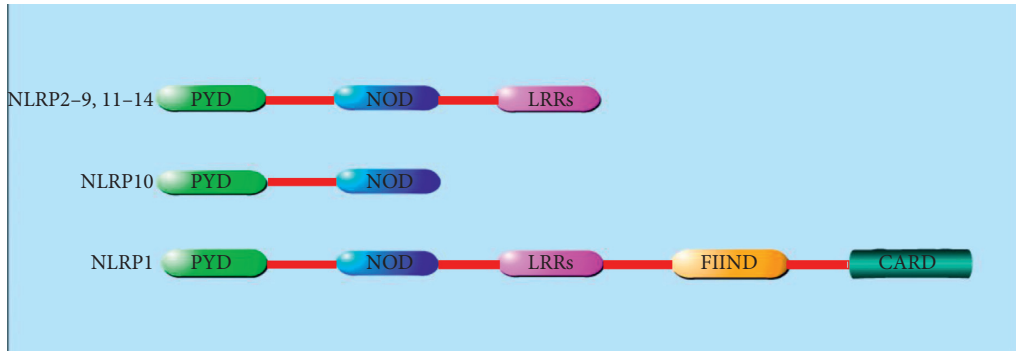

Figure 1: Structure of NLRP in humans. NLRP is the largest subfamily of NLR. All members in NLRP family have the pyrin domain (PYD) at the N-terminal and the nucleotide-binding oligomerization domain (NOD), also named as NACHT domain, in the middle. In addition, most members of NLRP (2–9, 11–14) have leucine-rich repeats (LRRs) at the C-terminal. The NLRP1's C-terminal has the caspase recruitment domain (CARD), function-to-find domain (FIIND), and leucine-rich repeats (LRRs).

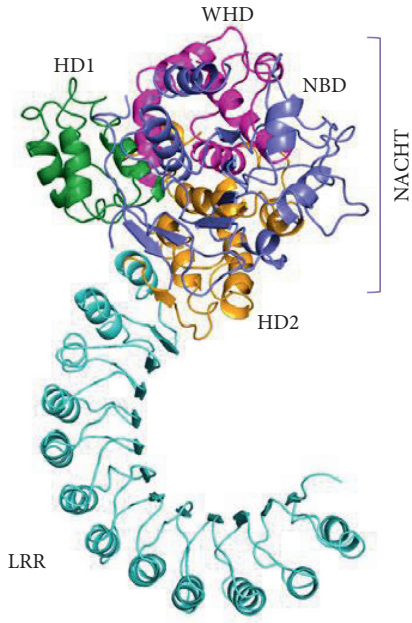

Figure 2: Cryo-EM structure overview. It is a ribbon diagram of the NLRP3 inflammasome with pyrin domains (PYD) deleted. Domains are colour coded in Figure 2. NLRP3 has an N-terminal pyrin domain, which interacts with the adaptor protein ASC via interactions between pyrin domains (PYD); a central adenosine triphosphatase (ATPase) domain known as NACHT, which comprises a nucleotide-binding domain (NBD), helical domain 1 (HD1), winged helix domain (WHD), and helical domain 2 (HD2); and a C-terminal leucine-rich repeat (LRR) domain [21].

presented that Ca^{2+} overloading of mitochondria was involved in NLRP3 activation [35]. In conclusion, Ca^{2+} mobilization may play an auxiliary role in NLRP3 inflammasome activation relatively.

2.2.2. The Second Hypothesis: Lysosomal Hypothesis. Some crystals or granular substances such as sodium urate crystals [39], calcium oxalate crystals [40], alum [41], asbestos [42], and β-amyloid [43] are phagocytized by phagocytes. The lysosome structure is damaged, and the protease in lysosomes, mainly cathepsin B, is released into the cytoplasm to activate NLRP3 [44]. This hypothesis includes two aspects: lysosome rupture and protease release. First, lysosome rupture undoubtedly plays an important role in the activation of NLRP3, but the exact mechanism is still not fully understood. Hornung et al. found that during the activation of NLRP3, the application of H^+-ATPase inhibitors inhibits the activation of NLRP3, suggesting that acidic environment was essential in NLRP3 activation [44]. Schorn et al. have proposed that lysosome lysis provides an acidic environment, and a large amount of Na^+ are released from the lysosome [45]. Increased intracellular osmotic pressure results in excessive intracellular water and decreased intracellular K^+ concentration, which may be further involved in NLRP3 activation [45]. Second, proteases released from the lysosome are essential in the activation of NLRP3. Studies have shown that inhibitors of cathepsin B significantly inhibit the activation of NLRP3, so cathepsin B is more concerned by the community [45]. It was reported that lysosomal cathepsin B was closely related to the release of IL-1β, demonstrating the importance of cathepsin B in the activation of NLRP3 [4◆6]. Similarly, how cathepsin B is involved in the activation of NLRP3 remains unclear.

2.2.3. The Third Hypothesis: ROS and Mitochondria Hypothesis. ROS pathway is often considered as a common pathway for NLRP3 inflammasome assembly since most of the activators induce ROS production and activate downstream of NLRP3 [47]. Mitochondria are the main production sites of ROS. mtROS and mtDNA produced with mitochondrial dysfunction are related to the activation of NLRP3 inflammasome [48]. Nakahira et al. found that mtROS caused by mitochondrial respiratory chain inhibition was crucial in the activation of NLRP3 induced by LPS and ATP [49]. Meanwhile, mtDNA was also released into the cytoplasm, which promoted NLRP3 activation [50]. However, some scholars have questioned whether the inhibition of NLRP3 focuses on the activation of LRP3, or the activation of NLRP3. A study has shown that the priming of NLRP3 is inhibited when antioxidants block mtROS [51].

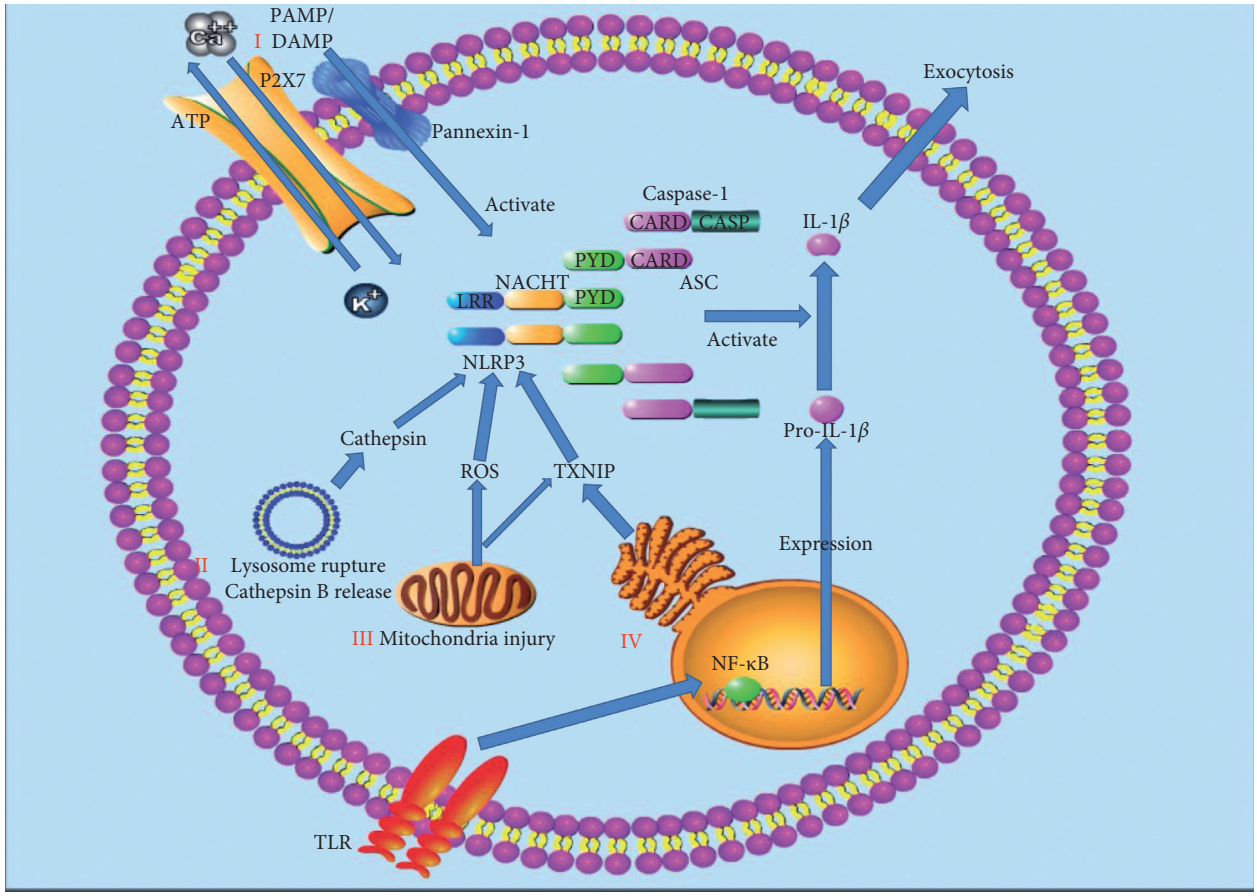

Figure 3: Activation of the NLRP3 inflammasome. Priming is initiated by the TLRs, which recognize and combine the corresponding signals to activate NF-κB at the transcriptional level, facilitating the expression of NLRP3 and various inflammatory precursors, such as IL-1β and IL-18 precursors in preparation for the next inflammatory response. NLRP3 is activated by related ligands via ionic flux (I), lysosome rupture and cathepsin B release (II), mitochondrial injury and reactive oxygen species (ROS) generation (III), and endoplasmic reticulum (ER) stress (IV). NLRP3 recruits ASC and procaspase-1 to assemble into the NLRP3 inflammasome. NLRP3 inflammasome which includes mature caspase-1 can promote the activation of proinflammatory mediators such as IL-1β and IL-18 and promote the occurrence of inflammatory response.

The direct mechanism of mtROS and NLRP3 still needs to be proved by experiments. In recent years, a study has found that thioredoxin interacting protein (TXNIP) is closely connected with the activation of NLRP3 [52]. TXNIP can be activated by ROS and then induce the generation of ROS in turn [52]. TXNIP is related to the redox of thioredoxin (TRX). When TXNIP binds to TRX, the produced ROS can make TRX oxidized [53]. TXNIP is isolated from the oxidized TRX and binds to the downstream of NLRP3 to participate in NLRP3 activation [54]. TXNIP is also involved in the indirect activation of NLRP3 through NEK7 activation [55]. During mitochondrial injury, cardiolipin in the mitochondrial membrane was also exposed [56]. Iyer et al. found that if the content of cardiolipin decreased, the activation of NLRP3 was also inhibited [57].

2.2.4. The Fourth Hypothesis: Endoplasmic Reticulum Stress Hypothesis. When stressors are applied to cells, they induce misfolded and unfolded proteins to accumulate in the endoplasmic reticulum cavity and disrupt Ca^{2+} balance, which in turn activates unfolded protein response (UPR) and apoptotic signaling pathways, which is called endoplasmic reticulum (ER) stress [58]. ER stress plays a crucial role in enhancing the resistance and adaptability of cells to injury and has an important impact on cell survival [58]. Mekahli et al. found that ER stress activated inflammasomes. Inositol-requiring enzyme 1α (IRE1α), activating transcription factor-6 (ATF6), and protein kinase R-like endoplasmic reticulum kinase (PERK) are ER stress transmembrane sensors which are involved in ROS production and NLRP3 activation [59]. Studies have proved that IRE1α and PERK also indirectly activate NLRP3 by increasing TXNIP [60]. On the other hand, the endoplasmic reticulum is an important intracellular calcium reservoir, and the entry of Ca^{2+} to the mitochondria from the endoplasmic reticulum [61] promotes ROS production, leading to NLRP3 activation.

3. NLRP3 Inflammasome and AS

3.1. Inflammation in AS. Inflammation runs through the beginning, progression, and complications of atherosclerosis [62]. Atherosclerosis is a complex, multimechanical disease.

Inflammatory mediators such as histamine, tumor necrosis factor (TNF), and interleukin-1 (IL-1) can lead to rupture and dysfunction of the vascular endothelium, thus causing a large number of inflammatory cells to gather at the injured situation and migrate into the subcutaneous tissue, inducing the inflammation [63]. The inflammation requires pattern recognition receptors (PRRs) to recognize and combine with pathogen/danger-associated molecular patterns (PAMPs/DAMPs), which can rapidly activate inflammasomes. NLRP3 inflammasome acts on the target tissues and prompts the functional changes of the target tissue to adapt to the harmful environment [64]. Duewell et al. found that cholesterol crystals promoted the secretion of saspase-1 and IL-1 by activating the NLRP3 inflammasome. The literature also reported that mice fed with high-fat diets showed increased caspase-1 expression after 3 weeks, and some papers proved that caspase-1 activation was positively correlated with lipid levels [65]. After oxidative modification, ox-LDLs have a strong effect on AS. Studies have found that ox-LDLs activate the NLRP3 inflammasome through the ROS pathway. Sheedy et al. further found that phagocytosis of ox-LDL promoted the activation of the NLRP3 inflammasome [66]. The above studies show that the NLRP3 inflammasome plays an important role in the process of AS.

Table 1: The role of NLRP3 inflammasome in AS patients.

Study type	Subjects	Effect of NLRP3 inflammasome	References
Clinical	The ascending aorta tissues of patients with CABG	The expression of NLRP3 is higher than that of patients without AS, which is positively correlated with the lesion degree of AS.	[67]
	Carotid atherosclerotic plaques in human	NLRP3, ASC, caspase-1, IL-1β, and IL-18 are highly expressed, especially in unstable plaques.	[68]
	The plaques of symptomatic AS patients	The expression of NLRP3-mRNA is higher than that of asymptomatic AS patients.	[69]
	The peripheral blood of CHD patients with ACS	The patients with ACS have higher levels of NLRP3 inflammasome.	[70]

CABG: coronary artery bypass grafting; CHD: chronic heart disease; ACS: acute coronary syndrome.

3.2. NLRP3 Inflammasome in AS Patients. In recent years, several population epidemiology studies have provided indirect evidence for the relationship between the NLRP3 inflammasome/IL-1β signaling pathway and AS, as shown in Table 1. The expression of NLRP3 in ascending aorta tissues of patients with coronary artery bypass grafting (CABG) is significantly higher than that of patients without AS, and it is positively correlated with the lesion degree of AS and risk factors of AS [67]. NLRP3 in the aorta was significantly correlated with the severity score of Gensini on the coronary artery [70]. The relevant components in the inflammasome signaling pathway of NLRP3, ASC, caspase-1, IL-1β, and IL-18 are highly expressed in human carotid atherosclerotic plaques, while expression in healthy mesenteric arteries is weak [68]. Compared with stable plaques, the levels of NLRP3, ASC, caspase-1, IL-1β, and IL-18 in unstable plaques are higher [68]. The expression of NLRP3-mRNA in the plaques of symptomatic AS patients is higher than that of asymptomatic AS patients [69]. Compared with non-CHD (nonchronic heart disease) patients, patients with CHD, especially those with acute coronary syndrome (ACS), have higher levels of mRNA and protein in peripheral blood of the NLRP3 inflammasome [70]. In ACS patients, NLRP3 is positively correlated with the degree of AS by clinical scores and lesion characteristics [70]. This study showed that the baseline concentration of NLRP3 was a promising prognostic index that effectively predicted MACE events through Grace and TIMI risk scores [70].

3.3. NLRPP3 Inflammasome in AS-Molded Animals. More and more studies have demonstrated that the NLRPP3 inflammasome is activated in atherosclerosis-molded animals and plays a crucial role in the development of atherosclerosis, as shown in Table 2. Wang et al. found that the expression of NLRP3 inflammasome was increased in ApoE$^{-/-}$ mice fed with a high-fat and high-protein diet [71]. Some studies have shown that plaque stability was increased and the development of atherosclerosis was inhibited after NLRP3 expression was silenced by the NLRP3 shRNA virus [72]. Abderrazak et al. found that NLRP3 gene knockout reduced the area of atherosclerotic plaque in the whole aorta and aortic sinus in ApoE$^{-/-}$ mice fed with a high-fat diet [73]. Arglabin, a plant-derived compound, inhibited the activity of the NLRP3 inflammasome and significantly reduced the production of IL-1α, IL-1β, and IL-18, reducing the production of proinflammatory mediators to alleviate atherosclerosis [73]. Duewell et al. found that in mice lacking the inflammasome components of NLRP3, the level of IL-18-dependent NLRP3 inflammasome in atherosclerosis caused by cholesterol crystals was reduced, which provides further clear evidence to support the importance of the NLRP3 inflammasome and cholesterol crystals in the development of atherosclerosis [65]. Shen et al. conducted relevant studies that polyunsaturated fatty acids in diet inhibited the activation of the NLRP3 inflammasome, and thus reduced the occurrence of atherosclerosis [76]. It was also reported that NLRP3 inhibitors such as MCC950 applying to ApoE$^{-/-}$ mice after four weeks showed that although the mice body quality, blood sugar, very low-density lipoprotein cholesterol (VLDL-c), low-density lipoprotein cholesterol (LDL-c), high-density lipoprotein cholesterol (HDL-c), triacylglycerol, and total cholesterols had no obvious changes, the area of atherosclerotic plaque decreased significantly, which in turn showed that MCC950 can inhibit the expression of NLRP3 for treatment of atherosclerosis [75]. These results suggest that inhibiting the expression of

Table 2: The effect of NLRP3 inflammasome inhibitors in AS-molded animals.

Study type	Subjects	Inhibitors	Effect	References
In vivo	ApoE$^{-/-}$ mice fed on a high-fat and high-protein diet	NLRP3 shRNA virus suspension (1.75×108 Tfu, 20 μL)	NLRP3 inflammasome inhibited; plaque stability increased; development of AS inhibited	[72]
	ApoE$^{-/-}$ mice fed on a high-fat diet	Arglabin	The activity of NLRP3 inflammasome inhibited; the production of proinflammatory mediators reduced	[73]
	ApoE$^{-/-}$ mice	Polyunsaturated fatty acid (vegetable oil and animal oil added into diets for additional 8–16 weeks)	The activation of NLRP3 inflammasome inhibited; the occurrence of AS reduced	[74]
	ApoE$^{-/-}$ mice	MCC950 (10 mg/kg)	The area of atherosclerotic plaque decreased significantly	[75]

the NLRP3 inflammasome reduces the development of atherosclerosis. The ox-LDLs [77], cholesterol crystals [65], and other substances induced the activation of the NLRP3 inflammasome and thus promoted the generation of atherosclerosis. Gage et al. found that compared with ApoE$^{-/-}$/caspase-1$^{-/-}$ double knockout mice, the extent of macrophage infiltration and the area of atherosclerotic plaque were significantly reduced in ApoE$^{-/-}$ mice [78]. To further clarify the exact relationship between the NLRP3 inflammasome and atherosclerosis, and the specific mechanism, we need to provide more reliable experimental evidence.

3.4. NLRP3 Inflammasome in Cells In Vitro. In the process of AS, a variety of cardiovascular damage factors can trigger the reaction of inflammatory cells such as macrophages, VECs, and VSMCs through activation of the NLRP3 inflammasome, resulting in a large release of inflammation mediators such as IL-1β and IL-18, which further induces the local and systemic inflammatory cascade, promoting the formation, vulnerability, and rupture of plaque. In recent years, the beneficial exploration of regulation of the NLRP3 inflammasome has also provided a new perspective for the treatment of AS (as shown in Figure 4).

3.4.1. NLRP3 Inflammasome and Macrophages. Macrophages play an important role in the early or late plaque formation and plaque rupture in AS [79]. In the early AS, NLRP3 derived from macrophages is involved in the anti-injury reactions of inflammation, which is beneficial to the stability of plaques [80]. Relatively, the NLRP3 inflammasome in the late AS makes excessive macrophage death and a large amount of lipid are released, which contributes to increase in lipid core and plaque vulnerability [80]. In recent years, a number of studies have proved that oxidized low-density lipoprotein (ox-LDL) and cholesterol crystals can activate the NLRP3 inflammasome and caspase-1, inducing macrophages to pyroptosis and leading to increase in the release of IL-1β and IL-18 [65]. The above factors prompt the inflammatory response of AS and reduce plaque stability. Regulation of NLRP3 in macrophages is vital in delaying the progress of AS and enhancing the stability of plaque. Silencing the *NLRP3* gene in mice inhibited the occurrence of inflammatory response, which slowed down the process of AS. Reducing the lipid core within the plaque improves plaque stability [72]. Also, specifically silencing mouse bone marrow *caspase-1/11* gene can significantly reduce the necrotic lipid core of plaque and enhance plaque stability [81]. Studies have found that MCC950, an NLRP3 inflammation inhibitor, can significantly improve the stability of mouse platelets because it inhibits the inflammatory response of macrophages [82]. MCC950 can also inhibit the transformation of macrophages into foam cells by inhibiting ox-LDL uptake and increasing cholesterol outflow, and thus the progression of AS is controlled [82].

3.4.2. NLRP3 Inflammasome and VECs. VECs comprise simple squamous epithelium, which is located in the inner layer of the vascular chamber and has a direct contact with the blood [83]. The dysfunction of VECs is an important link in the formation and development of AS [84]. Recent studies have shown that a variety of damage factors in AS can cause inflammatory response of vascular endothelial cells, and ox-LDL can promote NLRP3 inflammatory response through ROS mechanism, activate caspase-1, and induce heat shock of vascular endothelial cells [85]. Nicotine, as the most common risk, activates the NLRP3 inflammasome to promote the inflammatory response and even cell apoptosis of VECs, so it accelerates the process of AS [86]. The cytokines such as IL-1β, IL-18, *P*-selectin, intercellular adhesion molecule-l (ICAM-l), and vascular cell adhesion molecule-1 (VCAM-1) are increased in the inflammation of AS, which trigger the adhesion of the mononuclear phagocyte system and make AS deteriorate [87]. In addition, NLRP3-induced caspase-1 activation increases the expression of CXCL16 and its receptor CXCR6, which promotes the migration of T lymphocytes into subcutaneous tissues and promotes the inflammatory response of VECs [88]. It was found that hemodynamic abnormalities promoted the activation of NLRP3 and the secretion and release of IL-1β in human umbilical vein endothelial cells by activating sterol regulatory element binding protein 2 (SREBP2) [89].On the contrary, Yang et al. found that proanthocyanidin B2 inhibited the activation of the NLRP3 inflammasome in LPS-induced HUVECs by downregulating reactive oxygen species (ROS) level, and the activity of caspase-1 and IL-1β level was reduced

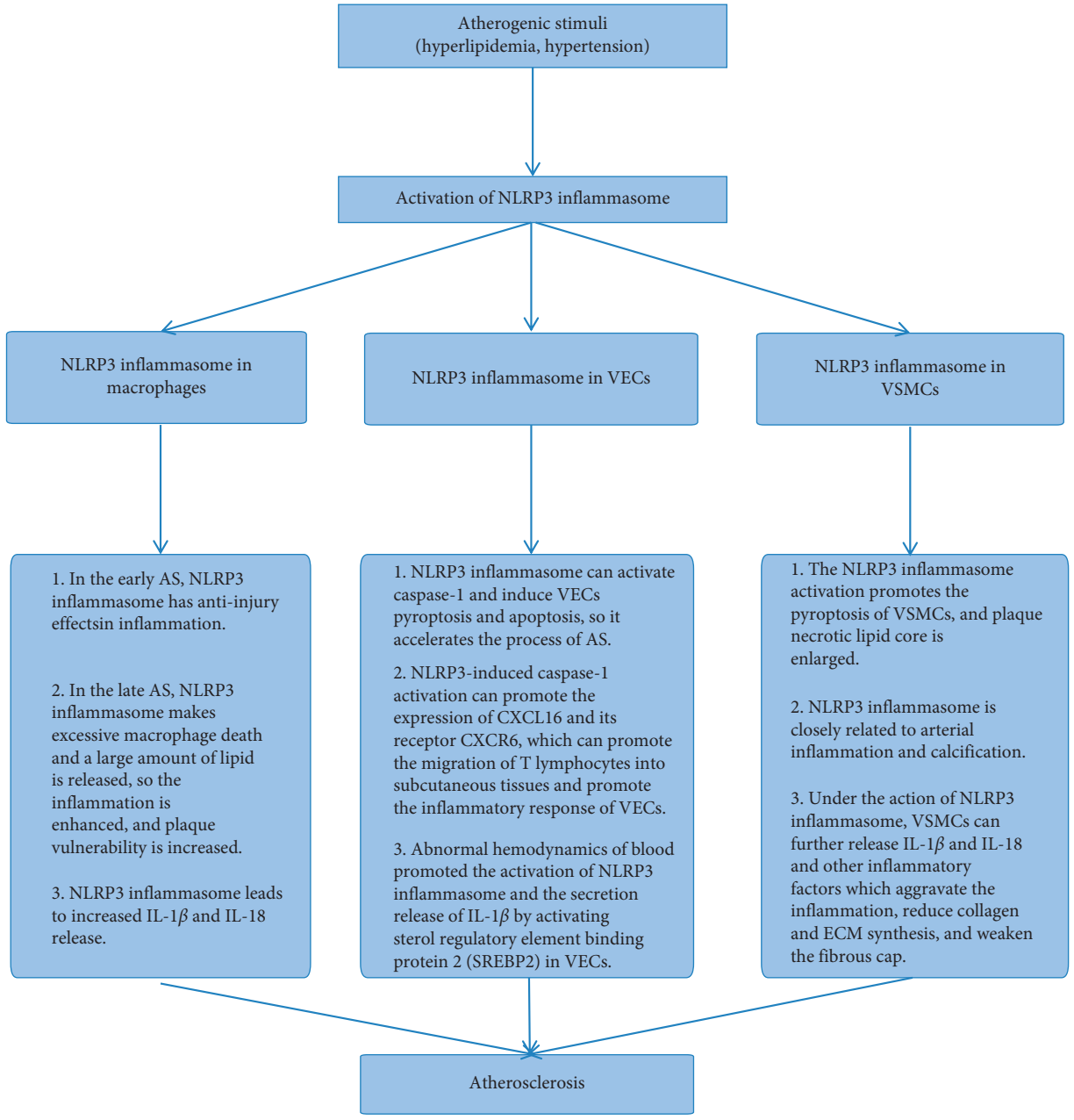

Figure 4: The role of the NLRP3 inflammasome in AS.

[90]. Mangiferin reduces ROS level in the endothelial cells to inhibit IRE1α phosphorylation and reduce ER stress [90, 91]. Thioredoxin interacting protein (TXNIP) expression was impeded, which inhibited NLRP3 activation and IL-1β release [91]. Regarding the NLRP3 signaling pathway as the target, melatonin can inhibit the pyroptosis of VECs through the MEG3/miR-223/NLRP3 signaling axis, and its substitute is expected to provide a new prospect for the control of AS [92]. Microrna-30c-5p inhibits NLRP3-induced inflammation in VECs via F0X03, which provides a further step forward for the prevention and treatment of AS [93].

3.4.3. NLRP3 Inflammasome and VSMCs. VSMCs are important cells of the middle membrane in coronary arteries [94]. In the early stage of AS, the activated VSMCs have a strong ability of proliferation and migration, which migrate from the middle membrane to the inner membrane [95]. By secreting an extracellular matrix, the fibrous cap is stabilized, which plays an important role in preventing plaque rupture. However, in the late stage of AS due to a large amount of lipid accumulation in the plaque, cholesterol activates a variety of proinflammatory genes in vascular smooth muscle cells, leading to the activation of NLRP3 inflammatory response in vascular smooth muscle cells, exacerbating the inflammatory response, and eventually resulting in vascular smooth muscle cells and plaque necrotic lipid nuclear heat sags [95]. Studies have found that calcium crystals make the NLRP3 inflammasome activated. It was reported that intracellular mRNA levels of NLRP3, ASC, and caspase-1 were

increased when β-glycerophosphate (β-GP) induced the primary rat aorta VSMCs to get crystallization on calcium. The level of IL-1β and VSMCs calcification was inhibited after the NLRP3 was silenced. At the same time, in the calcified tissue of the human artery, the levels of mRNA were significantly upregulated, and caspase-1 activity was increased [96]. It is suggested that the NLRP3 inflammasome is closely related to arterial inflammation and calcification. In a study by Usui et al., the *a*-smooth muscle actin (α-SMA), as a marker of VSMCs, was detected by the immunohistochemical method, and compared with ApoE$^{-/-}$ mice, the number of VSMCs at the inner membrane decreased significantly in ApoE$^{-/-}$/caspase-1$^{-/-}$ mice plaques [97]. Absent in melanoma- (AIM2-) related pattern recognition receptor can activate caspase-1 through the NLRP3 pathway, and then it mediates the inflammatory response of VSMCs by cutting GSDMD [98]. Under the action of the NLRP3 inflammasome, VSMCs also further released IL-1β and IL-18 and other inflammatory factors, which aggravated the inflammation, reduced collagen and ECM synthesis, and weakened the fibrous cap. Therefore, increased vulnerability of plaque lead to plaque erosion and rupture.

4. Therapy Targeting NLRP3 for AS

Because inflammatory response and NLRP3 inflammasome play an important role in the development of atherosclerosis, the NLRP3 inflammasome as the therapeutic target has become a hot topic in the research of atherosclerotic drugs. Emerging evidence suggests that the NLRP3 inflammasome could be considered as the potential therapeutic target for atherosclerosis, as shown in Table 3.

4.1. Natural Medicine and the Treatment for AS. Artemisinin is a natural peroxide lactone compound extracted from the plant *Artemisia annua* which showed vascular protection function. Artemisinin (50 or 100 mg/kg) can effectively improve formation and proliferation of foam cells and promote fibrosis in the intima of the aorta. It was reported that artemisinin inhibited inflammatory responses through the AMPK/NF-κB-NLRP3 pathway in macrophages [99].

Pretreating with rosmarinic acid (RA), the volume of nicotine-induced C-reactive protein (CRP) [86] will be dropped in VSMCs. In addition. RA also inhibited the activation of pyrin domains in the NLRP3 inflammasome and reduced the production of ROS after nicotine was involved in VSMCs. *In vivo* experiments suggested that RA played a protective role in nicotine-induced atherosclerosis *via* inhibiting the axis of ROS-NLRP3-CRP, and therefore RA was a potentially effective treatment for atherosclerosis, especially in smokers [100].

Curcumin significantly decreased the expression of NLRP3, caspase-1, and IL-1β in phorbol 12-myristate 13-acetate-(PMA-) induced macrophages. Curcumin is also partially involved in the phosphorylation of TLR4, MyD88, and IκB-α, as well as activating NF-κB. Therefore, curcumin inhibited NLRP3 inflammasome expression in PMA-induced macrophage by inhibiting TLR4/MyD88, NF-κB, and P2X7R [101].

Atherosclerosis is a chronic inflammatory disease mainly caused by the accumulation of cholesterol and the formation of cholesterol crystals (CCs) in the subcutaneous tissue. These CCs promote the development of the disease by activating the NLRP3 inflammasome and triggering a complex inflammatory response. Recently, many studies focused on whether ursodeoxycholic acid (UDCA) affected the formation of vascular CCs. It was reported that UDCA induced intracellular CC dissolution in macrophages, reducing the secretion of IL-1β. In summary, most of the data suggested that UDCA reduced CCs and attenuated NLRP3-dependent inflammation by increasing cholesterol solubility in mice [102].

It was observed that berberine suppressed IL-1β secretion in macrophages. In addition, Jiang et al. demonstrated that berberine reduced the activation of the NLRP3 inflammasome via the ROS-dependent pathway, which provided the evidence for the hypothesis that berberine alleviated NLRP3 inflammasome activation and reduced IL-β secretion from macrophages, showing an important therapeutic target in atherosclerosis therapy [103].

Dihydromyricetin (DHM) is a kind of natural flavonoids with antioxidant, anti-inflammatory, and other biological activities. In a study, palmitic acid (PA) treatment resulted in caspase-1 activation, lactate dehydrogenase (LDH) release, and positive-staining of propidium iodide in HUVECs. PA can promote the maturation and release of proinflammatory cytokines especially IL-1β by elevation of intracellular ROS and mtROS. In addition, transfection with NLRP3 inhibitors or treatment with NLRP3 siRNA effectively inhibited PA-induced pyroptosis, while pretreatment with total ROS or mtROS scavenger attenuated NLRP3 inflammasome activation and subsequent pyroptosis. DHM inhibited PA-induced high-temperature cell death by increasing cell viability and reducing caspase-1 and IL-1β release to improve cell membrane integrity. This study showed that DHM pretreatment significantly reduced intracellular ROS and mtROS levels and activated the Nrf2 signaling pathway [104]. In summary, these results suggested that the Nrf2 signaling pathway was obviously partially involved in the DHM-mediated improvement of PA-induced vascular events, suggesting the potential medicinal value of DHM against immune/inflammation-related diseases such as atherosclerosis.

Trimethylamine N-oxide (TMAO) is associated with endothelial dysfunction in atherosclerosis, a cardiovascular disease induced by vascular inflammation. TMAO induces scavenger receptors, adhesion molecules, and other genes associated with atherosclerosis in VECs. Apigenin is rich in celery and parsley, which prevents endothelial cells from artery injury [105]. Apigenin can reverse the transcription of LOX-1, SREC, SR-PSOX, NLRP3, TXNIP, VCAM-1, ICAM-1, and MCP-1, as well as the translation of LOX-1, adhesion molecule ICAM-1, and NLRP3 inflammasome. Apigenin also inhibited leukocyte adhesion and acetylated LDL uptake [105].

4.2. Clinical Medicine and the Treatment for AS. To evaluate the activation of inflammasomes in monocytes of patients

Table 3: The therapy targeting NLRP3 inflammasome for AS.

Therapy type	Medicine	Chemical structure	Effects and mechanisms	References
Natural medicine	Artemisinin (50, 100 mg/kg)	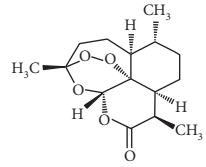	Vascular protection: the formation and proliferation of foam cells improved; the fibrosis in the intima of aorta promoted Inflammation inhibition: targeting the AMPK/NF-κB-NLRP3 pathway	[99]
	Rosmarinic acid (100 μM)	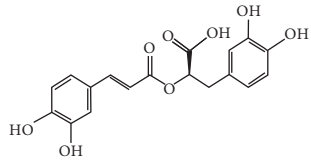	Playing a protective role in nicotine-induced AS via inhibiting the axis of ROS-NLRP3-CRP	[100]
	Curcumin (0–100 μM)	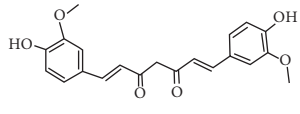	Inhibiting NLRP3 inflammasome in PMA-induced macrophage by inhibiting TLR4/MyD88, NF-κB, and P2X2R	[101]
	UDCA (20 μg/ml)	—	Attenuating NLRP3-dependent inflammation: reducing CCs; increasing cholesterol solubility	[102]
	Berberine (75 μM)	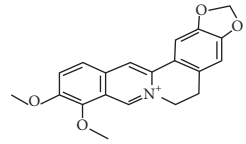	Alleviating NLRP3 inflammasome activation and reducing IL-1β secretion	[103]
	DHM (0.1, 0.5, and 1 μM)	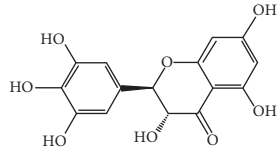	Antioxidant and anti-inflammatory activities: ROS reduced; the release of caspase-1 and IL-1β reduced	[104]
	Apigenin (50 μM)	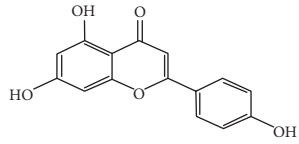	Endothelium protection: reversing the expression of adhesion molecule ICAM-1 and NLRP3 inflammasome	[105]

Table 3: Continued.

Therapy type	Medicine	Chemical structure	Effects and mechanisms	References
Clinical medicine	Colchicine (1 mg followed by 0.5 mg 1 hour later)	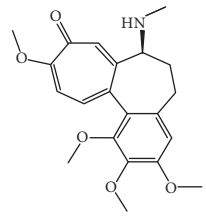	The levels of caspase-1 and IL-1β reduced	[106, 107]
	Statins (atovastatin 0–40 μM)	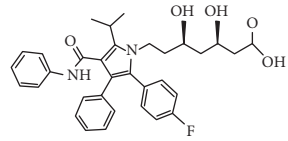	Inhibiting cholesterol synthesis; anti-inflammatory function	[108, 109]
	Dapagliflozin (1.0 mg/kg/d)	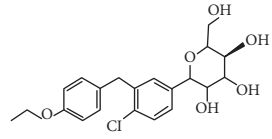	Inhibiting IL-1β secretion through the ROS-NLRP3-caspase-1 pathway	[110]
	Metformin (300 mg/kg/d, drinking water)	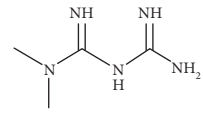	Anti-inflammatory function: reducing NLRP3 expression; inhibiting NLRP3 activation	[111]
Others	Dietary fiber	—	Antiatherogenic effects; anti-inflammatory effects	[112]
	Dietary PUFAs	—	Activating macrophage autophagy; inhibiting the activation of NLRP3 inflammasome	[112]
	Melatonin (20–2000 μM)	—	Anti-inflammatory effects; preventing apoptosis of endothelial cells; attenuating NLRP3 inflammasome activation	[74]

AMPK: adenosine monophosphate-activated protein kinase; CRP: C-reactive protein; PMA: phorbol 12-myristate 13-acetate; UDCA: ursodeoxycholic acid; CCs: cholesterol crystals; DHM: dihydromyricetin; TMAO: trimethylamine N-oxide; PUFAs: dietary polyunsaturated fatty acids.

with acute coronary syndrome (ACS) and the short-term oral administration of colchicine [113] (a recognized anti-inflammatory drug shown in clinical studies to have a protective effect on the heart), ACS patients ($n = 21$) were randomly divided into the oral colchicine group and the untreated group and compared with the untreated healthy control group ($n = 9$). Treatment for ACS with colchicine significantly reduced the levels of caspase-1 and IL-1β in the cells [106, 107].

Statins are very important in prevention and treatment for cardiovascular disease by inhibiting cholesterol synthesis. However, the beneficial effect of statins in cardiovascular disease may also be due to their role as anti-inflammatory mediators. Atorvastatin, a 3-hydroxy-3-methyglutaryl coenzyme A (HMG-CoA) inhibitor, significantly reduced the expression of NLRP3, caspase-1, and IL-1β in PMA-induced THP-1 cells. In addition, the NF-κB inhibitor decreased the expression of inflammatory mediators in inflammatory cells. It was suggested that the activation of the NF-κB pathway was involved in the regulation of the NLRP3 inflammasome [108, 109]. Therefore, atorvastatin plays an anti-inflammatory role by inhibiting the PMA-induced THP-1 monocyte via the TLR4/MyD88/NF-KB pathway. *In vitro* and *in vivo* treatment with simvastatin resulted in significantly lower expression levels in response to stimulation with CCs. Simvastatin inhibited expression of IL-1β, peripheral blood mononuclear cells (PBMCs), and CCs and then had protective effect on patients with cardiovascular disease [114].

Glucose cotransporter 2 (SGLT2) inhibitor has a good effect on glucose and fat metabolism, and it partially reverses the formation of atherosclerosis through inhibiting the infiltration of macrophages and enhancing the stability of the plaques. Dapagliflozin may have therapeutic abilities for diabetic atherosclerosis induced by a high-fat diet, and these benefits may depend on macrophages inhibiting IL-1β secretion through the ROS-NLRP3-caspase-1 pathway [110].

Metformin promotes the secretion of adenosine monophosphate-activated protein kinase (AMPK) and protein phosphatase 2A (PP2A). Data showed that metformin reduced the expression of NLRP3 and inhibited the activation of the NLRP3 inflammasome in ox-LDL-stimulated macrophages through increasing the expression of AMPK and PP2A [111]. Other *in vitro* experiments suggested that high glucose induced the accumulation of ROS and activated the NLRP3 inflammasome, which was significantly inhibited after treatment with metformin or the antioxidant N-acetyl-l-cysteine. In addition, the inhibitor complex C of AMPK hindered the anti-inflammatory effect of metformin, suggesting that metformin inhibited the high-glucose-induced NLRP3 inflammasome through AMPK activation. Glucose decreased the expression of TRX and increased the expression of TXNIP, in which metformin was also reversed. Metformin also inhibited the activation of the NLRP3 inflammasome in ApoE$^{-/-}$ mice and inhibited atherosclerosis in diabetes [115].

4.3. Other Treatments for AS. Via increasing cholesterol excretion, the dietary fiber (DF) to reduce the risk of atherosclerosis may occur through many mechanisms. Although macrophages are essential for lipid clearance, excessive uptake of cholesterol crystals (CCs) by these cells still induces the activation of the NLRP3 inflammasome and formation of foam cells. Therefore, the study investigated whether the water-soluble DF of chayote regulated the CCs in macrophage-like THP-1 cells. The health benefits of dietary fiber may exceed its physical properties for the gastrointestinal tract. Studies have evaluated the antiatherogenic effects of oat fiber and wheat bran fiber and explored their potential anti-inflammatory mechanisms. Animal experiments, pathology, and biological analysis have shown that cereal fiber can reduce the inflammatory response and atherosclerosis in ApoE$^{-/-}$mice. These effects are evident in oat fiber, which may be mediated by specific inhibition of the NLRP3 inflammasome pathway [112].

Dietary polyunsaturated fatty acids (PUFAs) reduce macrophage inflammation and delay the progress of atherosclerosis, but the accurate mechanisms are poorly understood. Through animal experiments, it was concluded that dietary PUFAs could reduce atherosclerosis by activating macrophage autophagy and inhibiting the activation of the NLRP3 inflammasome [112].

Melatonin has been reported to have a number of anti-inflammatory properties, shown to be effective against AS. Melatonin decreased expression of genes associated with the aortic endothelium, including NLRP3, ASC, cleaved caspase-1, NF-κB/GSDMD, GSDMD-N, and IL-1β. Through the MEG3/miR-223/NLRP3 axis [92], it can prevent apoptosis of endothelial cells in atherosclerosis. Current studies have shown that melatonin prevented the progression of atherosclerosis by inducing mitophagy and attenuating the activation of the NLRP3 inflammasome via the Sirt3/FOXO3a/Parkin signaling pathway [74].

5. Conclusion

"Inflammation theory" plays an important role in the development of atherosclerosis. NLRP3 inflammasome is pivotal in the stability of plaques owing to the ion flow, lysosome rupture, and ROS and endoplasmic reticulum stress mechanism, and then the NLRP3 inflammasome activation will produce mature inflammatory mediators such as IL-1β and caspase-1 which participate in the development of atherosclerosis. Most studies have proved that targeting at the initiation and activation of the NLRP3 inflammasome can effectively delay the process of atherosclerosis, and thus reduce the hospitalization rate of patients. However, clinical data are insufficient and some mechanisms about how the NLRP3 inflammasome participates in AS has not been explained clearly. Using drugs targeting at the NLRP3 inflammasome to treat atherosclerosis is promising, but it also needs further pharmacological studies to verify the efficacy and further experimental epidemiological studies to ensure the safety. In addition, to make the drugs widely used clinically, evidence-based medicine play an indispensable role.

Disclosure

Yang Liu and Chao Li are the co-first authors.

Conflicts of Interest

The authors declare no conflicts of interest, financial or otherwise.

Authors' Contributions

Yang Liu and Chao Li contributed equally to this work.

Acknowledgments

This work was supported by the National Nature Science Foundation of China (grant no. 81774242), Shandong Provincial Nature Science Foundation of China (grant no. ZR2018ZC1157), and special funding for Shandong Taishan Scholar Project (no. ts201712042).

References

[1] S. Taleb, "Inflammation in atherosclerosis," *Archives of Cardiovascular Diseases*, vol. 109, no. 12, pp. 708–715, 2016.

[2] I. Tabas, K. J. Williams, and J. Borén, "Subendothelial lipoprotein retention as the initiating process in atherosclerosis," *Circulation*, vol. 116, no. 16, pp. 1832–1844, 2007.

[3] A. C. Li and C. K. Glass, "The macrophage foam cell as a target for therapeutic intervention," *Nature Medicine*, vol. 8, no. 11, pp. 1235–1242, 2002.

[4] I. Tabas, "Macrophage death and defective inflammation resolution in atherosclerosis," *Nature Reviews Immunology*, vol. 10, no. 1, pp. 36–46, 2010.

[5] L. Fraemohs, E. Dejana, and C. Weber, "the role of junctional adhesion molecules in vascular inflammation," *Nature Reviews Immunology*, vol. 7, no. 6, pp. 467–477, 2007.

[6] R. Ross, "Atherosclerosis—an inflammatory disease," *New England Journal of Medicine*, vol. 340, no. 2, pp. 115–126, 1999.

[7] M. A. Birrell and S. Eltom, "The role of the NLRP3 Inflammasome in the pathogenesis of airway disease," *Pharmacology & Therapeutics*, vol. 130, no. 3, pp. 364–370, 2011.

[8] B. Singh, S. Arora, and V. Khanna, "Association of severity of COPD with IgE and interleukin-1 beta," *Monaldi Archives for Chest Disease = Archivio Monaldi per le Malattie del Torace*, vol. 73, no. 73, pp. 86-87, 2010.

[9] K. Schroder, R. Zhou, and J. Tschopp, "The NLRP3 inflammasome: a sensor for metabolic danger?" *Science*, vol. 327, no. 5963, pp. 296–300, 2010.

[10] F. A. Amaral, V. V. Costa, L. D. Tavares et al., "NLRP3 inflammasome-mediated neutrophil recruitment and hypernociception depend on leukotriene B4 in a murine model of gout," *Arthritis & Rheumatism*, vol. 64, no. 2, pp. 474–484, 2012.

[11] A.-C. Villani, M. Lemire, G. Fortin et al., "Common variants in the NLRP3 region contribute to Crohn's disease susceptibility," *Nature Genetics*, vol. 41, no. 1, pp. 71–76, 2009.

[12] B. Butts, R. A. Gary, S. B. Dunbar, and J. Butler, "The importance of NLRP3 inflammasome in heart failure," *Journal of Cardiac Failure*, vol. 21, no. 7, pp. 586–593, 2015.

[13] M. Takahashi, "NLRP3 inflammasome as a novel player in myocardial infarction," *International Heart Journal*, vol. 55, no. 2, pp. 101–105, 2014.

[14] D. Liu, X. Zeng, X. Li, J. L. Mehta, and X. Wang, "Role of NLRP3 inflammasome in the pathogenesis of cardiovascular diseases," *Basic Research in Cardiology*, vol. 113, no. 1, 2018.

[15] P. Libby, "Interleukin-1 beta as a target for atherosclerosis therapy," *Journal of the American College of Cardiology*, vol. 70, no. 18, pp. 2278–2289, 20.

[16] A. G. Mauro, A. Bonaventura, E. Mezzaroma, M. Quader, and S. Toldo, "NLRP3 inflammasome in acute myocardial infarction," *Journal of Cardiovascular Pharmacology*, vol. 74, no. 3, pp. 175–187, 2019.

[17] W. L. Vande, I. B. Stowe, P. Sacha et al., "MCC950/CRID3 potently targets the NACHT domain of wild-type NLRP3 but not disease-associated mutants for inflammasome inhibition," *PLoS Biology*, vol. 17, no. 9, Article ID e3000354, 2019.

[18] X. Liu, T. Pichulik, O.-O. Wolz et al., "Human NACHT, LRR, and PYD domain-containing protein 3 (NLRP3) inflammasome activity is regulated by and potentially targetable through Bruton tyrosine kinase," *Journal of Allergy and Clinical Immunology*, vol. 140, no. 4, pp. 1054–1067, 2017.

[19] Y. K. Kim, J.-S. Shin, and M. H. Nahm, "NOD-like receptors in infection, immunity, and diseases," *Yonsei Medical Journal*, vol. 57, no. 1, pp. 5–14, 2016.

[20] T. Pasqua, P. Pagliaro, C. Rocca, T. Angelone, and C. Penna, "Role of NLRP-3 inflammasome in hypertension: a potential therapeutic target," *Current Pharmaceutical Biotechnology*, vol. 19, no. 9, pp. 708–714, 2018.

[21] H. Sharif, L. Wang, W. L. Wang et al., "Structural mechanism for NEK7-licensed activation of NLRP3 inflammasome," *Nature*, vol. 570, no. 7761, pp. 338–343, 2019.

[22] Z. Hoseini, F. Sepahvand, B. Rashidi, A. Sahebkar, A. Masoudifar, and H. Mirzaei, "NLRP3 inflammasome: its regulation and involvement in atherosclerosis," *Journal of Cellular Physiology*, vol. 233, no. 3, pp. 2116–2132, 2018.

[23] J. Maharana, A. Vats, S. Gautam et al., "POP1 might be recruiting its type-Ia interface for NLRP3-mediated PYD-PYD interaction: insights from MD simulation," *Journal of Molecular Recognition*, vol. 30, no. 9, 2017.

[24] E. Eren and N. Özören, "The NLRP3 inflammasome: a new player in neurological diseases," *Turkish Journal of Biology*, vol. 43, no. 6, pp. 349–359, 2019.

[25] F. G. Bauernfeind, G. Horvath, A. Stutz et al., "Cutting edge: NF-κB activating pattern recognition and cytokine receptors license NLRP3 inflammasome activation by regulating NLRP3 expression," *The Journal of Immunology*, vol. 183, no. 2, pp. 787–791, 2009.

[26] L. Franchi, T. Eigenbrod, and G. Núñez, "Cutting edge: TNF-α mediates sensitization to ATP and silica via the NLRP3 inflammasome in the absence of microbial stimulation," *The Journal of Immunology*, vol. 183, no. 2, pp. 792–796, 2009.

[27] R. Gupta, S. Ghosh, B. Monks et al., "RNA and β-hemolysin of group BStreptococcusInduce interleukin-1β (IL-1β) by activating NLRP3 inflammasomes in mouse macrophages," *Journal of Biological Chemistry*, vol. 289, no. 20, pp. 13701–13705, 2014.

[28] J. J. Martinez-Garcia, H. Martinez-Banaclocha, D. Angosto-Bazarra et al., "P2X7 receptor induces mitochondrial failure in monocytes and compromises NLRP3 inflammasome activation during sepsis," *Nature Communications*, vol. 10, no. 1, p. 2711, 2019.

[29] D. Perregaux and C. A. Gabel, "Interleukin-1 beta maturation and release in response to ATP and nigericin. Evidence that potassium depletion mediated by these agents is a necessary and common feature of their activity," *Journal of Biological Chemistry*, vol. 269, no. 21, pp. 15195–15203, 1994.

[30] J. M. Kahlenberg and G. R. Dubyak, "Mechanisms of caspase-1 activation by P2X7 receptor-mediated K^+ release," *American Journal of Physiology-Cell Physiology*, vol. 286, no. 5, pp. C1100–C1108, 2004.

[31] R. Muñoz-Planillo, P. Kuffa, G. Martínez-Colón, B. L. Smith, T. M. Rajendiran, and G. Núñez, "K^+ efflux is the common trigger of NLRP3 inflammasome activation by bacterial toxins and particulate matter," *Immunity*, vol. 38, no. 6, pp. 1142–1153, 2013.

[32] V. Pétrilli, S. Papin, C. Dostert, A. Mayor, F. Martinon, and J. Tschopp, "Activation of the NALP3 inflammasome is triggered by low intracellular potassium concentration," *Cell Death & Differentiation*, vol. 14, no. 9, pp. 1583–1589, 2007.

[33] E. Carafoli and J. Krebs, "Why calcium? How calcium became the best communicator," *Journal of Biological Chemistry*, vol. 291, no. 40, pp. 20849–20857, 2016.

[34] J. Chu, L. M. Thomas, S. C. Watkins, L. Franchi, G. Núñez, and R. D. Salter, "Cholesterol-dependent cytolysins induce rapid release of mature IL-1β from murine macrophages in a NLRP3 inflammasome and cathepsin B-dependent manner," *Journal of Leukocyte Biology*, vol. 86, no. 5, pp. 1227–1238, 2009.

[35] T. Murakami, J. Ockinger, J. Yu et al., "Critical role for calcium mobilization in activation of the NLRP3 inflammasome," *Proceedings of the National Academy of Sciences*, vol. 109, no. 28, pp. 11282–11287, 2012.

[36] A. G. Baldwin, J. Rivers-Auty, M. J. D. Daniels et al., "Boron-based inhibitors of the NLRP3 inflammasome," *Cell Chemical Biology*, vol. 24, no. 11, pp. 1321–1335, 2017.

[37] Z. Zhong, Y. Zhai, S. Liang et al., "TRPM2 links oxidative stress to NLRP3 inflammasome activation," *Nature Communications*, vol. 4, p. 1611, 2013.

[38] K. Weber and J. D. Schilling, "Lysosomes integrate metabolic-inflammatory cross-talk in primary macrophage inflammasome activation," *Journal of Biological Chemistry*, vol. 289, no. 13, pp. 9158–9171, 2014.

[39] F. Martinon, V. Pétrilli, A. Mayor, A. Tardivel, and J. Tschopp, "Gout-associated uric acid crystals activate the NALP3 inflammasome," *Nature*, vol. 440, no. 7081, pp. 237–241, 2006.

[40] S. R. Mulay, O. P. Kulkarni, K. V. Rupanagudi et al., "Calcium oxalate crystals induce renal inflammation by NLRP3-mediated IL-1β secretion," *Journal of Clinical Investigation*, vol. 123, no. 1, pp. 236–246, 2013.

[41] M. Kool, V. Pétrilli, T. De Smedt et al., "Cutting edge: alum adjuvant stimulates inflammatory dendritic cells through activation of the NALP3 inflammasome," *The Journal of Immunology*, vol. 181, no. 6, pp. 3755–3759, 2008.

[42] R. A. Pietrofesa, P. Woodruff, W. T. Hwang et al., "The synthetic lignan secoisolariciresinol diglucoside prevents asbestos-induced NLRP3 inflammasome activation in murine macrophages," *Oxidative Medicine and Cellular Longevity*, vol. 2017, Article ID 7395238, 14 pages, 2017.

[43] A. Halle, V. Hornung, G. C. Petzold et al., "The NALP3 inflammasome is involved in the innate immune response to amyloid-β," *Nature Immunology*, vol. 9, no. 8, pp. 857–865, 2008.

[44] V. Hornung, F. Bauernfeind, A. Halle et al., "Silica crystals and aluminum salts activate the NALP3 inflammasome through phagosomal destabilization," *Nature Immunology*, vol. 9, no. 8, pp. 847–856, 2008.

[45] C. Schorn, B. Frey, K. Lauber et al., "Sodium overload and water influx activate the NALP3 inflammasome," *Journal of Biological Chemistry*, vol. 286, no. 1, pp. 35–41, 2011.

[46] D. Lian, J. Lai, Y. Wu et al., "Cathepsin B-mediated NLRP3 inflammasome formation and activation in angiotensin II-induced hypertensive mice: role of macrophage digestion dysfunction," *Cellular Physiology and Biochemistry*, vol. 50, no. 4, pp. 1585–1600, 2018.

[47] L. Minutoli, D. Puzzolo, M. Rinaldi et al., "ROS-mediated NLRP3 inflammasome activation in brain, heart, kidney, and testis ischemia/reperfusion injury," *Oxidative Medicine and Cellular Longevity*, vol. 2016, Article ID 2183026, 10 pages, 2016.

[48] Q. Liu, D. Zhang, D. Hu, X. Zhou, and Y. Zhou, "The role of mitochondria in NLRP3 inflammasome activation," *Molecular Immunology*, vol. 103, pp. 115–124, 2018.

[49] K. Nakahira, J. A. Haspel, V. A. K. Rathinam et al., "Autophagy proteins regulate innate immune responses by inhibiting the release of mitochondrial DNA mediated by the NALP3 inflammasome," *Nature Immunology*, vol. 12, no. 3, pp. 222–230, 2011.

[50] K. Shimada, T. R. Crother, J. Karlin et al., "Oxidized mitochondrial DNA activates the NLRP3 inflammasome during apoptosis," *Immunity*, vol. 36, no. 3, pp. 401–414, 2012.

[51] F. Bauernfeind, E. Bartok, A. Rieger, L. Franchi, G. Núñez, and V. Hornung, "Cutting edge: reactive oxygen species inhibitors block priming, but not activation, of the NLRP3 inflammasome," *The Journal of Immunology*, vol. 187, no. 2, pp. 613–617, 2011.

[52] Y. Han, X. Xu, C. Tang et al., "Reactive oxygen species promote tubular injury in diabetic nephropathy: the role of the mitochondrial ros-txnip-nlrp3 biological axis," *Redox Biology*, vol. 16, pp. 32–46, 2018.

[53] A. Harijith, D. L. Ebenezer, and V. Natarajan, "Reactive oxygen species at the crossroads of inflammasome and inflammation," *Frontiers in Physiology*, vol. 5, p. 352, 2014.

[54] R. Zhou, A. Tardivel, B. Thorens, I. Choi, and J. Tschopp, "Thioredoxin-interacting protein links oxidative stress to inflammasome activation," *Nature Immunology*, vol. 11, no. 2, pp. 136–140, 2010.

[55] Y. He, M. Y. Zeng, D. Yang, B. Motro, and G. Núñez, "NEK7 is an essential mediator of NLRP3 activation downstream of potassium efflux," *Nature*, vol. 530, no. 7590, pp. 354–357, 2016.

[56] L. A. O'Neill, "Cardiolipin and the Nlrp3 inflammasome," *Cell Metabolism*, vol. 18, no. 18, pp. 610–612, 2013.

[57] S. S. Iyer, Q. He, J. R. Janczy et al., "Mitochondrial cardiolipin is required for Nlrp3 inflammasome activation," *Immunity*, vol. 39, no. 2, pp. 311–323, 2013.

[58] H.-O. Rashid, R. K. Yadav, H.-R. Kim, and H.-J. Chae, "ER stress: autophagy induction, inhibition and selection," *Autophagy*, vol. 11, no. 11, pp. 1956–1977, 2015.

[59] D. Mekahli, G. Bultynck, J. B. Parys, H. De Smedt, and L. Missiaen, "Endoplasmic-reticulum calcium depletion and disease," *Cold Spring Harbor Perspectives in Biology*, vol. 3, no. 6, 2011.

[60] X. Chen, X. Guo, Q. Ge, Y. Zhao, H. Mu, and J. Zhang, "ER stress activates the NLRP3 inflammasome: a novel mechanism of atherosclerosis," *Oxidative Medicine and Cellular Longevity*, vol. 2019, Article ID 3462530, 18 pages, 2019.

[61] M. Okada, A. Matsuzawa, A. Yoshimura, and H. Ichijo, "The lysosome rupture-activated TAK1-JNK pathway regulates NLRP3 inflammasome activation," *Journal of Biological Chemistry*, vol. 289, no. 47, pp. 32926–32936, 2014.

[62] K. Feldmann, M. Grandoch, C. Kohlmorgen et al., "Decreased M1 macrophage polarization in dabigatran-treated Ldlr-deficient mice: implications for atherosclerosis and adipose tissue inflammation," *Atherosclerosis*, vol. 287, pp. 81–88, 2019.

[63] T.-T. Li, Z.-B. Wang, Y. Li, F. Cao, B.-Y. Yang, and H.-X. Kuang, "The mechanisms of traditional Chinese medicine underlying the prevention and treatment of atherosclerosis," *Chinese Journal of Natural Medicines*, vol. 17, no. 6, pp. 401–412, 2019.

[64] F. Anzai, S. Watanabe, H. Kimura et al., "Crucial role of NLRP3 inflammasome in a murine model of Kawasaki disease," *Journal of Molecular and Cellular Cardiology*, vol. 138, pp. 185–196, 2020.

[65] P. Duewell, H. Kono, K. J. Rayner et al., "NLRP3 inflammasomes are required for atherogenesis and activated by cholesterol crystals," *Nature*, vol. 464, no. 7293, pp. 1357–1361, 2010.

[66] F. J. Sheedy, A. Grebe, K. J. Rayner et al., "CD36 coordinates NLRP3 inflammasome activation by facilitating intracellular nucleation of soluble ligands into particulate ligands in sterile inflammation," *Nature Immunology*, vol. 14, no. 8, pp. 812–820, 2013.

[67] F. Zheng, S. Xing, Z. Gong, and Q. Xing, "NLRP3 inflammasomes show high expression in aorta of patients with atherosclerosis," *Heart, Lung and Circulation*, vol. 22, no. 9, pp. 746–750, 2013.

[68] X. Shi, W.-L. Xie, W.-W. Kong, D. Chen, and P. Qu, "Expression of the NLRP3 inflammasome in carotid atherosclerosis," *Journal of Stroke and Cerebrovascular Diseases*, vol. 24, no. 11, pp. 2455–2466, 2015.

[69] V. G. Paramel, L. Folkersen, R. J. Strawbridge et al., "NLRP3 inflammasome expression and activation in human atherosclerosis," *Journal of the American Heart Association*, vol. 5, no. 5, 2016.

[70] A. Afrasyab, P. Qu, Y. Zhao et al., "Correlation of NLRP3 with severity and prognosis of coronary atherosclerosis in acute coronary syndrome patients," *Heart and Vessels*, vol. 31, no. 8, pp. 1218–1229, 2016.

[71] R. Wang, Y. Wang, N. Mu et al., "Activation of NLRP3 inflammasomes contributes to hyperhomocysteinemia-aggravated inflammation and atherosclerosis in ApoE^{-} deficient mice," *Laboratory Investigation*, vol. 97, no. 8, pp. 922–934, 2017.

[72] F. Zheng, S. Xing, Z. Gong, W. Mu, and Q. Xing, "Silence of NLRP3 suppresses atherosclerosis and stabilizes plaques in apolipoprotein E-deficient mice," *Mediators of Inflammation*, vol. 2014, Article ID 507208, 8 pages, 2014.

[73] A. Abderrazak, D. Couchie, D. F. Darweesh Mahmood et al., "Response to letter regarding article, "Anti-inflammatory and antiatherogenic effects of the inflammasome NLRP3 inhibitor arglabin in ApoE2.Ki mice fed a high-fat diet"" *Circulation*, vol. 132, no. 21, pp. e250-1, 2015.

[74] S. Ma, J. Chen, J. Feng et al., "Melatonin ameliorates the progression of atherosclerosis via mitophagy activation and NLRP3 inflammasome inhibition," *Oxidative Medicine and Cellular Longevity*, vol. 2018, Article ID 9286458, 12 pages, 2018.

[75] T. van der Heijden, E. Kritikou, W. Venema et al., "NLRP3 inflammasome inhibition by MCC950 reduces atherosclerotic lesion development in apolipoprotein E-deficient mice-brief report," *Arteriosclerosis, Thrombosis, and Vascular Biology*, vol. 37, no. 8, pp. 1457–1461, 2017.

[76] L. Shen, Y. Yang, T. Ou et al., "Dietary PUFAs attenuate NLRP3 inflammasome activation via enhancing macrophage autophagy," *Journal of Lipid Research*, vol. 58, no. 9, pp. 1808–1821, 2017.

[77] R. Yin, X. Zhu, J. Wang et al., "MicroRNA-155 promotes the ox-LDL-induced activation of NLRP3 inflammasomes via the ERK1/2 pathway in THP-1 macrophages and aggravates atherosclerosis in ApoE$^{-/-}$ mice," *Annals of Palliative Medicine*, vol. 8, no. 5, pp. 676–689, 2019.

[78] J. Gage, M. Hasu, M. Thabet, and S. C. Whitman, "Caspase-1 deficiency decreases atherosclerosis in apolipoprotein E-null mice," *Canadian Journal of Cardiology*, vol. 28, no. 2, pp. 222–229, 2012.

[79] K. Rajamaki, J. Lappalainen, K. Oorni et al., "Cholesterol crystals activate the NLRP3 inflammasome in human macrophages: a novel link between cholesterol metabolism and inflammation," *PLoS One*, vol. 5, no. 7, Article ID e11765, 2010.

[80] I. Tabas and A. H. Lichtman, "Monocyte-Macrophages and T Cells in atherosclerosis," *Immunity*, vol. 47, no. 4, pp. 621–634, 2017.

[81] T. Hendrikx, M. L. J. Jeurissen, P. J. van Gorp et al., "Bone marrow-specific caspase-1/11 deficiency inhibits atherosclerosis development inLdlr$^{-/-}$ mice," *FEBS Journal*, vol. 282, no. 12, pp. 2327–2338, 2015.

[82] L. Chen, Q. Yao, S. Xu, H. Wang, and P. Qu, "Inhibition of the NLRP3 inflammasome attenuates foam cell formation of THP-1 macrophages by suppressing ox-LDL uptake and promoting cholesterol efflux," *Biochemical and Biophysical Research Communications*, vol. 495, no. 1, pp. 382–387, 2018.

[83] S. Hamanaka, A. Umino, H. Sato et al., "Generation of vascular endothelial cells and hematopoietic cells by blastocyst complementation," *Stem Cell Reports*, vol. 11, no. 4, pp. 988–997, 2018.

[84] M. A. Gimbrone and G. García-Cardeña, "Endothelial cell dysfunction and the pathobiology of atherosclerosis," *Circulation Research*, vol. 118, no. 4, pp. 620–636, 2016.

[85] Y. Yin, X. Li, X. Sha et al., "Early hyperlipidemia promotes endothelial activation via a caspase-1-sirtuin 1 pathway," *Arteriosclerosis, Thrombosis, and Vascular Biology*, vol. 35, no. 4, pp. 804–816, 2015.

[86] X. Wu, H. Zhang, W. Qi et al., "Nicotine promotes atherosclerosis via ROS-NLRP3-mediated endothelial cell pyroptosis," *Cell Death & Disease*, vol. 9, no. 2, p. 171, 2018.

[87] J. Mestas and K. Ley, "Monocyte-endothelial cell interactions in the development of atherosclerosis," *Trends in Cardiovascular Medicine*, vol. 18, no. 6, pp. 228–232, 2008.

[88] Y. Sheikine and A. Sirsjö, "CXCL16/SR-PSOX-A friend or a foe in atherosclerosis?" *Atherosclerosis*, vol. 197, no. 2, pp. 487–495, 2008.

[89] H. Xiao, M. Lu, T. Y. Lin et al., "Sterol regulatory element binding protein 2 activation of NLRP3 inflammasome in endothelium mediates hemodynamic-induced atherosclerosis susceptibility," *Circulation*, vol. 128, no. 6, pp. 632–642, 2013.

[90] H. Yang, L. Xiao, Y. Yuan et al., "Procyanidin B2 inhibits NLRP3 inflammasome activation in human vascular endothelial cells," *Biochemical Pharmacology*, vol. 92, no. 4, pp. 599–606, 2014.

[91] J. Song, J. Li, F. Hou, X. Wang, and B. Liu, "Mangiferin inhibits endoplasmic reticulum stress-associated thioredoxin-interacting protein/NLRP3 inflammasome activation with regulation of AMPK in endothelial cells," *Metabolism*, vol. 64, no. 3, pp. 428–437, 2015.

[92] Y. Zhang, X. Liu, X. Bai et al., "Melatonin prevents endothelial cell pyroptosis via regulation of long noncoding RNA MEG3/miR-223/NLRP3 axis," *Journal of Pineal Research*, vol. 64, no. 2, 2018.

[93] P. Li, X. Zhong, J. Li et al., "MicroRNA-30c-5p inhibits NLRP3 inflammasome-mediated endothelial cell pyroptosis through FOXO3 down-regulation in atherosclerosis," *Biochemical and Biophysical Research Communications*, vol. 503, no. 4, pp. 2833–2840, 2018.

[94] L. Fang, K. K. Wang, P. F. Zhang et al., "Nucleolin promotes Ang II-induced phenotypic transformation of vascular smooth muscle cells by regulating EGF and PDGF-BB," *Journal of Cellular and Molecular Medicine*, vol. 24, no. 2, pp. 1917–1933, 2020.

[95] M. R. Bennett, S. Sinha, and G. K. Owens, "Vascular smooth muscle cells in atherosclerosis," *Circulation Research*, vol. 118, no. 4, pp. 692–702, 2016.

[96] C. Wen, X. Yang, Z. Yan et al., "Nalp3 inflammasome is activated and required for vascular smooth muscle cell calcification," *International Journal of Cardiology*, vol. 168, no. 3, pp. 2242–2247, 2013.

[97] F. Usui, K. Shirasuna, H. Kimura et al., "Critical role of caspase-1 in vascular inflammation and development of atherosclerosis in Western diet-fed apolipoprotein E-deficient mice," *Biochemical and Biophysical Research Communications*, vol. 425, no. 2, pp. 162–168, 2012.

[98] S. M. Man, Q. Zhu, L. Zhu et al., "Critical role for the DNA sensor AIM2 in stem cell proliferation and cancer," *Cell*, vol. 162, no. 1, pp. 45–58, 2015.

[99] Y. Jiang, H. Du, X. Liu, X. Fu, X. Li, and Q. Cao, "Artemisinin alleviates atherosclerotic lesion by reducing macrophage inflammation via regulation of AMPK/NF-κB/NLRP3

inflammasomes pathway," *Journal of Drug Targeting*, vol. 28, no. 1, pp. 70–79, 2020.

[100] Y. Yao, J. Mao, S. Xu et al., "Rosmarinic acid inhibits nicotine-induced C-reactive protein generation by inhibiting NLRP3 inflammasome activation in smooth muscle cells," *Journal of Cellular Physiology*, vol. 234, no. 2, pp. 1758–1767, 2019.

[101] F. Kong, B. Ye, J. Cao et al., "Curcumin represses NLRP3 inflammasome activation via TLR4/MyD88/NF-kappaB and P2X7R signaling in PMA-induced macrophages," *Frontiers in Pharmacology*, vol. 7, p. 369, 2016.

[102] N. Bode, A. Grebe, A. Kerksiek et al., "Ursodeoxycholic acid impairs atherogenesis and promotes plaque regression by cholesterol crystal dissolution in mice," *Biochemical and Biophysical Research Communications*, vol. 478, no. 1, pp. 356–362, 2016.

[103] Y. Jiang, K. Huang, X. Lin et al., "Berberine attenuates NLRP3 inflammasome activation in macrophages to reduce the secretion of interleukin-1beta," *Annals of Clinical and Laboratory Science*, vol. 47, no. 6, pp. 720–728, 2017.

[104] Q. Hu, T. Zhang, L. Yi, X. Zhou, and M. Mi, "Dihydromyricetin inhibits NLRP3 inflammasome-dependent pyroptosis by activating the Nrf2 signaling pathway in vascular endothelial cells," *Biofactors*, vol. 44, no. 2, pp. 123–136, 2018.

[105] K. Yamagata, K. Hashiguchi, H. Yamamoto, and M. Tagami, "Dietary apigenin reduces induction of LOX-1 and NLRP3 expression, leukocyte adhesion, and acetylated low-density lipoprotein uptake in human endothelial cells exposed to trimethylamine-N-oxide," *Journal of Cardiovascular Pharmacology*, vol. 74, no. 6, pp. 558–565, 2019.

[106] S. Robertson, G. J. Martínez, C. A. Payet et al., "Colchicine therapy in acute coronary syndrome patients acts on caspase-1 to suppress NLRP3 inflammasome monocyte activation," *Clinical Science*, vol. 130, no. 14, pp. 1237–1246, 2016.

[107] G. J. Martínez, D. S. Celermajer, and S. Patel, "The NLRP3 inflammasome and the emerging role of colchicine to inhibit atherosclerosis-associated inflammation," *Atherosclerosis*, vol. 269, pp. 262–271, 2018.

[108] F. Kong, B. Ye, L. Lin, X. Cai, W. Huang, and Z. Huang, "Atorvastatin suppresses NLRP3 inflammasome activation via TLR4/MyD88/NF-κB signaling in PMA-stimulated THP-1 monocytes," *Biomedicine & Pharmacotherapy*, vol. 82, pp. 167–172, 2016.

[109] S. Peng, L. W. Xu, X. Y. Che et al., "Atorvastatin inhibits inflammatory response, attenuates lipid deposition, and improves the stability of vulnerable atherosclerotic plaques by modulating autophagy," *Frontiers in Pharmacology*, vol. 9, p. 438, 2018.

[110] W. Leng, X. Ouyang, X. Lei et al., "The SGLT-2 inhibitor dapagliflozin has a therapeutic effect on atherosclerosis in diabetic ApoE$^{(-/-)}$ mice," *Mediators Inflamm*, vol. 2016, Article ID 6305735, 13 pages, 2016.

[111] L. Zhang, L. Lu, X. Zhong et al., "Metformin reduced NLRP3 inflammasome activity in Ox-LDL stimulated macrophages through adenosine monophosphate activated protein kinase and protein phosphatase 2A," *European Journal of Pharmacology*, vol. 852, pp. 99–106, 2019.

[112] R. Zhang, S. Han, Z. Zhang et al., "Cereal fiber ameliorates high-fat/cholesterol-diet-induced atherosclerosis by modulating the NLRP3 inflammasome pathway in ApoE$^{-/-}$ mice," *Journal of Agricultural and Food Chemistry*, vol. 66, no. 19, pp. 4827–4834, 2018.

[113] F. Hoss and E. Latz, "Inhibitory effects of colchicine on inflammasomes," *Atherosclerosis*, vol. 273, pp. 153-154, 2018.

[114] A. J. Boland, N. Gangadharan, P. Kavanagh et al., "Simvastatin suppresses interleukin iβ release in human peripheral blood mononuclear cells stimulated with cholesterol crystals," *Journal of Cardiovascular Pharmacology and Therapeutics*, vol. 23, no. 6, pp. 509–517, 2018.

[115] G. Tang, F. Duan, W. Li et al., "Metformin inhibited Nod-like receptor protein 3 inflammasomes activation and suppressed diabetes-accelerated atherosclerosis in ApoE$^{-/-}$ mice," *Biomedicine & Pharmacotherapy*, vol. 119, Article ID 109410, 2019.

Hindawi
Evidence-Based Complementary and Alternative Medicine
Volume 2020, Article ID 4517587, 9 pages
https://doi.org/10.1155/2020/4517587

Review Article

Involvement of Cathepsins in Innate and Adaptive Immune Responses in Periodontitis

Xu Yan,[1] Zhou Wu,[2,3] Biyao Wang,[1] Tianhao Yu,[1] Yue Hu,[1] Sijian Wang,[4] Chunfu Deng,[3] Baohong Zhao,[4] Hiroshi Nakanishi,[5] and Xinwen Zhang[4]

[1]*The VIP Department, School and Hospital of Stomatology, China Medical University, Liaoning Provincial Key Laboratory of Oral Diseases, Shenyang 110002, China*
[2]*Department of Aging Science and Pharmacology, Faculty of Dental Science, Kyushu University, Fukuoka 812-8582, Japan*
[3]*OBT Research Center, Faculty of Dental Science, Kyushu University, Fukuoka 812-8582, Japan*
[4]*Center of Implant Dentistry, School and Hospital of Stomatology, China Medical University, Liaoning Provincial Key Laboratory of Oral Diseases, Shenyang 110002, China*
[5]*Department of Pharmacology, Faculty of Pharmacy, Yasuda Women's University, Hiroshima 731-0153, Japan*

Correspondence should be addressed to Zhou Wu; zhouw@dent.kyushu-u.ac.jp and Xinwen Zhang; zhangxinwen@cmu.edu.cn

Received 9 January 2020; Revised 27 February 2020; Accepted 7 March 2020; Published 31 March 2020

Guest Editor: Young-Su Yi

Periodontitis is an infectious disease whereby the chronic inflammatory process of the periodontium stimulated by bacterial products induces specific host cell responses. The activation of the host cell immune system upregulates the production of inflammatory mediators, comprising cytokines and proteolytic enzymes, which contribute to inflammation and bone destruction. It has been well known that periodontitis is related to systemic inflammation which links to numerous systemic diseases, including diabetes and arteriosclerosis. Furthermore, periodontitis has been reported in association with neurodegenerative diseases such as Alzheimer's disease (AD) in the brain. Regarding immune responses and inflammation, cathepsin B (CatB) plays pivotal role for the induction of IL-1β, cathepsin K- (CatK-) dependent active toll-like receptor 9 (TLR9) signaling, and cathepsin S (CatS) which involves in regulating both TLR signaling and maturation of the MHC class II complex. Notably, both the production and proteolytic activities of cathepsins are upregulated in chronic inflammatory diseases, including periodontitis. In the present review, we focus on the roles of cathepsins in the innate and adaptive immune responses within periodontitis. We believe that understanding the roles of cathepsins in the immune responses in periodontitis would help to elucidate the therapeutic strategies of periodontitis, thus benefit for reduction of systemic diseases as well as neurodegenerative diseases in the global aging society.

1. Introduction

Immune responses, including the innate and adaptive immune responses, are components of a defensive mechanism which has become increasingly specialized with evolution. The human immune system is able to generate great quantities of specialized cells and molecules capable of recognizing and eliminating an apparently unlimited diversity of foreign invaders by functioning cooperatively [1]. Of note, although these specialized cells and molecules accumulate at inflammatory sites to efficiently remove invading agents, they may also amplify the inflammatory response and impair the surrounding tissues [2]. Therefore, under the inflammatory conditions, the inflammatory-responsive cell-related immune responses must be tightly controlled. Periodontitis is a chronic infectious disease whereby chronic inflammation of the periodontium involves interactions among bacterial products, numerous cell populations, and inflammatory mediators. The initiation of periodontitis might be attributed to dental plaques and complex and diverse microbial biofilms that form on the teeth. In particular, substances released from these biofilms, including lipopolysaccharides (LPS), antigens, and other virulence factors, gain access to the gingival tissues. As a

result, the innate and adaptive immune responses are elicited, thus leading to the activation of host defense cells. Collectively, inflammatory mediators, which comprise cytokines and proteolytic enzymes, induce tissue destruction and bone resorption [3].

Cathepsin, a term derived from the Greek word kathepsein (meaning to digest), is a protease that is functionally active in a slightly acidic environment. There are 11 human cysteine cathepsin isoforms, referred to as B, C, F, H, K, L, O, S, V, X, and W [4]. Cathepsins are primarily intracellular enzymes responsible for nonspecific bulk proteolysis in the endosomal/lysosomal system, which degrades both intracellular and extracellular proteins [5]. However, cathepsins are involved in producing immune modulators by the limited proteolysis processing. For example, cathepsin B (CatB) involves in the production of interleukin-1β (IL-1β) [6, 7] and TNF-α [8] and cathepsin K (CatK) involves in toll-like receptor 9 (TLR9) activation [9]. In addition, cathepsin S (CatS) mediates TLR signaling transduction and regulates major histocompatibility complex (MHC) class II-dependent $CD4^+$ T-cell activation [10]. Indeed, both the production and proteolytic activities of CatS are upregulated under conditions closely related to chronic inflammatory diseases, including periodontitis [11]. In the present review, we summarize the current knowledge on the involvement of cathepsins in regulating innate and adaptive immune responses in periodontitis. Given the roles of cathepsins in immune/inflammatory responses, the regulation of cathepsins will be helpful for the management of cellular immune responses in patients with periodontitis, and thus beneficial to prevent and relax the systemic diseases as well as neurodegenerative diseases in the global aging society.

2. Innate and Adaptive Immune Responses in Periodontitis

2.1. Periodontal Pathogens and TLRs. Periodontitis is caused by specific bacterial infection. The bacterial species living in polymicrobial biofilms or below the gingival margin proliferate largely as a result of the inflammation initiated by specific subgingival species. It is widely accepted that specific microorganisms are associated with specific periodontal diseases, and the search for the periodontal pathogens responsible for distinct periodontal conditions is under way [12, 13]. The "red complex," which is composed of the pathogens *Porphyromonas gingivalis*, *Tannerella forsythia*, and *Treponema denticola*, has been shown to exist in the biofilms where progressive periodontitis is shown [14]. Bacterial components, such as LPS, peptidoglycans, lipoteichoic acids, proteases, and toxins, which stimulate the inflammatory activity, can be detected in the biofilms on the surface of the tooth [15]. Antigens and toxic products released by bacteria, such as LPS and peptidoglycans, are identified by TLRs on the surface of host cells and can trigger cellular signaling of host cells [16]. On the host side, the diverse inflammatory cell types and resident cells of the tissues respond to bacterial infection and induce cellular immune responses that are innate and adaptive immune responses [17]. TLRs can detect multiple pathogen-related molecular patterns, including LPS, bacterial lipoproteins, lipoteichoic acids, flagellin, CpGDNA of bacteria and viruses, double-stranded RNA, and single-stranded viral RNA [18]. To date, 11 different TLRs (TLR1–11) have been identified [16]. It has been known that lipopolysaccharides from *Porphyromonas gingivalis* (*P. gingivalis* LPS) is recognized by TLR2/TLR4 [19, 20] while flagellin in *Tannerella forsythia* is recognized by TLR5 [21]. The TLR pathway is crucial in the immune responses in periodontitis because TLRs are bound to their corresponding antigens, which triggers intracellular immune responses to produce inflammatory-related mediators [22].

2.2. Macrophages in Periodontitis. Macrophages are myeloid cells of hematopoietic origin, which play important role in the local immune responses [23]. The major functions of macrophages include elimination of invading bacteria, recruitment of immune cells to the site of infection, production of cytokines and chemokines, and activation of the adaptive immune response through TLR signaling [22]. The functions of activated macrophages are regulated by mediators produced by T cells. The classically activated macrophages (M1) are regulated by interferon (IFN)-γ and LPS [24], while alternatively activated macrophages (M2) are produced in response to IL-4 or IL-13 [25]. M2 macrophages have been shown to play a role in relief of inflammation and thus have decreased capacity to produce cytokines. Macrophages express high levels of TLR2 and TLR4 [26], which shift to the M1 phenotype in gingival tissues of patients with chronic periodontitis [27]. Interestingly, M1 macrophages can transform into M2 macrophages by exosomes derived from gingival mesenchymal stem cells, which is beneficial for suppressing the immune responses [28].

Accumulating studies have demonstrated that macrophage serves as an important route for local immune responses in periodontitis because macrophage can produce multiple proinflammatory mediators, including tumor necrosis factor (TNF-α) and IL-1β and IL-6 through activating the nuclear factor kappa-light-chain-enhancer of activated B (NF-κB) pathway [29]. In addition to the contribution to innate immune response, TNF-α also serves as a significant route for alveolar bone resorption in periodontitis for inducing the differentiation and activation of osteoclasts [30]. IL-1β activates generation of matrix metalloproteinase (MMP)-9 in periodontitis [31] and promotes the expression of the receptor activator of nuclear factor kappa-B ligand (RANKL), contributing to osteoclastogenesis in periodontitis [32, 33]. A recent report has shown that IL-1β-expressed inflammatory macrophages produce amyloid β (the main component of the hall marker in the brain of AD patients) in the gingival tissues of the patients with periodontitis as well as in the liver of mice after chronic systemic *P. gingivalis* infection, indicating that inflammatory macrophages in periodontitis may contribute to neurodegenerative diseases such as AD [34]. IL-6 triggers the generation of vascular endothelial growth factor (VEGF) and MMP-1, making great contribution to the development of periodontitis [35] and synergic effects of IL-1β and IL-6 upregulate MMPs,

contributing to the tissue destruction in periodontitis by collagen degradation and bone resorption [36]. It is noted that chemical ablation of macrophages in mice prevents the *P. gingivalis*-induced alveolar bone resorption, demonstrating important roles for macrophages during periodontitis [37].

2.3. Dendritic Cells in Periodontitis. Dendritic cells (DCs) are located adjacent to the epithelia of blood vessels and the mucosa that shield soft tissues from microbial invasion. Bacteria or antigen-antibody complexes of bacteria or bacterial products that breach the epithelia and mucosa will encounter DCs and induce DC responses. DCs are typically the first immune cells to encounter and respond to invading microorganisms [38]. The nature of this DC response is essential in determining the type of acquired immune response that is induced. Adaptive immune response relies on the formation of appropriate peptides from foreign proteins and the consequent presentation on MHC I or II complexes [39], and DCs are able to initiate the elimination of the MHC II-associated chaperone invariant chain (Ii) from MHC II [40, 41]. Upon the stimulation by pathogens, such as *P. gingivalis*, antigen presentation by DCs leads to the activation and subsequent differentiation of $CD4^+$ T cells [36]. The unique immune-stimulatory activity of DC stems from their ability to efficiently capture and present antigens and optimally express cytokines after *P. gingivalis* LPS stimulation [42]. Naïve DCs are found in large numbers in gingival tissues, and DCs are matured in the inflamed gingival tissues from patients with periodontitis [43] which particularly serve as immune stimulators [44]. Considering the roles of DCs for cytokine production and differentiation of $CD4^+$ T cells, DCs are reckoned to be the bridge between the innate and adaptive immune responses in periodontitis.

2.4. T Cells in Cellular Immune Responses. T cells can be activated in response to oral bacterial antigens [45], and $CD4^+$ T cells play key roles in the development of a mouse model of periodontitis [46]. $CD4^+$ T-cell-dependent responses are initiated by the recognition of MHC class II peptide complexes on antigen-presenting cells (APCs), such as DCs and macrophages. During the process, the invariant chain is sequentially degraded to leupeptin-induced peptide 10 (lip10) and ultimately to class II-associated Ii peptide (CLIP), which remains in the peptide-binding groove [47, 48]. Then, CLIP is removed from the class II molecules catalyzed by the human leukocyte antigen DM which is capable of binding with antigenic peptides. Subsequently, the CLIP complex is transported to the cell surface, on which the antigen is presented to cognate T cells, initiating an immune response [49]. The naïve $CD4^+$ T helper (Th0) cells can differentiate into $CD4^+$ cell subtypes, including Th1, Th2, Th17, and regulatory T cells (Tregs), depending on the cytokines which are produced. In the presence of IL-12, Th1 cells are derived by IFN-γ and TNF-α, while Th2 cells are derived in the presence of IL-4, which produce IL-4, IL-5, and IL-10. Th17 cells, which secrete IL-17, IL-23, and IL-22, are derived in the presence of TGF-β, IL-1β, and IL-6. In contrast, Tregs are raised in the presence of TGF-β, which secretes the immunosuppressive cytokines IL-10 and TGF-β. In the participation of immune responses, IL-17 stimulates the production of inflammatory mediators, including TNF-α, IL-6, and IL-1β, while Tregs effectively regulate the resolution of inflammation [50, 51]. An in vitro study has reported that $CD4^+$ T cells with its proinflammatory cytokines IFN-γ and IL-6 serve as important routes for alveolar bone resorption in mice infected with *P. gingivalis* [46]. Tregs and Th17 cells have been demonstrated in periodontal tissues which are involved in periodontal disease processes [52]. Th17 cells promote bone destruction [51, 53], while Tregs protect alveolar bone by inhibiting osteoclastogenesis [54]. Therefore, the plasticity and cross-talk in T-cell subsets are vital for the regulation of the cellular immune response during periodontitis and therapeutic strategies comprising Tregs inhibiting the immuno-inflammatory response and restoring alveolar bone homeostasis [55]. Indeed, the effect of antibiotic therapy in regulating Treg-Th17 plasticity in humans with periodontitis is demonstrated [56].

3. Involvement of Cathepsin B in Innate Immune Responses

3.1. CatB in Periodontitis. CatB, functioning as an endopeptidase at neutral pH, is also found in the extralysosomal sites involving the cytosol, plasma membrane, and pericellular spaces [57]. In the noninvasive diagnostic body fluid, gingival crevicular fluid (GCF), CatB was detected mainly in macrophages when monocytes were migrating into the gingival crevice [58, 59]. The protease activity of CatB in GCF is closely associated with the GCF volume and the severity of periodontitis [60, 61]. CatB in GCF plays a major role in the pathology of periodontitis with respect to connective tissue breakdown and bone resorption. It is demonstrated that there is an imbalance between cathepsin B and the endogenous inhibitor cystatin C, with the elevated level of cathepsin B and a decreased level of cystatin C [62]. As a result of the proteinases from *P. gingivalis* infection, the hemostasis of CatB activity is disrupted, contributing to the destruction in periodontitis [63]. Therefore, the activity and the amount of cathepsin B and cystatin C in GCF can potentially serve as a predictor of attachment loss and an indicator of the progression of the disease [61, 64, 65]. CatB plays a significant role in promoting chronic inflammation in periodontitis. It is reported that CatB regulates the expression of collagens III and IV by fibroblasts in response to a TLR2 agonist, *P. gingivalis* LPS [66]. Moreover, CatB recently has been determined to be involved in the production of amyloid β, the main component of the hall marker in the brain of AD patients, in the macrophages in the gingival tissues of the patients with periodontitis and in the liver of mice after chronic systemic *P. gingivalis* infection [67].

3.2. CatB in IL-1β Processing. IL-1β is recognized as the master mediator in innate immune responses, and two signals are required for IL-1β processing. One is NF-κB-

dependent pro-IL-1β production, and the other is caspase-1-dependent proteolytic processing of pro-IL-1β to mature IL-1β. CatB plays a critical role in both signals of IL-1β processing because CatB involves in NF-κB activation [68] and activation of caspase-1 [6, 7]. We have demonstrated that CatB was colocalized with caspase-1, and treatment with CA-074Me, a specific CatB inhibitor, markedly inhibited caspase-1 expression, resulting in a decreased production of IL-1β [69–71]. These findings are consistent with the observations that IL-1β and CatB are colocalized in phagolysosomes, and that the secretion of IL-1β is through the exocytosis of phagolysosomes in LPS-activated human monocytes [72]. The CatB expression is upregulated in the macrophages which involves the production of IL-1β and amyloid β in gingival tissues of the patients with periodontitis [67, 73]. Furthermore, CatB indirectly involves in the activation of caspase-1 through the proteolytic maturation of caspase-11 [74].

3.3. CatB in TNF-α Trafficking. Membrane-associated (m) TNF-α is a type II transmembrane precursor which is delivered from the *trans*-Golgi network to the recycling endosome [75, 76]. Membrane-associated TNF-α is transported to the cell surface, where it is cleaved by the TNF-α-converting enzyme [77]. Membrane fusion among the TNF-α-containing vesicles from the trans-Golgi network, the recycling endosomes, and the cell surface membrane is mediated by the interactions among various *trans*-soluble-*N*-ethylmaleimide-sensitive factor-attachment protein SNAP receptor (SNARE) family members [78]. Recent studies have revealed that the accumulation of newly synthesized mTNF-α originally occurs in the Golgi complex [79]. The mTNF-containing vesicles are then translocated from the *trans*-Golgi network to the recycling endosome and subsequently to the cell surface through two different membrane fusion processes [75, 76]. The first fusion process is mediated by Q-SNAREs, including syntaxin 6, syntaxin 7, and vesicle transport, through interacting with t-SNARE homolog 1b (Vit1b) of the Golgi complex TNF-α carrier vesicle and the R-SNARE vesicle-associated membrane protein 3 (VAMP3) of the recycling endosome. The second fusion process is mediated by the interactions between VAMP3 of the recycling endosome and the Q-SNARE complex which consists of syntaxin 4 and SNAP-23. LPS triggers expression of the Q-SNARE components, including syntaxin 4 and SNAP-23 for the accommodation of increased trafficking during TNF-α secretion in macrophages [80].

A recent report shows that cytosolic CatB is imperative for fusion of the TNF-α-containing vesicles to the plasma membrane [8]. CatB can be localized in the nucleus and downregulate transcriptions [81]. However, there is no difference in the levels of syntaxin 4 and SNAP-23 in the CA-074Me-treated or CatB−/− macrophages, suggesting that CatB does not downregulate the SNARE components. There is a possibility that CatB has functions in regulating TNF-α vesicle trafficking through regulation of the SNARE components, either at the transcriptional or posttranslational levels in THP-1 and primary human monocytic cells considering that CatB was reported to be involved in both transcription and posttranslational protein processes, such as protein [82] and thyroglobulin [83]. A new role for intracellular CatB activity involved in TNF-α signaling is suggested in the report [8].

Therefore, CatB plays a critical role in regulating innate immune responses in periodontitis by controlling production of IL-1β and TNF-α.

4. Involvement of Cathepsin S in Adaptive Immune Responses

4.1. CatS in Periodontitis. The general role of CatS is breaking down antigenic and antimicrobial peptides, involving antigen processing and presentation [84–86]. In addition, CatS also serves as an elastase, destroying extracellular matrix proteins, comprising collagen and proteins of the bacterial outer membrane [84, 87]. CatS is generated by immune cells, including macrophages and DCs [88, 89]. In an analysis of healthy buccal gingival tissues from Rhesus monkeys, the transcription of CatS was altered in aged healthy tissues compared with younger animals. These age-related immune pathways were associated with periodontal health [90]. CatS was also found to be upregulated in rats with experimental periodontitis and human patients with periodontitis [11, 91]. CatS is recognized as one of the hub proteins in the protein-protein interaction network of 726 differentially expressed genes in periodontitis and plays an essential role in bone loss involved in periodontitis progression [58, 91].

4.2. CatS in MHC II Antigen Presenting and CD4$^+$ T-Cell Activation. CatS is essential in MHC II antigen processing and presentation [92, 93]. Indeed, CatS null mice show a considerable variation in generation of MHC II-bound Ii fragments, and presentation due to the fact that the Ii degradation in professional APCs is substantially diminished, where CatS is abundantly expressed [94, 95]. In addition, endocytosis selectively targets exogenous material to CatS in human DCs [96]. Enrichment of MHC II molecules within late endocytic structures has consistently been seen in splenic DCs of CatS-deficient mice [97]. Pharmacological or genetic inhibition of CatS results in defective TLR2 signaling in the *P. gingivalis* LPS-exposed DCs, indicating CatS may be involved in innate immune responses [10, 42].

4.3. CatS in Promoting of Th1 and Th17. Cathepsin S, which is predominantly generated by monocytes/macrophages and DCs, is involved in the ultimate proteolytic cleavage stage of the invariant chain in APCs during TLR2 signaling [48, 85, 88]. DCs induce the differentiation of naïve CD4$^+$ T cells into various subpopulations, comprising Th1 (IFN-γ) or Th17 (Th17) [98, 99]. Recently, we reported that CatS is crucial for the differentiation of naïve CD4$^+$ T cells [10]. We have found that CatS deficiency significantly relieves lower Th1 cell responses, accompanied with a decreased level of IFN-γ [10]. Moreover, we have demonstrated that CatS

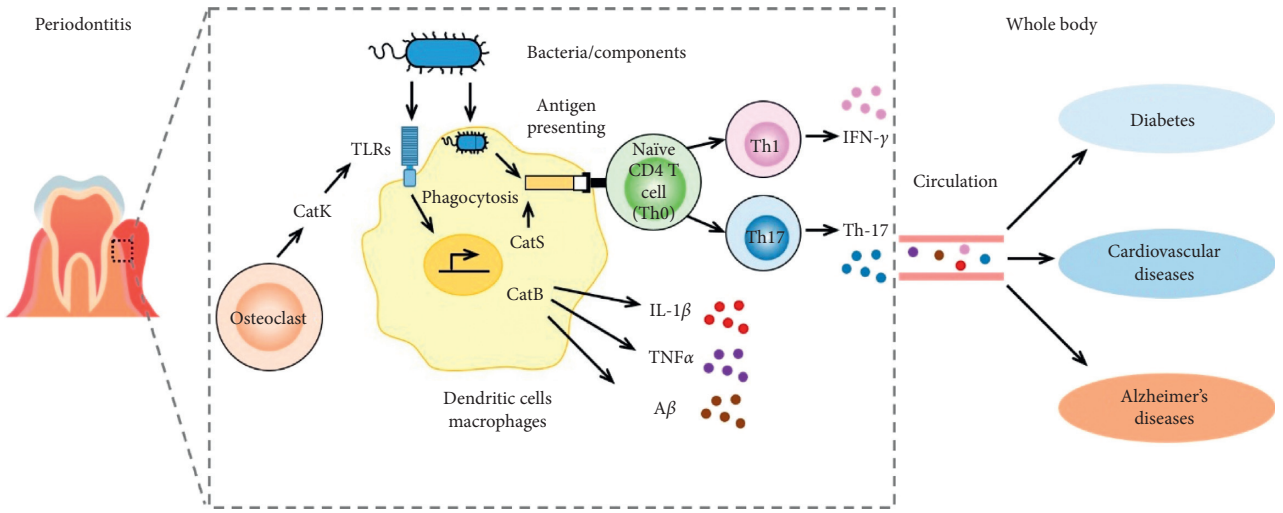

FIGURE 1: A schematic illustration of the cathepsin-related immune responses in periodontitis linking to the diseases within the whole body. In the bacteria (components)-stimulated cells, cathepsin B involves in activation of TLR signaling to produce IL-1β, TNF-α, and amyloid (A) β, and cathepsin S involves in maturation of MHC class II for driving $CD4^+$ (helper) T cells to produce IFN-γ (Th1) and IL-17 (Th17). Cathepsin K involves in activation of the TLR/autophagy pathway to produce type I interferon (IFN). The periodontitis cathepsin-related proinflammatory mediators involve in systemic diseases and Alzheimer's disease via the circulation.

promotes differentiation of Th17 cells in response to *P. gingivalis* LPS-exposed DCs through protease-activated receptor (PAR) 2-dependent IL-6 production [42]. Subsequently, the increased IL-6 triggers the differentiation of Th17 cells, illustrating the significant role of CatS in the differentiation of Th17 cells, after the exposure to *P. gingivalis* LPS [42]. Considering the critical roles of CatS in adaptive immune responses through promoting the differentiation of both Th1 and Th17 cells in periodontitis, CatS may provide a novel therapeutic target for treatment of periodontitis.

5. Involvement of Cathepsin K in Immune Responses

5.1. CatK in Periodontitis. Cathepsin K (CatK) is dominantly generated by osteoclasts, which serves as an important regulator for bone resorption [100]. CatK is essential for normal bone resorption via degrading collagens and gelatin, the latter being a hydrolysis product of collagen [101, 102]. And it also dissolves type I collagen, the major component of the organic bone matrix [103]. Recently, several studies have demonstrated that CatK plays a crucial role in alveolar bone resorption in patients with periodontitis. It is reported that there are elevated levels of CatK in GCF of patients with periodontitis and periimplantitis [104–107]. Once the hemostasis is destroyed, bone resorption will occur in periodontitis. In patients with chronic periodontitis, CatK levels were greatly elevated in smokers compared to nonsmokers, indicating a positive influence of smoking on CatK [108]. Moreover, CatK in GCF is not only derived from osteoclasts, but also from fibroblasts, macrophages, and gingival epithelial cells, contributing to the attachment loss and alveolar bone resorption [109]. Pharmacologic or genetic inhibition of CatK results in defective TLR9 signaling in DCs in response to unmethylated CpGDNA, without affecting antigen-presenting ability [110].

5.2. CatK in Autophagy. The elevated level of CatK not only directly induces bone resorption, but also makes impact on innate immune indirectly contributing to periodontitis and even autoimmune diseases, especially rheumatoid arthritis (RA) [9]. As the level of CatK is elevated, there would be an activated TLR9 signaling in DCs and macrophages and consequently, osteoclastic bone resorption [103, 110]. The CpGDNA can be recognized by TLR9, which can trigger autophagy [111–113]. In response to the activation of TLR9, the autophagy protein microtubule-associated protein 1A/1B-light chain 3 (LC3) aggregates IκB kinase α (IKKα) for type I interferon generation [112]. Moreover, there is a significant increase in the TLR9 downstream proteins (IKKβ and MYD88) and TFEB, which are greatly correlated with autophagy, in response to the activation of TLR9 [114, 115]. Coinciding with the conclusion that the activation of TLR9 can induce the downstream autophagy pathway, the inhibition of CatK can suppress this response via down-regulating the expression of TLR9 [9, 116]. Therefore, CatK may involve in innate immune responses in periodontitis through the TLR/autophagy pathway.

6. Conclusion

The involvement of cathepsins in the immune responses of periodontitis contribute to systemic diseases, including diabetes, cardiovascular diseases, and neurodegenerative disease, including AD, especially increasing in aged population (Figure 1). We believe that regulation of cathepsins, including CatB, CatS, and CatK, in cellular immune responses in patients with periodontitis will be beneficial for

reduction of systemic diseases and neurodegenerative diseases in the global aging society.

Conflicts of Interest

The authors declare no conflicts of interest.

Acknowledgments

This work was financially supported by grants from the National Natural Science Foundation of China (no. 81700977 and 81500858), the Technology Project Program of Liaoning Province of China (no. 20170541059) from the Nature Sciences Foundation of Liaoning Province of China, and the Japanese KAKENHI Grant no. 16K11478 (grants-in-aid for scientific research to Z.W.). The authors would like to thank the Department of Aging Science and Pharmacology, Faculty of Dental Science, Kyushu University, Fukuoka, Japan, for their support and allowing them to use their facilities.

References

[1] D. M. Clancy, G. P. Sullivan, H. B. T. Moran et al., "Extracellular neutrophil proteases are efficient regulators of IL-1, IL-33, and IL-36 cytokine activity but poor effectors of microbial killing," *Cell Reports*, vol. 22, no. 11, pp. 2937–2950, 2018.

[2] S. J. Weiss, "Tissue destruction by neutrophils," *The New England Journal of Medicine*, vol. 320, no. 6, pp. 365–376, 1989.

[3] E. M. Cardoso, C. Reis, and M. C. Manzanares-Céspedes, "Chronic periodontitis, inflammatory cytokines, and interrelationship with other chronic diseases," *Postgraduate Medicine*, vol. 130, no. 1, pp. 98–104, 2018.

[4] B. Turk, D. Turk, and V. Turk, "Lysosomal cysteine proteases: more than scavengers," *Biochimica et Biophysica Acta*, vol. 1477, no. 1-2, pp. 98–111, 2000.

[5] V. Turk, B. Turk, and D. Turk, "New embo members' review: lysosomal cysteine proteases: facts and opportunities," *The EMBO Journal*, vol. 20, no. 17, pp. 4629–4633, 2001.

[6] R. I. Campden and Y. Zhang, "The role of lysosomal cysteine cathepsins in NLRP3 inflammasome activation," *Archives of Biochemistry and Biophysics*, vol. 670, pp. 32–42, 2019.

[7] Y. Zhang, Y. Chen, Y. Zhang, P.-L. Li, and X. Li, "Contribution of cathepsin B-dependent Nlrp3 inflammasome activation to nicotine-induced endothelial barrier dysfunction," *European Journal of Pharmacology*, vol. 865, p. 172795, 2019.

[8] S.-D. Ha, A. Martins, K. Khazaie, J. Han, B. M. Chan, and S. O. Kim, "Cathepsin B is involved in the trafficking of TNF-alpha-containing vesicles to the plasma membrane in macrophages," *The Journal of Immunology*, vol. 181, no. 1, pp. 690–697, 2008.

[9] W. Wei, J. Ren, W. Yin et al., "Inhibition of Ctsk modulates periodontitis with arthritis via downregulation of TLR9 and autophagy," *Cell Proliferation*, vol. 53, no. 1, Article ID e12722, 2020.

[10] X. Zhang, Z. Wu, Y. Hayashi, R. Okada, and H. Nakanishi, "Peripheral role of cathepsin S in Th1 cell-dependent transition of nerve injury-induced acute pain to a chronic pain state," *Journal of Neuroscience*, vol. 34, no. 8, pp. 3013–3022, 2014.

[11] S. Memmert, A. Damanaki, A. V. B. Nogueira et al., "Role of cathepsin S in periodontal inflammation and infection," *Mediators of Inflammation*, vol. 2017, Article ID 4786170, 10 pages, 2017.

[12] G. A. Weijden, M. F. Timmerman, E. Reijerse, G. N. Wolffe, A. J. Winkelhoff, and U. Velden, "The prevalence of *A. actinomycetemcomitans*, *P. gingivalis* and *P. intermedia* in selected subjects with periodontitis," *Journal of Clinical Periodontology*, vol. 21, no. 9, pp. 583–588, 1994.

[13] A. Mombelli, "Microbiological monitoring," *Journal of Clinical Periodontology*, vol. 23, no. 3, pp. 251–257, 1996.

[14] S. Schulz, M. Porsch, I. Grosse, K. Hoffmann, H.-G. Schaller, and S. Reichert, "Comparison of the oral microbiome of patients with generalized aggressive periodontitis and periodontitis-free subjects," *Archives of Oral Biology*, vol. 99, pp. 169–176, 2019.

[15] T. R. Fitzsimmons, S. Ge, and P. M. Bartold, "Compromised inflammatory cytokine response to *P. gingivalis* LPS by fibroblasts from inflamed human gingiva," *Clinical Oral Investigations*, vol. 22, no. 2, pp. 919–927, 2018.

[16] K. Takeda and S. Akira, "Toll-like receptors," *Current Protocols in Immunology*, vol. 109, no. 1, 2015.

[17] T. E. Van Dyke and A. J. van Winkelhoff, "Infection and inflammatory mechanisms," *Journal of Clinical Periodontology*, vol. 40, no. 14, pp. S1–S7, 2013.

[18] T. Kawai and S. Akira, "The role of pattern-recognition receptors in innate immunity: update on toll-like receptors," *Nature Immunology*, vol. 11, no. 5, pp. 373–384, 2010.

[19] K. Q. de Andrade, C. L. C. Almeida-da-Silva, and R. Coutinho-Silva, "Immunological pathways triggered by *Porphyromonas gingivalis* and *Fusobacterium nucleatum*: therapeutic possibilities?" *Mediators of Inflammation*, vol. 2019, Article ID 7241312, 20 pages, 2019.

[20] T. Maekawa, J. L. Krauss, T. Abe et al., "*Porphyromonas gingivalis* manipulates complement and TLR signaling to uncouple bacterial clearance from inflammation and promote dysbiosis," *Cell Host & Microbe*, vol. 15, no. 6, pp. 768–778, 2014.

[21] M. R. Benakanakere, Q. Li, M. A. Eskan et al., "Modulation of TLR2 protein expression by miR-105 in human oral keratinocytes," *Journal of Biological Chemistry*, vol. 284, no. 34, pp. 23107–23115, 2009.

[22] B. Song, Y. Zhang, L. Chen et al., "The role of toll-like receptors in periodontitis," *Oral Diseases*, vol. 23, no. 2, pp. 168–180, 2017.

[23] C. Varol, A. Mildner, and S. Jung, "Macrophages: development and tissue specialization," *Annual Review of Immunology*, vol. 33, no. 1, pp. 643–675, 2015.

[24] C. M. Minutti, B. García-Fojeda, A. Sáenz et al., "Surfactant protein A prevents IFN-γ/IFN-γ receptor interaction and attenuates classical activation of human alveolar macrophages," *The Journal of Immunology*, vol. 197, no. 2, pp. 590–598, 2016.

[25] D. R. Herbert, B. Douglas, and K. Zullo, "Group 2 innate lymphoid cells (ILC2): type 2 immunity and helminth immunity," *International Journal of Molecular Sciences*, vol. 20, no. 9, 2019.

[26] H. AlQallaf, Y. Hamada, S. Blanchard, D. Shin, R. Gregory, and M. Srinivasan, "Differential profiles of soluble and cellular toll like receptor (TLR)-2 and 4 in chronic periodontitis," *PLoS One*, vol. 13, no. 12, Article ID e0200231, 2018.

[27] J. Yang, Y. Zhu, D. Duan et al., "Enhanced activity of macrophage M1/M2 phenotypes in periodontitis," *Archives of Oral Biology*, vol. 96, pp. 234–242, 2018.

[28] R. Wang, Q. Ji, C. Meng et al., "Role of gingival mesenchymal stem cell exosomes in macrophage polarization under inflammatory conditions," *International Immunopharmacology*, no. 81, Article ID 106030, 2019.

[29] Y. Xiao, C. Li, M. Gu et al., "Protein disulfide isomerase silence inhibits inflammatory functions of macrophages by suppressing reactive oxygen species and NF-κB pathway," *Inflammation*, vol. 41, no. 2, pp. 614–625, 2018.

[30] T. Tenkumo, L. Rojas-Sanchez, J. R. Vanegas Saenz et al., "Reduction of inflammation in a chronic periodontitis model in rats by TNF-alpha gene silencing with a topically applied siRNA-loaded calcium phosphate paste," *Acta Biomaterialia*, vol. 105, pp. 263–279, 2020.

[31] R. Cheng, Z. Wu, M. Li, M. Shao, and T. Hu, "Interleukin-1beta is a potential therapeutic target for periodontitis: a narrative review," *International Journal of Oral Science*, vol. 12, no. 1, p. 2, 2020.

[32] G. N. Belibasakis and N. Bostanci, "The RANKL-OPG system in clinical periodontology," *Journal of Clinical Periodontology*, vol. 39, no. 3, pp. 239–248, 2012.

[33] N. C.-N. Huynh, V. Everts, P. Pavasant, and R. S. Ampornaramveth, "Interleukin-1β induces human cementoblasts to support osteoclastogenesis," *International Journal of Oral Science*, vol. 9, no. 12, p. e5, 2017.

[34] C. Fu, Z. Wei, and D. Zhang, "PTEN inhibits inflammatory bone loss in ligature-induced periodontitis via IL1 and TNF-alpha," *BioMed Research International*, vol. 2019, Article ID 6712591, 9 pages, 2019.

[35] K. Naruishi and T. Nagata, "Biological effects of interleukin-6 on Gingival Fibroblasts: cytokine regulation in periodontitis," *Journal of Cellular Physiology*, vol. 233, no. 9, pp. 6393–6400, 2018.

[36] J. L. Hor, P. G. Whitney, A. Zaid, A. G. Brooks, W. R. Heath, and S. N. Mueller, "Spatiotemporally distinct interactions with dendritic cell subsets facilitates $CD4^+$ and $CD8^+$ T cell activation to localized viral infection," *Immunity*, vol. 43, no. 3, pp. 554–565, 2015.

[37] R. S. Lam, N. M. O'Brien-Simpson, J. C. Lenzo et al., "Macrophage depletion abates *Porphyromonas gingivalis*-induced alveolar bone resorption in mice," *Journal of Immunology*, vol. 193, no. 5, pp. 2349–2362, 2014.

[38] S. C. Eisenbarth, "Dendritic cell subsets in T cell programming: location dictates function," *Nature Reviews Immunology*, vol. 19, no. 2, pp. 89–103, 2019.

[39] T. Zavasnik-Bergant and B. Turk, "Cysteine proteases: destruction ability versus immunomodulation capacity in immune cells," *Biological Chemistry*, vol. 388, no. 11, pp. 1141–1149, 2007.

[40] K. Honey and A. Y. Rudensky, "Lysosomal cysteine proteases regulate antigen presentation," *Nature Reviews Immunology*, vol. 3, no. 6, pp. 472–482, 2003.

[41] R. D. A. Wilkinson, R. Williams, C. J. Scott, and R. E. Burden, "Cathepsin S: therapeutic, diagnostic, and prognostic potential," *Biological Chemistry*, vol. 396, no. 8, pp. 867–882, 2015.

[42] M. Dekita, Z. Wu, J. Ni et al., "Cathepsin S is involved in Th17 differentiation through the upregulation of IL-6 by activating PAR-2 after systemic exposure to lipopolysaccharide from Porphyromonas gingivalis," *Frontiers in Pharmacology*, vol. 8, p. 470, 2017.

[43] J. Carrion, E. Scisci, B. Miles et al., "Microbial carriage state of peripheral blood dendritic cells (DCs) in chronic periodontitis influences DC differentiation, atherogenic potential," *The Journal of Immunology*, vol. 189, no. 6, pp. 3178–3187, 2012.

[44] G. R. Souto, C. M. Queiroz-Junior, M. H. de Abreu, F. O. Costa, and R. A. Mesquita, "Pro-inflammatory, Th1, Th2, Th17 cytokines and dendritic cells: a cross-sectional study in chronic periodontitis," *PLoS One*, vol. 9, no. 3, Article ID e91636, 2014.

[45] N. R. Bennett, D. B. Zwick, A. H. Courtney, and L. L. Kiessling, "Multivalent antigens for promoting B and T cell activation," *ACS Chemical Biology*, vol. 10, no. 8, pp. 1817–1824, 2015.

[46] P. J. Baker, M. Dixon, R. T. Evans, L. Dufour, E. Johnson, and D. C. Roopenian, "$CD4^+$ T cells and the proinflammatory cytokines gamma interferon and interleukin-6 contribute to alveolar bone loss in mice," *Infection and Immunity*, vol. 67, no. 6, pp. 2804–2809, 1999.

[47] T. Y. Nakagawa, W. H. Brissette, P. D. Lira et al., "Impaired invariant chain degradation and antigen presentation and diminished collagen-induced arthritis in cathepsin S null mice," *Immunity*, vol. 10, no. 2, pp. 207–217, 1999.

[48] R. J. Riese, G.-P. Shi, J. Villadangos et al., "Regulation of CD1 function and NK1.1+ T cell selection and maturation by cathepsin S," *Immunity*, vol. 15, no. 6, pp. 909–919, 2001.

[49] J. A. Villadangos, R. J. Riese, C. Peters, H. A. Chapman, and H. L. Ploegh, "Degradation of mouse invariant chain: roles of cathepsins S and D and the influence of major histocompatibility complex polymorphism," *Journal of Experimental Medicine*, vol. 186, no. 4, pp. 549–560, 1997.

[50] N. Gagliani, M. C. A. Vesely, A. Iseppon et al., "Th17 cells transdifferentiate into regulatory T cells during resolution of inflammation," *Nature*, vol. 523, no. 7559, pp. 221–225, 2015.

[51] T. Okui, Y. Aoki, H. Ito, T. Honda, and K. Yamazaki, "The presence of $IL\text{-}17^+/FOXP3^+$ double-positive cells in periodontitis," *Journal of Dental Research*, vol. 91, no. 6, pp. 574–579, 2012.

[52] V. P. B. Parachuru, D. E. Coates, T. J. Milne, H. M. Hussaini, A. M. Rich, and G. J. Seymour, "Forkhead box P3-positive regulatory T-cells and interleukin 17-positive T-helper 17 cells in chronic inflammatory periodontal disease," *Journal of Periodontal Research*, vol. 49, no. 6, pp. 817–826, 2014.

[53] K. Bunte and T. Beikler, "Th17 cells and the IL-23/IL-17 Axis in the pathogenesis of periodontitis and immune-mediated inflammatory diseases," *International Journal of Molecular Sciences*, vol. 20, no. 14, 2019.

[54] Y. K. Han, Y. Jin, Y. B. Miao, T. Shi, and X. P. Lin, "$CD8^+$ $Foxp3^+$ T cells affect alveolar bone homeostasis via modulating Tregs/Th17 during induced periodontitis: an adoptive transfer experiment," *Inflammation*, vol. 41, no. 5, pp. 1791–1803, 2018.

[55] E. A. Cafferata, A. Jerez, R. Vernal, G. Monasterio, N. Pandis, and C. M. Faggion Jr., "The therapeutic potential of regulatory T lymphocytes in periodontitis: a systematic review," *Journal of Periodontal Research*, vol. 54, no. 3, pp. 207–217, 2019.

[56] M. Rajendran, S. Looney, N. Singh et al., "Systemic antibiotic therapy reduces circulating inflammatory dendritic cells and Treg-Th17 plasticity in periodontitis," *The Journal of Immunology*, vol. 202, no. 9, pp. 2690–2699, 2019.

[57] H. Hentze, X. Y. Lin, M. S. K. Choi, and A. G. Porter, "Critical role for cathepsin B in mediating caspase-1-dependent interleukin-18 maturation and caspase-1-

independent necrosis triggered by the microbial toxin nigericin," *Cell Death & Differentiation*, vol. 10, no. 9, pp. 956–968, 2003.

[58] B. Zhao, M. Takami, A. Yamada et al., "Interferon regulatory factor-8 regulates bone metabolism by suppressing osteoclastogenesis," *Nature Medicine*, vol. 15, no. 9, pp. 1066–1071, 2009.

[59] S. W. Cox, E. M. Rodriguez-Gonzalez, V. Booth, and B. M. Eley, "Secretory leukocyte protease inhibitor and its potential interactions with elastase and cathepsin B in gingival crevicular fluid and saliva from patients with chronic periodontitis," *Journal of Periodontal Research*, vol. 41, no. 5, pp. 477–485, 2006.

[60] K. Kunimatsu, K. Yamamoto, E. Ichimaru, Y. Kato, and I. Kato, "Cathepsins B, H and L activities in gingival crevicular fluid from chronic adult periodontitis patients and experimental gingivitis subjects," *Journal of Periodontal Research*, vol. 25, no. 2, pp. 69–73, 1990.

[61] E. Ichimaru, M. Tanoue, M. Tani et al., "Cathepsin B in gingival crevicular fluid of adult periodontitis patients: identification by immunological and enzymological methods," *Inflammation Research*, vol. 45, no. 6, pp. 277–282, 1996.

[62] R. Elkaim, S. Werner, L. Kocgozlu, and H. Tenenbaum, "*P. gingivalis* regulates the expression of cathepsin B and cystatin C," *Journal of Dental Research*, vol. 87, no. 10, pp. 932–936, 2008.

[63] M. Abrahamson, M. Wikstrom, J. Potempa, S. Renvert, and A. Hall, "Modification of cystatin C activity by bacterial proteinases and neutrophil elastase in periodontitis," *Molecular Pathology*, vol. 50, no. 6, pp. 291–297, 1997.

[64] B. M. Eley and S. W. Cox, "The relationship between gingival crevicular fluid cathepsin B activity and periodontal attachment loss in chronic periodontitis patients: a 2-year longitudinal study," *Journal of Periodontal Research*, vol. 31, no. 6, pp. 381–392, 1996.

[65] H. Y. Chen, S. W. Cox, and B. M. Eley, "Cathepsin B, alpha2-macroglobulin and cystatin levels in gingival crevicular fluid from chronic periodontitis patients," *Journal of Clinical Periodontology*, vol. 25, no. 1, pp. 34–41, 1998.

[66] X. Li, Z. Wu, J. Ni et al., "Cathepsin B regulates collagen expression by fibroblasts via prolonging TLR2/NF-kappaB activation," *Oxidative Medicine and Cellular Longevity*, vol. 2016, Article ID 7894247, 12 pages, 2016.

[67] R. Nie, Z. Wu, J. Ni et al., "Porphyromonas gingivalis infection induces amyloid-β accumulation in monocytes/macrophages," *Journal of Alzheimer's Disease*, vol. 72, no. 2, pp. 479–494, 2019.

[68] J. Ni, Z. Wu, C. Peterts, K. Yamamoto, H. Qing, and H. Nakanishi, "The critical role of proteolytic relay through cathepsins B and E in the phenotypic change of microglia/macrophage," *Journal of Neuroscience*, vol. 35, no. 36, pp. 12488–12501, 2015.

[69] Z. Wu, L. Sun, S. Hashioka et al., "Differential pathways for interleukin-1β production activated by chromogranin A and amyloid β in microglia," *Neurobiology of Aging*, vol. 34, no. 12, pp. 2715–2725, 2013.

[70] K. Terada, J. Yamada, Y. Hayashi et al., "Involvement of cathepsin B in the processing and secretion of interleukin-1β in chromogranin A-stimulated microglia," *Glia*, vol. 58, no. 1, pp. 114–124, 2010.

[71] L. Sun, Z. Wu, Y. Hayashi et al., "Microglial cathepsin B contributes to the initiation of peripheral inflammation-induced chronic pain," *Journal of Neuroscience*, vol. 32, no. 33, pp. 11330–11342, 2012.

[72] C. Andrei, C. Dazzi, L. Lotti, M. R. Torrisi, G. Chimini, and A. Rubartelli, "The secretory route of the leaderless protein interleukin 1β involves exocytosis of endolysosome-related vesicles," *Molecular Biology of the Cell*, vol. 10, no. 5, pp. 1463–1475, 1999.

[73] Y. Liu, Z. Wu, X. Zhang et al., "Leptomeningeal cells transduce peripheral macrophages inflammatory signal to microglia in reponse to *Porphyromonas gingivalis* LPS," *Mediators of Inflammation*, vol. 2013, Article ID 407562, 11 pages, 2013.

[74] S.-J. Kang, S. Wang, H. Hara et al., "Dual role of caspase-11 in mediating activation of caspase-1 and caspase-3 under pathological conditions," *Journal of Cell Biology*, vol. 149, no. 3, pp. 613–622, 2000.

[75] R. Z. Murray, J. G. Kay, D. G. Sangermani, and J. L. Stow, "A role for the phagosome in cytokine secretion," *Science*, vol. 310, no. 5753, pp. 1492–1495, 2005.

[76] R. Z. Murray, F. G. Wylie, T. Khromykh, D. A. Hume, and J. L. Stow, "Syntaxin 6 and Vti1b form a novel SNARE complex, which is up-regulated in activated macrophages to facilitate exocytosis of tumor necrosis factor-α," *Journal of Biological Chemistry*, vol. 280, no. 11, pp. 10478–10483, 2005.

[77] R. A. Black, C. T. Rauch, C. J. Kozlosky et al., "A metalloproteinase disintegrin that releases tumour-necrosis factor-α from cells," *Nature*, vol. 385, no. 6618, pp. 729–733, 1997.

[78] J. L. Stow, A. P. Manderson, and R. Z. Murray, "SNAREing immunity: the role of SNAREs in the immune system," *Nature Reviews Immunology*, vol. 6, no. 12, pp. 919–929, 2006.

[79] W. Shurety, A. Merino-Trigo, D. Brown, D. A. Hume, and J. L. Stow, "Localization and post-Golgi trafficking of tumor necrosis factor-alpha in macrophages," *Journal of Interferon & Cytokine Research*, vol. 20, no. 4, pp. 427–438, 2000.

[80] J. K. Pagan, F. G. Wylie, S. Joseph et al., "The t-SNARE syntaxin 4 is regulated during macrophage activation to function in membrane traffic and cytokine secretion," *Current Biology*, vol. 13, no. 2, pp. 156–160, 2003.

[81] M. C. Pizzorno, "Nuclear cathepsin B-like protease cleaves transcription factor YY1 in differentiated cells," *Biochimica et Biophysica Acta (BBA)—Molecular Basis of Disease*, vol. 1536, no. 1, pp. 31–42, 2001.

[82] I. Jutras and T. L. Reudelhuber, "Prorenin processing by cathepsin B in vitro and in transfected cells," *FEBS Letters*, vol. 443, no. 1, pp. 48–52, 1999.

[83] A. D. Dunn and J. T. Dunn, "Cysteine proteinases from human thyroids and their actions on thyroglobulin," *Endocrinology*, vol. 123, no. 2, pp. 1089–1097, 1988.

[84] D. P. Dickinson, "Cysteine peptidases of mammals: their biological roles and potential effects in the oral cavity and other tissues in health and disease," *Critical Reviews in Oral Biology and Medicine: An Official Publication of the American Association of Oral Biologists*, vol. 13, no. 3, pp. 238–275, 2002.

[85] H. Nakanishi, "Microglial functions and proteases," *Molecular Neurobiology*, vol. 27, no. 2, pp. 163–176, 2003.

[86] P.-M. Andrault, S. A. Samsonov, G. Weber et al., "Antimicrobial peptide LL-37 is both a substrate of cathepsins S and K and a selective inhibitor of cathepsin L," *Biochemistry*, vol. 54, no. 17, pp. 2785–2798, 2015.

[87] P. Pietschmann, U. Foger-Samwald, W. Sipos, and M. Rauner, "The role of cathepsins in osteoimmunology,"

Critical Reviews in Eukaryotic Gene Expression, vol. 23, no. 1, pp. 11–26, 2013.

[88] S. Petanceska, P. Canoll, and L. A. Devi, "Expression of rat cathepsin S in phagocytic cells," *Journal of Biological Chemistry*, vol. 271, no. 8, pp. 4403–4409, 1996.

[89] V. Zavasnik-Bergant, A. Sekirnik, R. Golouh, V. Turk, and J. Kos, "Immunochemical localisation of cathepsin S, cathepsin L and MHC class II-associated p41 isoform of invariant chain in human lymph node tissue," *Biological Chemistry*, vol. 382, no. 5, pp. 799–804, 2001.

[90] O. A. Gonzalez, M. J. Novak, S. Kirakodu et al., "Comparative analysis of gingival tissue antigen presentation pathways in ageing and periodontitis," *Journal of Clinical Periodontology*, vol. 41, no. 4, pp. 327–339, 2014.

[91] L. Song, J. Yao, Z. He, and B. Xu, "Genes related to inflammation and bone loss process in periodontitis suggested by bioinformatics methods," *BMC Oral Health*, vol. 15, p. 105, 2015.

[92] T. Zavasnik-Bergant and B. Turk, "Cysteine cathepsins in the immune response," *Tissue Antigens*, vol. 67, no. 5, pp. 349–355, 2006.

[93] Z. Meng, W. Klinngam, M. C. Edman, and S. F. Hamm-Alvarez, "Interferon-gamma treatment in vitro elicits some of the changes in cathepsin S and antigen presentation characteristic of lacrimal glands and corneas from the NOD mouse model of Sjogren's syndrome," *PLoS One*, vol. 12, no. 9, Article ID e0184781, 2017.

[94] G.-P. Shi, J. A. Villadangos, G. Dranoff et al., "Cathepsin S required for normal MHC class II peptide loading and germinal center development," *Immunity*, vol. 10, no. 2, pp. 197–206, 1999.

[95] J. Bania, E. Gatti, H. Lelouard et al., "Human cathepsin S, but not cathepsin L, degrades efficiently MHC class II-associated invariant chain in nonprofessional APCs," *Proceedings of the National Academy of Sciences*, vol. 100, no. 11, pp. 6664–6669, 2003.

[96] M. Reich, P. F. van Swieten, V. Sommandas et al., "Endocytosis targets exogenous material selectively to cathepsin S in live human dendritic cells, while cell-penetrating peptides mediate nonselective transport to cysteine cathepsins," *Journal of Leukocyte Biology*, vol. 81, no. 4, pp. 990–1001, 2007.

[97] C. Driessen, R. A. R. Bryant, A.-M. Lennon-Duménil et al., "Cathepsin S controls the trafficking and maturation of MHC class II molecules in dendritic cells," *Journal of Cell Biology*, vol. 147, no. 4, pp. 775–790, 1999.

[98] P. McGuirk and K. H. G. Mills, "Pathogen-specific regulatory T cells provoke a shift in the Th1/Th2 paradigm in immunity to infectious diseases," *Trends in Immunology*, vol. 23, no. 9, pp. 450–455, 2002.

[99] L. E. Harrington, R. D. Hatton, P. R. Mangan et al., "Interleukin 17-producing $CD4^+$ effector T cells develop via a lineage distinct from the T helper type 1 and 2 lineages," *Nature Immunology*, vol. 6, no. 11, pp. 1123–1132, 2005.

[100] M. Novinec and B. Lenarčič, "Cathepsin K: a unique collagenolytic cysteine peptidase," *Biological Chemistry*, vol. 394, no. 9, pp. 1163–1179, 2013.

[101] M. Matsumoto, M. Kogawa, S. Wada et al., "Essential role of p38 mitogen-activated protein kinase in cathepsin K gene expression during osteoclastogenesis through association of NFATc1 and PU.1," *Journal of Biological Chemistry*, vol. 279, no. 44, pp. 45969–45979, 2004.

[102] A. H. Aguda, P. Panwar, X. Du, N. T. Nguyen, G. D. Brayer, and D. Brömme, "Structural basis of collagen fiber degradation by cathepsin K," *Proceedings of the National Academy of Sciences*, vol. 111, no. 49, pp. 17474–17479, 2014.

[103] B. R. Troen, "The regulation of cathepsin K gene expression," *Annals of the New York Academy of Sciences*, vol. 1068, no. 1, pp. 165–172, 2006.

[104] L. Funkelstein, M. Beinfeld, A. Minokadeh, J. Zadina, and V. Hook, "Unique biological function of cathepsin L in secretory vesicles for biosynthesis of neuropeptides," *Neuropeptides*, vol. 44, no. 6, pp. 457–466, 2010.

[105] G. Garg, A. R. Pradeep, and M. K. Thorat, "Effect of nonsurgical periodontal therapy on crevicular fluid levels of cathepsin K in periodontitis," *Archives of Oral Biology*, vol. 54, no. 11, pp. 1046–1051, 2009.

[106] N. Yamalik, S. Gunday, K. Kilinc, E. Karabulut, E. Berker, and T. F. Tozum, "Analysis of cathepsin-K levels in biologic fluids from healthy or diseased natural teeth and dental implants," *The International Journal of Oral & Maxillofacial Implants*, vol. 26, no. 5, pp. 991–997, 2011.

[107] N. Yamalik, S. Günday, S. Uysal, K. Kilinç, E. Karabulut, and T. F. Tözüm, "Analysis of cathepsin-K activity at tooth and dental implant sites and the potential of this enzyme in reflecting alveolar bone loss," *Journal of Periodontology*, vol. 83, no. 4, pp. 498–505, 2012.

[108] P. Gajendran, H. Parthasarathy, and A. Tadepalli, "Comparative evaluation of cathepsin K levels in gingival crevicular fluid among smoking and nonsmoking patients with chronic periodontitis," *Indian Journal of Dental Research*, vol. 29, no. 5, pp. 588–593, 2018.

[109] A. Beklen, A. Al-Samadi, and Y. Konttinen, "Expression of cathepsin K in periodontitis and in gingival fibroblasts," *Oral Diseases*, vol. 21, no. 2, pp. 163–169, 2015.

[110] M. Asagiri, T. Hirai, T. Kunigami et al., "Cathepsin K-dependent toll-like receptor 9 signaling revealed in experimental arthritis," *Science*, vol. 319, no. 5863, pp. 624–627, 2008.

[111] D. De Nardo, "Toll-like receptors: activation, signalling and transcriptional modulation," *Cytokine*, vol. 74, no. 2, pp. 181–189, 2015.

[112] K. Hayashi, M. Taura, and A. Iwasaki, "The interaction between IKKalpha and LC3 promotes type I interferon production through the TLR9-containing LAPosome," *Science Signaling*, vol. 11, no. 528, 2018.

[113] X. Li, Y. Cen, Y. Cai et al., "TLR9-ERK-mTOR signaling is critical for autophagic cell death induced by CpG oligodeoxynucleotide 107 combined with irradiation in glioma cells," *Scientific Reports*, vol. 6, no. 1, p. 27104, 2016.

[114] C.-S. Shi and J. H. Kehrl, "MyD88 and trif target beclin 1 to trigger autophagy in macrophages," *Journal of Biological Chemistry*, vol. 283, no. 48, pp. 33175–33182, 2008.

[115] A. Criollo, L. Senovilla, H. Authier et al., "The IKK complex contributes to the induction of autophagy," *The EMBO Journal*, vol. 29, no. 3, pp. 619–631, 2010.

[116] W. Pan, W. Yin, L. Yang et al., "Inhibition of Ctsk alleviates periodontitis and comorbid rheumatoid arthritis via downregulation of the TLR9 signalling pathway," *Journal of Clinical Periodontology*, vol. 46, no. 3, pp. 286–296, 2019.

Hindawi
Evidence-Based Complementary and Alternative Medicine
Volume 2020, Article ID 1303524, 10 pages
https://doi.org/10.1155/2020/1303524

Review Article

Research Progress on Anti-Inflammatory Effects and Mechanisms of Alkaloids from Chinese Medical Herbs

Sicong Li,[1] **Xin Liu**,[2] **Xiaoran Chen**,[1] **and Lei Bi**[2]

[1]*School of Pharmacy, Peking University Health Science Centre, Beijing, China*
[2]*School of Traditional Chinese Medicine, Beijing University of Traditional Chinese Medicine, Beijing 100029, China*

Correspondence should be addressed to Xin Liu; xinliu1011@126.com

Received 8 January 2020; Accepted 17 February 2020; Published 18 March 2020

Guest Editor: Tae Jin lee

As the spectrum of diseases keeps changing and life pace keeps going faster, the probability and frequency of diseases caused by human inflammatory reactions also keep increasing. How to develop effective anti-inflammatory drugs has become the hotspot of researches. It has been found that alkaloids from Chinese medical herbs have anti-inflammatory, analgesic, antitumor, anticonvulsant, diuretic, and antiarrhythmic effects, among which the anti-inflammatory effect is very prominent and commonly used in the treatment of rheumatoid arthritis, ankylosing spondylitis, and other rheumatic immune diseases, but its mechanism of action has not been well explained. Based on this, this paper will classify alkaloids according to structural types and review the plant sources, applicable diseases, and anti-inflammatory mechanisms of 16 kinds of alkaloids commonly used in clinical treatment, such as berberine, tetrandrine, and stephanine, with the aim of providing a reference for drug researches and clinical applications.

1. Introduction

Inflammation has been considered as the main risk factor of rheumatic immune diseases. As the incidence rate of this disease keeps increasing in recent years, how to effectively resist inflammation has attracted widespread attentions. The application of anti-inflammatory Chinese medical herbs not only enjoys a long history, a wide range of sources, and rich varieties, but also has complex and diverse pharmacological effects. Therefore, it has become a research hotspot to search for anti-inflammatory active ingredients in Chinese medical herbs, among which alkaloids are of great representativeness. Alkaloids are nitrogen-containing organic compounds with an alkali like properties. They are widely distributed in *Tripterygium wilfordii* and *Begonia kunmingshanensis* of Celastraceae; *Sinomenium acutum*, *Stephania tetrandra* S. Moore, and *Menispermum dauricum* DC. of Menispermaceae [1]; *Coptis chinensis* Franch., *Aconitum carmichaelii*, *Aconitum kusnezoffii* Reichb., *Aconitum carmichaelii* Debx., and *Clematis chinensis* Osbeck of Ranunculaceae; *Gentiana macrophylla* Pall. and *Gentiana scabra Bunge*. of Gentianaceae, and so on [2]. Some alkaloids have strong anti-inflammatory activities and play important roles in the treatment of rheumatoid arthritis, Behcet's disease, ankylosing spondylitis, myasthenia gravis, systemic lupus erythematosus, dermatomyositis, and other rheumatic immune diseases [3]. The following is a comprehensive review of researches on alkaloids from Chinese medical herbs. By taking chemical structure as the classification standard, anti-inflammatory effects and possible mechanisms of various alkaloids are introduced in detail, which are expected to lay the foundation for follow-up researches and developments of anti-inflammatory drugs.

2. Isoquinoline Alkaloids

Isoquinoline alkaloids are widely distributed in 27 sections of plants, such as Menispermaceae, Berberidaceae, Papaveraceae, and Ranunculaceae [4]. Isoquinoline alkaloids, taking isoquinoline or tetrahydroisoquinoline as the basic parent nucleus, can be divided into 20 categories, including simple isoquinoline, benzylisoquinoline, phenethyl isoquinoline, naphthyl isoquinoline, aporphine, morphine,

phenanthridine, and pyrrolidine. Isoquinoline alkaloids have anti-inflammatory, analgesic, spasmolysis, antibacterial, and relieving asthma effects [5]. Among them, berberine, tetrandrine, dauricine, sinomenine, lycorine, and stephanine have good anti-inflammatory effects.

2.1. Berberine. Berberine, a kind of benzylisoquinoline alkaloid extracted from the rhizome of *Coptis chinensis* Franch., the bark of *Phellodendron chinensis* Schneid., and *Daemonorops margaritae* (Hance) Becc. [6], has therapeutic effects on rheumatoid arthritis, delayed type hypersensitivity, ulcerative colitis, autoimmune tubulointerstitial nephritis, and other rheumatic autoimmune diseases [7]. 8 mg/kg of berberine subcutaneously injected to rats can inhibit rats' paw swelling induced by carrageenan and mice's auricle swelling induced by xylene. Intraperitoneal injection of berberine (50 mg/kg) can inhibit the increased skin capillary permeability caused by histamine [8].

Intraperitoneal injection of 30 mg/kg of berberine for 8 days can inhibit the increased prostaglandin E2 (PGE2) in paw swelling mice induced by formalin [9]. The mechanism is that berberine can inhibit PGE2 synthesis by reducing the concentration of cyclooxygenase-2 (COX-2). Oral administration of berberine (1.5 mg/ml) can inhibit the delayed hypersensitivity induced by dinitrofluorobenzene in mice [10], by means of inhibiting the production and secretion of interferon-γ, interleukin-1 (IL-1), tumor necrosis factor (TNF-α), interleukin-2 (IL-2), interleukin-8 (IL-8), interleukin-6 (IL-6), and monocyte chemotactic protein-1 (MCP-1) [11]. Berberine has a therapeutic effect on autoimmune nephritis of rats induced by alloantigens, such as primary anti-glomerular basement membrane and Heymann nephritis. It can inhibit the excretion of urinary protein and reduce serum creatinine content and pathological changes of glomerulus [12].

In terms of diseases in the digestive system, berberine can protect the gastric mucosa from chemical factors. Berberine can inhibit the activation of nuclear factor kappa-B (NF-κB) and the transcription of inflammatory cytokines in ulcerative colitis mice induced by dextran sodium sulfate [13]. Berberine can inhibit not only the adhesion between endothelial cells and polymorphonuclear leukocytes activated by IL-1 and tumor necrosis factor-α (TNF-α) but also the adhesion of polymorphonuclear leukocytes and vascular endothelial cells activated by TNF-α, so as to reduce the infiltration of inflammatory cells and lesions of colonic mucosa [14].

2.2. Tetrandrine. Tetrandrine is a kind of bisbenzylisoquinoline alkaloid extracted from the root of *Stephania tetrandra* S. Moore. and *Stephania japonica* (Thumb.) Miers [15]. It has therapeutic effects on gout, osteoarthritis, and systemic lupus erythematosus. Tetrandrine can significantly inhibit rats' joint swelling caused by carrageenan or formaldehyde and increased vascular permeability in rats induced by histamine [16]. Intraperitoneal injection of 20 mg/kg of tetrandrine can significantly reduce the amount of hydrothorax, protein exudation, and leukocyte migration in rats with pleurisy caused by carrageenan [17]. The effect of inhibiting leukocyte migration is stronger than the effect of inhibiting the exudation of hydrothorax and proteins. Intraperitoneal injection of 20 mg/kg of tetrandrine also significantly reduces the activity of neutrophils (Neu-PLA2) and the acellular component (ACC-PLA2) [18]. Tetrandrine in the treatment of experimental auricular burns plays a direct excitatory adrenal function. Tetrandrine not only inhibits cyclooxygenase (COX)-2 and nitric oxide synthase (iNOS) by interfering with NF-κB/COX-2 signaling pathway, but also inhibits histamine, platelet-derived growth factor (PDGF), IL-1β, and TNF-α in inflammatory reactions and promotes the expression of the anti-inflammatory cytokine IL-10 [19].

Intragastric administration of 6.25 mg/kg of tetrandrine can reduce the concentration of nitric oxide in serum and pancreatic tissue of rats with acute hemorrhagic necrotizing pancreatitis, reduce the activity of phospholipase A2, and inhibit the activation of NF-κB, thus inhibiting the production of IL-6, IL-8, and TNF-α inflammatory factors, as well as reducing the inflammatory response of pancreas [20].

In the inflammatory model of RAW264.7 cells induced by lipopolysaccharide (LPS), tetrandrine can not only inhibit the phosphorylation of NF-κB inhibitor α, but also reduce the production of nitric oxide (NO) and prostaglandin E2 (PGE2), and the expression of matrix metalloproteinase-3 (MMP-3) and tissue metalloproteinase inhibitor-1 (TIMP-1) [21].

2.3. Dauricine. Dauricine, a kind of benzylisoquinoline alkaloid extracted from the rhizome and rattan of *Menispermum dauricum DC* [22], has therapeutic effects on rheumatoid arthritis, ischemic stroke, coronary atherosclerotic heart disease, and ventricular premature beat.

Dauricine can significantly improve neurological deficit symptoms and reduce the apoptosis rate of neurons in ischemic brain tissue [23]. Moreover, it can inhibit the expression of nuclear factor KB, intercellular adhesion molecule-1, and cyclooxygenase-2. Intraperitoneal injection of 40 mg/kg of dauricine can effectively reduce liver injury in mice induced by CCl_4. Its mechanism is related to inhibiting the expression of TGF β1 and TNF-α [24].

In vitro studies, it is identified that pretreatment of dauricine can dose-dependently inhibit not only the contents of NO, IL-1β, IL-6, TNF-α, and intercellular adhesion molecule-1 (ICAM-1), but also the activity of inducible nitric oxide synthase (iNOS), myeloperoxidase (MPO), and cyclooxygenase-2 (COX-2) in LPS-stimulated macrophages [25].

Intraperitoneal injection of 50 mg/kg of dauricine, with pharmacological actions similar to hydrocortisone, can inhibit the increased capillary permeability caused by histamine and acetic acid, inflammatory edema caused by xylene in mice, and edema of hind paws caused by carrageenan in rats [26]. Dauricine has the same anti-inflammatory effect on adrenalectomized rats. The anti-inflammatory effect of dauricine at the same dosage in normal rats is stronger than that in adrenalectomized rats. Dauricine can also reduce the

content of ascorbic acid in adrenal glands. It can be concluded that dauricine also has an indirect anti-inflammatory effect by stimulating the pituitary adrenal cortex system [27].

2.4. Sinomenine. Sinomenine, a kind of benzyl alkaloid, is extracted from the stem and root of *Sinomenium acutum* (Thunb.) Rehd. et Wils. [28]. It can be used in the treatment of rheumatoid arthritis, chronic nephritis, ankylosing spondylitis, myocardial ischemia, ventricular premature beats, and other rapid arrhythmias. Sinomenine can inhibit the foot swelling caused by egg white, formaldehyde, or carrageenan [29].

Oral administration of 30 mg/kg of sinomenine can not only inhibit the activity of iNOS and COX-2 in rats but also inhibit the synthesis and release of PGE2 and leukotriene in inflammatory areas. Sinomenine can alleviate LPS-induced lung inflammation by inhibiting the expression of nitric oxide (NO), myeloperoxidase (MPO), TNF-α, and IL-6 [30].

Sinomenine achieves the anti-inflammatory effect by inhibiting NF-κB and JNK signaling pathways. The mechanism is that it inhibits the expression of TNF-α mRNA and IL-1β mRNA in synovial cells by inhibiting NF-κB activity [31]. Sinomenine can not only inhibit the synthesis of prostaglandin F2a (PGF2a) and leukotriene in macrophages, but also reduce the synthesis of nitric oxide (NO) in cells [32]. Sinomenine can prevent the aggregation of neutrophils caused by complement activation, so as to improve rat antigenic arthritis caused by calf serum albumin. It is found that sinomenine can inhibit the proliferation of lymphocytes induced by mitosis and mixed lymphocyte culture. At the same time, the concentration of IL-1, IL-6, TNF, and other inflammatory cytokines in the supernatant of cultured cells decreases [33]. Moreover, sinomenine has the ability to inhibit inflammation in LPS-stimulated macrophages by regulating CD14/TLR4, JAK2/STAT3 pathway, and calcium signal through alpha 7nAChR [34].

2.5. Lycorine. Lycorine, a kind of pyrrolidine alkaloid extracted from the bulb of *Lycoris radiata* (L′ Her.) Herb., has a therapeutic effect on osteoarthritis, deformable osteitis, gout, ankylosing spondylitis, and other rheumatic autoimmune diseases. Intravenous injection of 3 mg/kg of lycorine has a therapeutic effect on formalin arthritis in rabbits and protein arthritis in rats [35]. In the endotoxic shock model mice, 80% of the mice in normal saline group die of endotoxic shock within 40 hours after injecting LPS. After intravenous injection of 40 mg/kg of lycorine, the survival rate of mice gets to 60%, rather than 20% in the normal saline control group [36].

Tolerance ability of inflammatory factors in mice gets improved after injecting lycorine. It is found that lycorine (5 μm) can inhibit activities of iNOS and cyclooxygenase-2 induced by LPS. The inhibitory effect is stronger than that of dexamethasone. In addition, lycorine can also inhibit the production of PGE2 and IL-6 in macrophages to play an antipyretic and analgesic role [37].

A STAT signaling pathway is one of the common pathways of physiological and pathological reactions in the human body. JAK-STAT pathway gets involved in the signal transduction and regulation of many important inflammatory/anti-inflammatory cytokines [38]. STATs are many cytoplasmic proteins that bind to the DNA of the target gene regulatory region. They are conjugated to tyrosine phosphorylation signals to complete transcriptional regulation. It is found that lycorine (5 μM) inhibited the activation of STAT1 and STAT3 stimulated by LPS [39].

2.6. Stephanine. Stephanine, a kind of simple isoquinoline alkaloid, is extracted from the root and tuber of *Menispermum japonicum* Thunb. [40]. It has a therapeutic effect on rheumatoid arthritis, osteoarthritis, and gout. Stephanine has an obvious inhibitory effect on xylene induced inflammatory edema, toe swelling induced by egg white, and adjuvant arthritis. Intraperitoneal injection of 10 mg/kg of stephanine can reduce myeloperoxidase (MPO) activity and contents of TNF-α, IL-1β, and IL-6 in the mammary gland tissue of mastitis rats induced by LPS [41]. Stephanine at this dosage can not only inhibit p65 phosphorylation and IκB degradation, but also improve the pathological changes of breast tissue. Intraperitoneal injection of 20 mg/kg of stephanine can reduce the expression of NF-κB, phospho-p38 MAPK, phospho-JNK, NLRP3, and IL-1β in the brain tissue of mice with focal cerebral ischemia, so as to play an anti-inflammatory role [42]. Intragastric administration of 15 g/kg of stephanine can not only reduce the content of ICAM-1, IL-1β, and IL-18 but also increase the content of IL-12 in peripheral blood and nasal lavage fluid [43].

3. Piperidine Alkaloids

Piperidine alkaloids are derived from lysine, including piperidine, indolicidin, and quinolizidine. These alkaloids can be found in *Sophora flavescens* Ait., *Diphasiastrum veitchii*., *Piper nigrum* L., *Lobelia chinensis* Lour., etc. [44]. Piperidine alkaloids have anti-inflammatory, anticonvulsant, anticancer, and antiarrhythmic effects. Among them, aloperine, sophoridine, and matrine have good anti-inflammatory effects [1].

3.1. Aloperine. Aloperine, extracted from *Sophora alopecuroides*, has therapeutic effects on myocardial ischemia-reperfusion injury, acute renal injury, asthma, ventricular hypertrophy, pulmonary hypertension, and other cardiovascular diseases [45]. The concentration of IL-6, TNF-α, and IL-1β in H9c2 cardiomyocytes decreases significantly after intragastric administration of 50 mg/L of aloperine for 48 hours, which suggests that aloperine can alleviate myocardial ischemia-reperfusion injury by inhibiting inflammatory response [46]. Intragastric administration of 40 mg/kg of aloperine for 14 days can reduce the levels of IL-6, IL-1β, TNF-α, NO, MCP-1, ADMA, ICAM-1, and VCAM-1, thus inhibiting the myocardial fibrosis and ventricular hypertrophy caused by isoproterenol [47].

IL-6 and TGF-β1 play an important role in the development of pulmonary hypertension. Pulmonary hypertension is often accompanied by a large number of inflammatory cells

infiltration into pulmonary vascular lesions. The expression levels of NF-κB, TNF-α, and IL-1β protein significantly reduce after intragastric administration of 100 mg/kg of aloperine [48]. The result of flow cytometry shows that 0.5 mM of aloperine can reduce the expression levels of NF-κ, Bp65, p-IKKα, p-IκBα, TNF-α, and CyclinE1 [49]. After the application of aloperine, the injury of pulmonary vascular endothelial cells gets significantly improved, the shape of the nucleus of endothelial cells becomes basically normal, and the expansion of the Golgi body and endoplasmic reticulum gets improved. It suggests that rotenone can improve pulmonary hypertension induced by monocrotaline through the NF-κB p65 signaling pathway [50].

In terms of respiratory diseases, intragastric administration of 40 mg/kg of aloperine can improve lung function, alleviate asthma symptoms, and inhibit inflammatory responses in asthmatic mice. The mechanism is related to the regulation of the NF-κB inflammatory signal pathway and the reduction of TNF-α and IL-1β levels [51].

3.2. Sophoridine. Sophoridine, extracted from the roots of *Sophora flavescens*, has therapeutic effects on rheumatoid arthritis and ankylosing spondylitis, as well as organ damage caused by endotoxin and exogenous toxicant [52]. Intragastric administration of 40 mg/kg of sophoridine can reduce the increased permeability of capillaries and inhibit the auricle swelling induced by xylene [53]. Intraperitoneal injection of 5 mg/kg of sophoridine for 3 days in advance can prevent the lung and kidney injury caused by endotoxin and reduce the congestion, edema, and blood seepage into lung tissue as well as edema and inflammatory cell infiltration in renal tubular epithelial cells [54]. Its anti-inflammatory mechanism is to downregulate the expression of lipopolysaccharide recognition receptor, lipopolysaccharide-binding protein, CD14, and TLR4, as well as the transcription of nuclear factor c-Jun and c-fos genes. Sophoridine inhibits not only the phosphorylation of p38 mitogen-activated protein kinase (p38 MAPK) but also the expression and release of IL-6, TNF-α, and NO [55]. Continuously intraperitoneal injection of 125 mg/kg of sophoridine for 8 weeks significantly inhibits acute liver injury in mice induced by carbon tetrachloride [56]. The damage of liver tissue in mice gets alleviated, which appears as the orderly arrangement of hepatocytes, the reduction of focal necrosis, cell balloon degeneration, steatosis, and interstitial inflammation. The protective mechanism of sophoridine is related to its inhibition of cyclooxygenase-2 activity and the reduction of TNF-α and other inflammatory cytokines [57].

3.3. Matrine. Matrine, extracted from the root of *Sophora flavescens*, has therapeutic effects on rheumatoid arthritis, psoriasis, ulcerative colitis, ankylosing spondylitis, asthma, acute lung injury, acute respiratory distress syndrome, and cerebral infarction [58].

Hypodermic injection of 25 mg/kg of marine can inhibit the swelling of auricle caused by croton oil, the acute inflammatory swelling of the toes caused by carrageenan, or egg white [59]. Moreover, it can inhibit the increased capillary permeability in the abdominal cavity caused by acetic acid in both normal mice and adrenalectomized mice.

In terms of respiratory diseases, 3 hours after endotoxin injection, intraperitoneal injection of marine (10 mg/kg) can resist the pathological changes of lung tissue in mice caused by lipopolysaccharide and reduce pulmonary edema, pulmonary vascular leakage, and rise in temperature [60]. Moreover, it can not only inhibit the activity of myeloperoxidase (MPO) and malondialdehyde (MDA) but also reduce the content of TNF-α, IL-1β, and IL-6. Matrine can inhibit airway inflammation by inhibiting the signal transduction of NF-κB in airway epithelial cells of asthmatic mice, reducing the expression of SOCS3 as well as the production of reactive oxygen species (ROS) and inflammatory factors in alveolar macrophages [61].

Matrine also has a protective effect on lung injury caused by ulcerative colitis. The mechanism is to enhance the anti-inflammatory and scavenging oxygen free radical ability of lung tissue and upregulate the repair factors in lung and gut tissue by increasing the expression of ZO-1 and Occludin, which are closely related to the mucosa of lung tissue. Matrine has a strong inhibitory effect on TNF-α and can effectively reduce the secretion of IL-1α and IL-8 [62].

In terms of nervous system diseases, injecting matrine (30mg/kg) into the jugular vein can inhibit the activity of 12/15-lipoxygenase and the expression of NF-κB, TLR4, and TLR2 in ischemic brain tissue [63]. Moreover, it can reduce not only the nerve function defect of right middle cerebral artery occlusion model rats but also the volume of local cerebral infarction. The results above suggest that matrine has an obvious neuroprotective effect on ischemic brain tissues.

In vitro, matrine at the dosage of 50 μmol/L can significantly inhibit the expression of IL-6, IL-8, TNF-α, NF-κB, and intracellular adhesion molecule 1 in colon epithelial cells induced by lipopolysaccharide. Matrine at the dosage of 100 μmol/L can significantly resist the inflammatory damage of colon epithelial cells induced by lipopolysaccharide [64].

4. Terpene Alkaloids

Terpene alkaloids come from mevalonic acid. They can be classified into four categories, which include monoterpenes, sesquiterpenes, diterpenes, and triterpenes. Terpene alkaloids have antihypertensive, analgesic, anti-inflammatory, antipyretic, and sedative effects. Among them, gentianine, aconitine, and bulleyaconitine A have good anti-inflammatory effects [65].

4.1. Gentianine. Gentianine, a kind of monoterpene alkaloid, is extracted from the root of *Gentiana scabra* Bunge., the whole herb of *Gentiana algida* Pall., and the seeds from *Trigonella foenum-graecum*. Intraperitoneal injection of 90 mg/kg of gentianine for 10 days can reduce not only the increase of capillary permeability caused by egg white but also the formaldehyde-induced foot swelling in rats, accelerating the swelling to subside as well [66]. The effect is equivalent to 200 mg/kg of sodium salicylate but does not

lead to gastrointestinal bleeding [67]. The content of vitamin C in adrenal gland of rats significantly decreases after injecting gentianine. But this effect disappears after the removal of the pituitary gland. Therefore, it can be concluded that the anti-inflammatory effect of gentianine is related to hypophyseal-adrenocortical functions.

Gentianine inhibits IL-1β-induced inflammatory responses in rats' articular chondrocytes by inhibiting the activity of P38, extracellular regulated protein kinases (ERK), and c-Jun N-terminal kinase (JNK). In addition, gentianine can also inhibit the release of matrix metalloproteinases (MMPs) induced by IL-1β and promote the expression of type II collagen [68]. Oral administration of 50 mg/kg of gentianine for 12 weeks can reduce body weight and visceral fat mass in mice, which was associated with reduced levels of inflammatory cytokines (NF-κb1, TNF-α, and IL-6). Oral administration of gentianine at the dosage of 60 mg/kg for 7 days has a therapeutic effect on contact dermatitis induced by 1-fluoro-2,4-dinitrofluorobenzene (DNFB) [69]. Gentianine can inhibit epidermal hyperplasia and immune cell infiltration, as well as reducing the production of TNF-α, IFN-α, IL-6, and MCP-1 in inflammatory tissues.

4.2. Aconitine. Aconitine, a kind of diterpene alkaloids extracted from the root tuber of *Aconitum carmichaeli* Debx., has a therapeutic effect on rheumatoid arthritis, ankylosing spondylitis, and other autoimmune diseases [70]. Oral administration, subcutaneous injection, or intramuscular injection of aconitine can significantly reduce the content of ascorbic acid in the adrenal glands of rats. This effect cannot be blocked by pentobarbital and chlorpromazine. Oral administration of 0.1 mg/kg of aconitine has inhibitory effects on the edema of toes in rats caused by carrageenan, ear swelling in mice caused by croton oil, and joint swelling in rats caused by formaldehyde [71]. The effect of aconitine exerted on the symptoms above is stronger than indometacin. Intragastric administration of 60 mg/L of aconitine can improve the acute lung injury in rats caused by lipopolysaccharide, by means of inhibiting the activation of NF-κB, reducing the contents of inflammation transcription factor NF-κB and inflammatory mediators TNF-α, IL-6, and IL-1β. Moreover, no evidence has been founded to support aconitine's toxicity to the cells of the lung tissue [72].

4.3. Bulleyaconitine A. Bulleyaconitine A, a kind of aconitine diterpenoid alkaloids, is extracted from the root tuber of *Aconitum kusnezoffii* Rchb. [73]. Nowadays, bulleyaconitine A has been widely used in the clinical treatment of rheumatoid arthritis, ankylosing spondylitis, knee osteoarthritis, and gout. Bulleyaconitine A has an obvious anti-inflammatory effect by inhibiting the phagocytic function of macrophages as well as the release of nitric oxide, INF-γ, and PGE2 [74]. Intraperitoneal injection of 0.48 mg/kg for 7 consecutive days can effectively reduce the content of IL-4, IL-10, IL-6, TNF-α, and MCP-1 produced by LPS-induced RAW264.7 cells [75]. Intraperitoneal injection of 0.48 mg/kg can not only decrease the expression of NF-κB1 and PKC-δ in the NF-κB signaling pathway in the lung tissues of asthmatic mice, but also reduce the contents of IL-4, IL-10, TNF-α, and MCP-1 in bronchoalveolar lavage fluid [76].

5. Purine Alkaloids

Purine alkaloids have the same purine ring structure and can be transformed into each other under specific conditions, mainly including caffeine, theophylline, theobromine, xanthine, and hypoxanthine. Among them, theophylline has a good anti-inflammatory effect and has been widely used in the clinical treatment of Chronic Obstructive Pulmonary Disease (COPD) and other pulmonary diseases.

5.1. Theophylline. Theophylline, extracted from tea and cocoa beans, has the functions of anti-inflammatory, bronchiectasis, immunity regulation, and improving the contractility of septal muscle. It has therapeutic effects on bronchial asthma, emphysema, and heart failure [77]. Theophylline exerts anti-inflammatory effects by inhibiting the release of phosphodiesterase and neuropeptides. At appropriate levels, theophylline strongly inhibits antigen-activated late-phase reactions, which are associated with the inhibition of the activation of neutrophils and the release of inflammatory mediators induced by phosphodiesterase. Theophylline has direct dilating effects on the smooth muscle of the respiratory tract [78]. Theophylline also inhibits adenosine receptor, increases the release of interleukin-10, and inhibits the transcriptional expression of NF-κB and the activation of inflammatory cells and T cells from peripheral blood to airway mucosa metastasis, thus playing an anti-inflammatory and immune regulatory role. Oral administration of 0.1 g of theophylline twice a day can reduce the contents of IL-4, IL-5, IL-6, IL-8, IL-17, TNF-α, and C-reactive protein (CRP) in COPD patients. Moreover, theophylline of this dosage can increase the activity and expression of histone deacetylase-2 in the blood of COPD patients and improve the sensitivity of the human body to glucocorticoids [79].

Moreover, a low dosage of theophylline can inhibit the abnormal expression of ET-1 induced by inflammatory cytokines in smooth muscle, which is one of its mechanisms of reducing the hyperresponsiveness of asthmatic airway.

6. Organic Amine Alkaloids

Organic amine alkaloid is a kind of important alkaloid. Nitrogen atoms in this alkaloid are not combined in a ring structure. Colchicine, betaine, ephedrine, demecolcine, and leonurine belong to this kind of alkaloids.

6.1. Colchicine. Colchicine, extracted from the seeds and bulbs of *Colchicum autumnale* L., has been now widely used in the treatment of gout and the first choice for acute gout attacks. The 2016 European rheumatic union guidelines for the treatment of gout [80] suggests that colchicine is almost equivalent to nonsteroidal anti-inflammatory drugs and

glucocorticoids and the guidelines advocates to start the treatment of gout with low doses of colchicine.

Monosodium urate crystal deposition is the central link in the pathogenesis of gouty arthritis. When neutrophils phagocytize monosodium urate crystals, lysosomes can be induced to release a chemokine derived from glycopeptide crystals, which can significantly amplify the recruitment of neutrophils. Colchicine, by means of inhibiting the aggregation of neutrophils at the joints, weakens neutrophils' phagocytosis towards monosodium urate crystals and reduces the inflammatory response caused by partial neutrophils [81]. Moreover, colchicine can change the expression of L-selectin in neutrophils and the distribution of E-selectin in endothelial cells, so as to inhibit the release of leukotriene B4, as well as the adhesion, exudation, and recruitment of neutrophils [82]. Colchicine can inhibit not only the chemotaxis, adhesion, and superoxidation of neutrophils but also the process and release of NOD-like receptor heat protein domain-related protein inflammasomes and interleukin-1β.

In terms of heart disease, oral administration of 1.5 mg of colchicine for 5 days can reduce hypersensitive C-reactive protein (hs-CRP), IL-1, IL-6, IL-8, and Neutrophilic Alkaline Phosphatase 3 (NALP3) levels in patients' serum with acute myocardial infarction [83]. Moreover, it can not only improve the expression of IL-1, apoptosis-related microprotein ASC, cysteine, proteinase-caspase-1, and NLRP3 mRNA in peripheral blood but also reduce the myocardial damage mediated by the inflammatory response. Colchicine can prevent the recurrence of atrial fibrillation after radiofrequency ablation, which is closely related to the reduction of the contents of interleukin-6 and CRP. Vascular atherosclerotic disease is a chronic immune inflammatory disease and smoking is an independent risk factor for atherosclerosis disease. After the oral administration of colchicine (0.1 mg/(kg·d)) for eight weeks, the contents of intercellular adhesion molecule-1 (ICAM-1), vascular adhesion molecules-1 (VCAM-1), monocyte chemoattractant protein-1 (MCP-1), IL-6, IL-1β, and TNF-α in the aorta of mice exposed to tobacco for a long period of time could be reduced to achieve the purpose of vascular protection [84].

7. Indole Alkaloid

Indole alkaloids, mainly derived from tryptophan, are the largest and most complex alkaloids. Indole alkaloids are divided into four groups: simple indoles, tryptophan indole, hemiterpenoid indoles, and monoterpene indoles.

7.1. Rhynchophylline. Rhynchophylline, a kind of monoterpene indole alkaloids, is the highest in the content of *Uncaria rhynchophylla* (Miq.) Miq. ex Havil. [85]. It has therapeutic effects on epilepsy, hypertension, and Parkinson's diseases. Rhynchophylline can significantly increase the pain threshold of mice and inhibit auricle swelling by reducing capillary permeability caused by xylene [86]. In vitro, 5 μg/μL of rhynchophylline can inhibit the production of IL-1β and TNF-α in dopaminergic neurons and glial cells induced by lipopolysaccharide, so as to protect neurons. Rhynchophylline can also inhibit the phosphorylation of p38 MAPK, then block the nuclear translocation of NF-κB, and inhibit its transcriptional function, so as to inhibit the vascular endothelial cell damage caused by intermittent hypoxia [87].

7.2. Brucine. Brucine, a kind of monoterpene indole alkaloids extracted from the mature seeds of *Strychnos nux-vomica* Linn., has therapeutic effects on myasthenia gravis, rheumatoid arthritis, and hemiplegia caused by cerebrovascular diseases [88]. Brucine can inhibit auricle swelling caused by xylene in mice. Oral administration of 3 mg/kg of brucine can inhibit adjuvant arthritis in rats and reduce the concentrations of NO and NOS in serum, thus reducing the destruction of articular cartilage and protecting the function of chondrocytes [89]. In myasthenia gravis model rats, brucine can not only reduce the serum level of acetylcholine receptor antibody and IL-6, but also inhibit the activation of T cells and B cells.

8. Summary

As people learn more and more about nature, Chinese medical herbs have become important sources for the creation of new medicines. The purpose of researches on the anti-inflammatory effects and mechanisms of alkaloids in Chinese materia medica is to find new anti-inflammatory drugs with high selectivity and strong effect and improve the effectiveness, safety, and economy of the current clinical treatment in rheumatoid arthritis, ankylosing spondylitis, and other rheumatic immune diseases.

There are many side effects of drugs currently used in the treatment of rheumatic immune diseases. Nonsteroidal anti-inflammatory drugs can increase the risk of gastrointestinal bleeding. Glucocorticoids can not only raise blood sugar and blood pressure but also aggravate osteoporosis. Immunosuppressive agents can give rise to fungal or atypical pathogen infections. Alkaloids in Chinese materia medica have unique advantages in the treatment of rheumatic immune diseases. They exert anti-inflammatory effects through multiple targets, without adverse reactions mentioned above. Their anti-inflammatory mechanisms include stimulating the pituitary adrenal cortex axis, promoting the release of adrenal cortex hormones, inhibiting the release of inflammatory mediators, interleukins, and tumor necrosis factors, and regulating the level of nitric oxide, the expression of cytokine mRNA, and so on [90].

Anti-inflammatory alkaloids can be mainly divided into the following categories: isoquinoline alkaloids, indole alkaloids, pyridine alkaloids, terpenoid alkaloids, organic amine alkaloids, etc. This article summarizes anti-inflammatory mechanisms of alkaloids in Chinese materia medica, in order to provide a reference for screening active ingredients with anti-inflammatory effects and finding new therapeutic targets. However, the studies above are limited to animal experiments, and some of their mechanisms need further study. We will continue to explore the

anti-inflammatory effects of alkaloids in Chinese materia medica in clinical practice and contribute our efforts to the development of new drugs with anti-inflammatory effects.

Disclosure

The funder has no role in the manuscript writing, editing, approval, or decision to publish.

Conflicts of Interest

The authors declare that they have no conflicts of interest.

Authors' Contributions

Sicong Li and Xin Liu contributed equally to this article. They are both responsible for the initial outline, draft writing, revisions for intellectual content, and final approval. Xiaoran Cheng and Lei Bi were responsible for data interpretation, presentation, draft writing, and revisions for intellectual content.

Acknowledgments

The authors would like to thank all the scholars who have made outstanding contributions to the internationalization of traditional Chinese medicine.

References

[1] W. Li, Y. Li, Y. Zhao, and L. Ren, "The protective effects of aloperine against ox-LDL-induced endothelial dysfunction and inflammation in HUVECs," *Artificial Cells, Nanomedicine, and Biotechnology*, vol. 48, no. 1, pp. 107–115, 2020.

[2] U. H. Ren Hasan, A. M. Uttra et al., "Phytochemicals targeting matrix metalloproteinases regulating tissue degradation in inflammation and rheumatoid arthritis," *Phytomedicine*, vol. 66, Article ID 153134, 2020.

[3] T. Wei, X. Xiaojun, and C. Peilong, "Magnoflorine improves sensitivity to doxorubicin (DOX) of breast cancer cells via inducing apoptosis and autophagy through AKT/mTOR and p38 signaling pathways," *Biomedicine & Pharmacotherapy*, vol. 121, Article ID 109139, 2020.

[4] H. Ardalani, A. Hadipanah, and A. Sahebkar, "Medicinal plants in the treatment of peptic ulcer disease: a review," *Mini-Reviews in Medicinal Chemistry*, vol. 20, 2019.

[5] J. Jiang, T. Ma, L. Zhang et al., "The transdermal performance, pharmacokinetics and anti-inflammatory pharmacodynamics evaluation of harmine-loaded ethosomes," *Drug Development and Industrial Pharmacy*, vol. 46, no. 1, pp. 1–21, 2019.

[6] C.-J. Kim, T. W. Kim, C. J. Kim et al., "Mitochondrial dysfunction as a cause of neurological diseases," *International Neurourology Journal*, vol. 23, no. 1, pp. S3–S4, 2019.

[7] H. Wang, S. Tu, S. Yang et al., "Berberine modulates LPA function to inhibit the proliferation and inflammation of FLS-RA via p38/ERK MAPK pathway mediated by LPA1," *Evidence-Based Complementary and Alternative Medicine*, vol. 2019, Article ID 2580207, 8 pages, 2019.

[8] J. Song, Q. Wu, J. Jiang et al., "Berberine reduces inflammation of human dental pulp fibroblast via miR-21/KBTBD7 axis," *Archives of Oral Biology*, vol. 110, Article ID 104630, 2020.

[9] M. Yao, X. Fan, B. Yuan et al., "Berberine inhibits NLRP3 Inflammasome pathway in human triple-negative breast cancer MDA-MB-231 cell," *BMC Complementary and Alternative Medicine*, vol. 19, no. 1, p. 216, 2019.

[10] Z.-C. Yu, Y.-X. Cen, B.-H. Wu et al., "Berberine prevents stress-induced gut inflammation and visceral hypersensitivity and reduces intestinal motility in rats," *World Journal of Gastroenterology*, vol. 25, no. 29, pp. 3956–3971, 2019.

[11] M. Takahara, A. Takaki, S. Hiraoka et al., "Berberine improved experimental chronic colitis by regulating interferon-gamma- and IL-17A-producing lamina propria CD4(+) T cells through AMPK activation," *Science Reports*, vol. 9, no. 1, p. 11934, 2019.

[12] W. Zhang, J.-H. Xu, T. Yu, and Q.-K. Chen, "Effects of berberine and metformin on intestinal inflammation and gut microbiome composition in db/db mice," *Biomedicine & Pharmacotherapy*, vol. 118, Article ID 109131, 2019.

[13] K. Chen, Q. Chen, N. Wu et al., "Berberine ameliorates spatial learning memory impairment and modulates cholinergic anti-inflammatory pathway in diabetic rats," *Frontiers in Pharmacology*, vol. 10, p. 1003, 2019.

[14] M. Beba, K. Djafarian, and S. Shab-Bidar, "Effect of Berberine on C-reactive protein: a systematic review and meta-analysis of randomized controlled trials," *Complementary Therapies in Medicine*, vol. 46, pp. 81–86, 2019.

[15] Y. Jia, Y. Miao, M. Yue, M. Shu, Z. Wei, and Y. Dai, "Tetrandrine attenuates the bone erosion in collagen-induced arthritis rats by inhibiting osteoclastogenesis via spleen tyrosine kinase," *The FASEB Journal*, vol. 32, no. 6, pp. 3398–3410, 2018.

[16] G. Qin, B. Gui, J. Xie et al., "Tetrandrine alleviates nociception in a rat model of migraine via suppressing S100B and p-ERK activation in satellite glial cells of the trigeminal Ganglia," *Journal of Molecular Neuroscience*, vol. 64, no. 1, pp. 29–38, 2018.

[17] N. Bhagya and K. R. Chandrashekar, "Tetrandrine-a molecule of wide bioactivity," *Phytochemistry*, vol. 125, pp. 5–13, 2016.

[18] L.-N. Gao, Q.-S. Feng, X.-F. Zhang, Q.-S. Wang, and Y.-L. Cui, "Tetrandrine suppresses articular inflammatory response by inhibiting pro-inflammatory factors via NF-κB inactivation," *Journal of Orthopaedic Research*, vol. 34, no. 9, pp. 1557–1568, 2016.

[19] X. Yuan, B. Tong, Y. Dou, X. Wu, Z. Wei, and Y. Dai, "Tetrandrine ameliorates collagen-induced arthritis in mice by restoring the balance between Th17 and Treg cells via the aryl hydrocarbon receptor," *Biochemical Pharmacology*, vol. 101, pp. 87–99, 2016.

[20] G. Bao, C. Li, L. Qi, N. Wang, and B. He, "Tetrandrine protects against oxygen-glucose-serum deprivation/reoxygenation-induced injury via PI3K/AKT/NF-κB signaling pathway in rat spinal cord astrocytes," *Biomedicine & Pharmacotherapy*, vol. 84, pp. 925–930, 2016.

[21] B. Qiao, H. Wang, C. Wang, M. Liang, K. Huang, and Y. Li, "Dauricine negatively regulates lipopolysaccharide- or cecal ligation and puncture-induced inflammatory response via NF-κB inactivation," *Archives of Biochemistry and Biophysics*, vol. 666, pp. 99–106, 2019.

[22] Z. Pu, S. Ma, L. Wang et al., "Corrigendum to "Amyloid-beta degradation and neuroprotection of dauricine mediated by unfolded protein response in a Caenorhabditis elegans model of Alzheimer's disease" [Neuroscience 392C (2018) 25–37]," *Neuroscience*, vol. 404, p. 557, 2019.

[23] X. Zhou, Y. Q. Qu, Z. Zheng et al., "Novel dauricine derivatives suppress cancer via autophagy-dependent cell death," *Bioorganic Chemistry*, vol. 83, pp. 450–460, 2019.

[24] H. Li, X. Chen, and S.-J. Zhou, "Dauricine combined with clindamycin inhibits severe pneumonia co-infected by influenza virus H5N1 and Streptococcus pneumoniae in vitro and in vivo through NF-κB signaling pathway," *Journal of Pharmacological Sciences*, vol. 137, no. 1, pp. 12–19, 2018.

[25] S. Y. Zhang and J. Q. Ren, "Dauricine inhibits viability and induces cell cycle arrest and apoptosis via inhibiting the PI3K/Akt signaling pathway in renal cell carcinoma cells," *Molecular Medicine Reports*, vol. 17, no. 5, pp. 7403–7408, 2018.

[26] M.Y. Wu, S. F. Wang, C. Z. Cai et al., "Natural autophagy blockers, dauricine (DAC) and daurisoline (DAS), sensitize cancer cells to camptothecin-induced toxicity," *Oncotarget*, vol. 8, no. 44, pp. 77673–77684, 2017.

[27] H. Jin, S. Shen, X. Chen, D. Zhong, and J. Zheng, "CYP3A-mediated apoptosis of dauricine in cultured human bronchial epithelial cells and in lungs of CD-1 mice," *Toxicology and Applied Pharmacology*, vol. 261, no. 3, pp. 248–254, 2012.

[28] H. Yang, J. Wang, X. Chen et al., "Effects of sinomenine in LPS-associated diseases are related to inhibition of LBP, Mac-1, and L-selectin levels," *Journal of Veterinary Pharmacology and Therapeutics*, vol. 42, no. 6, pp. 732–737, 2019.

[29] L. Zhang, W. Zhang, B. Zheng, and N. Tian, "Sinomenine attenuates traumatic spinal cord injury by suppressing oxidative stress and inflammation via Nrf2 pathway," *Neurochemical Research*, vol. 44, no. 4, pp. 763–775, 2019.

[30] R.-L. Tian, Y.-K. Zhi, L. Yi et al., "Sinomenine regulates CD14/TLR4, JAK2/STAT3 pathway and calcium signal via α7nAChR to inhibit inflammation in LPS-stimulated macrophages," *Immunopharmacology and Immunotoxicology*, vol. 41, no. 1, pp. 172–177, 2019.

[31] Z.-t. Feng, T. Yang, X.-q. Hou et al., "Sinomenine mitigates collagen-induced arthritis mice by inhibiting angiogenesis," *Biomedicine & Pharmacotherapy*, vol. 113, Article ID 108759, 2019.

[32] Y. Liu, Y. Sun, Y. Zhou et al., "Sinomenine hydrochloride inhibits the progression of plasma cell mastitis by regulating IL-6/JAK2/STAT3 pathway," *International Immunopharmacology*, Article ID 106025, 2019.

[33] W. Wang, X. Yang, Q. Chen et al., "Sinomenine attenuates septic-associated lung injury through the Nrf2-Keap1 and autophagy," *Journal of Pharmacy and Pharmacology*, vol. 72, no. 2, pp. 259–270, 2020.

[34] B. Gao, Y. Wu, Y. J. Yang et al., "Sinomenine exerts anticonvulsant profile and neuroprotective activity in pentylenetetrazole kindled rats: involvement of inhibition of NLRP1 inflammasome," *Journal of Neuroinflammation*, vol. 15, no. 1, p. 152, 2018.

[35] L. Ning, S. Wan, Z. Jie et al., "Lycorine induces apoptosis and G1 phase Arrest through ROS/p38 MAPK signaling pathway in human osteosarcoma cells in vitro and in vivo," *Spine*, vol. 45, no. 3, pp. 126–139, 2020.

[36] W. Liu, Q. Zhang, Q. Tang et al., "[Corrigendum] Lycorine inhibits cell proliferation and migration by inhibiting ROCK1/cofilininduced actin dynamics in HepG2 hepatoblastoma cells," *Oncology Reports*, vol. 42, no. 6, p. 2856, 2019.

[37] H. J. Park, M. Gholam-Zadeh, J. H. Suh et al., "Lycorine attenuates autophagy in osteoclasts via an axis of mROS/TRPML1/TFEB to reduce LPS-induced bone loss," *Oxidative Medicine and Cellular Longevity*, vol. 2019, Article ID 8982147, 11 pages, 2019.

[38] L. Yang, J. H. Zhang, X. L. Zhang et al., "Tandem mass tag-based quantitative proteomic analysis of lycorine treatment in highly pathogenic avian influenza H5N1 virus infection," *PeerJ*, vol. 7, Article ID e7697, 2019.

[39] H. Hu, S. Wang, D. Shi et al., "Lycorine exerts antitumor activity against osteosarcoma cells in vitro and in vivo xenograft model through the JAK2/STAT3 pathway," *OncoTargets and Therapy*, vol. 12, pp. 5377–5388, 2019.

[40] P. M. Le, V. Srivastava, T. T. Nguyen et al., "Stephanine from Stephania venosa (blume) spreng showed effective antiplasmodial and anticancer activities, the latter by inducing apoptosis through the reverse of mitotic exit," *Phytotherapy Research*, vol. 31, no. 9, pp. 1357–1368, 2017.

[41] H. Wang, X. Cheng, S. Kong et al., "Synthesis and structure-activity relationships of a series of Aporphine derivatives with antiarrhythmic activities and acute toxicity," *Molecules*, vol. 21, no. 12, pp. 22–24, 2016.

[42] C. Desgrouas, N. Taudon, S.-S. Bun et al., "Ethnobotany, phytochemistry and pharmacology of Stephania rotunda Lour," *Journal of Ethnopharmacology*, vol. 154, no. 3, pp. 537–563, 2014.

[43] B. Baghdikian, V. Mahiou-Leddet, S. Bory et al., "New antiplasmodial alkaloids from Stephania rotunda," *Journal of Ethnopharmacology*, vol. 145, no. 1, pp. 381–385, 2013.

[44] H. Dong, Y. Zhang, L. Fang et al., "Combinative application of pH-zone-refining and conventional high-speed counter-current chromatography for preparative separation of alkaloids from Stephania kwangsiensis," *Journal of Chromatography B*, vol. 879, no. 13-14, pp. 945–949, 2011.

[45] Z. Ren, X. Wang, X. Chen et al., "Identification of Aloperine as an anti-apoptotic Bcl2 protein inhibitor in glioma cells," *PeerJ*, vol. 7, Article ID e7652, 2019.

[46] Q. Mao, F. Guo, X. Liang et al., "Aloperine Activates the PI3K/Akt pathway and protects against coronary microembolisation-induced myocardial injury in rats," *Pharmacology*, vol. 104, no. 1-2, pp. 90–97, 2019.

[47] H. I. Yu, H. C. Shen, S. H. Chen et al., "Autophagy modulation in human thyroid cancer cells following aloperine treatment," *International Journal of Molecular Sciences*, vol. 20, no. 21, 2019.

[48] J.-S. Liu, C.-Y. Huo, H.-H. Cao et al., "Aloperine induces apoptosis and G2/M cell cycle arrest in hepatocellular carcinoma cells through the PI3K/Akt signaling pathway," *Phytomedicine*, vol. 61, Article ID 152843, 2019.

[49] Z. Chang, P. Zhang, M. Zhang et al., "Aloperine suppresses human pulmonary vascular smooth muscle cell proliferation via inhibiting inflammatory response," *Chinese Journal of Physiology*, vol. 62, no. 4, pp. 157–165, 2019.

[50] N. Zhang, Y. Dou, L. Liu et al., "SA-49, a novel aloperine derivative, induces MITF-dependent lysosomal degradation of PD-L1," *EBioMedicine*, vol. 40, pp. 151–162, 2019.

[51] D. Tian, Y. Li, X. Li et al., "Aloperine inhibits proliferation, migration and invasion and induces apoptosis by blocking the Ras signaling pathway in human breast cancer cells," *Molecular Medicine Reports*, vol. 18, no. 4, pp. 3699–3710, 2018.

[52] H. Zhuang, X. Dai, X. Zhang, Z. Mao, and H. Huang, "Sophoridine suppresses macrophage-mediated immunosuppression through TLR4/IRF3 pathway and subsequently upregulates $CD8^+$ T cytotoxic function against gastric cancer," *Biomedicine & Pharmacotherapy*, vol. 121, Article ID 109636, 2020.

[53] R. Wang, H. Liu, Y. Shao et al., "Sophoridine inhibits human colorectal cancer progression via targeting MAPKAPK2," *Molecular Cancer Research*, vol. 17, no. 12, pp. 2469–2479, 2019.

[54] G. Ren, G. Ding, H. Zhang et al., "Antiviral activity of sophoridine against enterovirus 71 in vitro," *Journal of Ethnopharmacology*, vol. 236, pp. 124–128, 2019.

[55] X. D. Chen, X. Y. Hua, X. M. Kong et al., "[Sophoridine inhibits the proliferation of human gastric cancer MKN45 cells and promotes apoptosis]," *Sheng Li Xue Bao*, vol. 70, no. 4, pp. 391–396, 2018.

[56] D. Li, L. Dai, X. Zhao et al., "Novel sophoridine derivatives bearing phosphoramide mustard moiety exhibit potent antitumor activities in vitro and in vivo," *Molecules*, vol. 23, no. 8, 2018.

[57] Z. Yue, T. Si, Z. Pan et al., "Sophoridine suppresses cell growth in human medulloblastoma through FoxM1, NF-kappaB and AP-1," *Oncology Letters*, vol. 14, no. 6, pp. 7941–7946, 2017.

[58] S. Zhang, S. Guo, X. b. Gao et al., "Matrine attenuates high-fat diet-induced in vivo and ox-LDL-induced in vitro vascular injury by regulating the PKCα/eNOS and PI3K/Akt/eNOS pathways," *Journal of Cellular and Molecular Medicine*, vol. 23, no. 4, pp. 2731–2743, 2019.

[59] P. Li, J. Lei, G. Hu et al., "Matrine mediates inflammatory response via gut microbiota in TNBS-induced murine colitis," *Frontiers in Physiology*, vol. 10, p. 28, 2019.

[60] X. Yu, H. J. Seow, H. Wang et al., "Matrine reduces cigarette smoke-induced airway neutrophilic inflammation by enhancing neutrophil apoptosis," *Clinical Science*, vol. 133, no. 4, pp. 551–564, 2019.

[61] W. W. Li, T. Y. Wang, B. Cao et al., "Synergistic protection of matrine and lycopene against lipopolysaccharideinduced acute lung injury in mice," *Molecular Medicine Reports*, vol. 20, no. 1, pp. 455–462, 2019.

[62] J. Zhou, W. Ma, X. Wang et al., "Matrine suppresses reactive oxygen species (ROS)-Mediated MKKs/p38-induced inflammation in oxidized low-density lipoprotein (ox-LDL)-Stimulated macrophages," *Medical Science Monitor*, vol. 25, pp. 4130–4136, 2019.

[63] Q. Li, J. Xu, Z. He et al., "The effects of matrine in combination with docetaxel on castration-resistant (Androgen-Independent) prostate cancer," *Cancer Management and Research*, vol. 11, pp. 10125–10133, 2019.

[64] W.-W. Jiang, Y.-M. Wang, X.-Y. Wang, Q. Zhang, S.-M. Zhu, and C.-L. Zhang, "Role and mechanism of matrine alone and combined with acitretin for HaCaT cells and psoriasis-like murine models," *Chinese Medical Journal*, vol. 132, no. 17, pp. 2079–2088, 2019.

[65] C. Wenjin and W. Jianwei, "Protective effect of gentianine, a compound from du huo Ji sheng tang, against Freund's complete adjuvant-induced arthritis in rats," *Inflammation*, vol. 40, no. 4, pp. 1401–1408, 2017.

[66] G. O. Anyanwu, Nisar-ur-Rehman, C. E. Onyeneke, and K. Rauf, "Medicinal plants of the genus Anthocleista-a review of their ethnobotany, phytochemistry and pharmacology," *Journal of Ethnopharmacology*, vol. 175, pp. 648–667, 2015.

[67] X. Rauf, S. Tang, Y. Jin et al., "Determination of the metabolic profile of gentianine after oral administration to rats by high performance liquid chromatography/electrospray ionization-trap mass spectrometry," *Journal of Chromatography B*, vol. 989, pp. 98–103, 2015.

[68] S. H. Tiong, C. Y. Looi, A. Arya et al., "Vindogentianine, a hypoglycemic alkaloid from Catharanthus roseus (L.) G. Don (Apocynaceae)," *Fitoterapia*, vol. 102, pp. 182–188, 2015.

[69] H. Vaidya, R. K. Goyal, and S. K. Cheema, "Anti-diabetic activity of swertiamarin is due to an active metabolite, gentianine, that upregulates PPAR-γ gene expression in 3T3-L1 cells," *Phytotherapy Research*, vol. 27, no. 4, pp. 624–627, 2013.

[70] F. Peng, N. Zhang, C. Wang et al., "Aconitine induces cardiomyocyte damage by mitigating BNIP3-dependent mitophagy and the TNFalpha-NLRP3 signalling axis," *Cell Proliferation*, vol. 53, no. 1, Article ID e12701, 2020.

[71] T. Guo, N. Cheng, J. Zhao, X. Hou, Y. Zhang, and N. Feng, "Novel nanostructured lipid carriers-loaded dissolving microneedles for controlled local administration of aconitine," *International Journal of Pharmaceutics*, vol. 572, Article ID 118741, 2019.

[72] Y. Wang, Y. Shan, Y. Wang et al., "Aconitine inhibits androgen synthesis enzymes by rat immature Leydig cells via down-regulating androgen synthetic enzyme expression in vitro," *Chemico-Biological Interactions*, vol. 312, Article ID 108817, 2019.

[73] X. Zhan, W. Zhang, T. Sun et al., "Bulleyaconitine A effectively relieves allergic lung inflammation in a murine asthmatic model," *Medical Science Monitor*, vol. 25, pp. 1656–1662, 2019.

[74] M. X. Xie, H. Q. Zhu, R. P. Pang et al., "Mechanisms for therapeutic effect of bulleyaconitine A on chronic pain," *Molecular Pain*, vol. 14, Article ID 1744806918797243, 2018.

[75] M. X. Xie, J. Yang, R. P. Pang et al., "Bulleyaconitine A attenuates hyperexcitability of dorsal root ganglion neurons induced by spared nerve injury: the role of preferably blocking Nav1.7 and Nav1.3 channels," *Molecular Pain*, vol. 14, Article ID 1744806918778491, 2018.

[76] M.-X. Xie, R.-P. Pang, J. Yang et al., "Bulleyaconitine A preferably reduces tetrodotoxin-sensitive sodium current in uninjured dorsal root ganglion neurons of neuropathic rats probably via inhibition of protein kinase C," *Pain*, vol. 158, no. 11, pp. 2169–2180, 2017.

[77] Y. Bin, Y. Xiao, D. Huang et al., "Theophylline inhibits cigarette smoke-induced inflammation in skeletal muscle by upregulating HDAC2 expression and decreasing NF-κB activation," *American Journal of Physiology-Lung Cellular and Molecular Physiology*, vol. 316, no. 1, pp. L197–L205, 2019.

[78] T. Mitani, T. Takaya, N. Harada et al., "Theophylline suppresses interleukin-6 expression by inhibiting glucocorticoid receptor signaling in pre-adipocytes," *Archives of Biochemistry and Biophysics*, vol. 646, pp. 98–106, 2018.

[79] L. Gallelli, D. Falcone, R. Cannataro et al., "Theophylline action on primary human bronchial epithelial cells under proinflammatory stimuli and steroidal drugs: a therapeutic rationale approach," *Drug Design, Development and Therapy*, vol. 11, pp. 265–272, 2017.

[80] P. Richette, M. Doherty, E. Pascual et al., "2016 updated EULAR evidence-based recommendations for the management of gout," *Annals of the Rheumatic Diseases*, vol. 76, no. 1, pp. 29–42, 2017.

[81] N. Saini, D. Singh, and R. Sandhir, "Bacopa monnieri prevents colchicine-induced dementia by anti-inflammatory action," *Metabolic Brain Disease*, vol. 34, no. 2, pp. 505–518, 2019.

[82] A. Berdeli, O. Senol, and G. Talay, "Treatment of familial mediterranean fever with canakinumab in patients who are unresponsive to colchicine," *European Journal of Rheumatology*, vol. 6, no. 2, pp. 85–88, 2019.

[83] B. Tucker, R. Kurup, J. Barraclough et al., "Colchicine as a novel therapy for suppressing chemokine production in patients with an acute coronary syndrome: a pilot study," *Clinical Therapeutics*, vol. 41, no. 10, pp. 2172–2181, 2019.

[84] Y. Liang, H.-F. Zhou, M. Tong, L. Chen, K. Ren, and G.-J. Zhao, "Colchicine inhibits endothelial inflammation via NLRP3/CRP pathway," *International Journal of Cardiology*, vol. 294, p. 55, 2019.

[85] L. Hongyan, Z. Mengjiao, W. Chunyan, and H. Yaruo, "Rhynchophylline attenuates neurotoxicity in tourette syndrome rats," *Neurotoxicity Research*, vol. 36, no. 4, pp. 679–687, 2019.

[86] Y. Yaruo, J. Sun, S. Zhu et al., "The role of rhynchophylline in alleviating early brain injury following subarachnoid hemorrhage in rats," *Brain Research*, vol. 1631, pp. 92–100, 2016.

[87] H. C. Hsu, N. Y. Tang, C. H. Liu et al., "Antiepileptic effect of Uncaria rhynchophylla and rhynchophylline involved in the initiation of c-Jun N-terminal kinase phosphorylation of MAPK signal pathways in acute seizures of Kainic acid-treated rats," *Evidence-Based Complementary and Alternative Medicine*, vol. 2013, Article ID 961289, 2013.

[88] M. Zhang, C. Wang, H.-l. Cai, J. Wen, and P.-f. Fang, "Licorice extracts attenuate nephrotoxicity induced by brucine through suppression of mitochondria apoptotic pathway and STAT3 activation," *Current Medical Science*, vol. 39, no. 6, pp. 890–898, 2019.

[89] Z. P. Chen, W. Liu, H. X. Chen et al., "[Brucine chitosan thermosensitive hydrogel for intra-articular injection]," *Yao Xue Xue Bao*, vol. 47, no. 5, pp. 652–656, 2012.

[90] H. S. Foyet, W. E. Keugong, A. H. Ngatanko et al., "Anticholinesterase and antioxidant potential of hydromethanolic extract of Ziziphus mucronata (rhamnaceae) leaves on scopolamine-induced memory and cognitive dysfunctions in mice," *Evidence-Based Complementary and Alternative Medicine*, vol. 2019, Article ID 4568401, 2019.

Hindawi
Evidence-Based Complementary and Alternative Medicine
Volume 2020, Article ID 3495836, 15 pages
https://doi.org/10.1155/2020/3495836

Research Article

Electroacupuncture Ameliorates Cerebral I/R-Induced Inflammation through DOR-BDNF/TrkB Pathway

Yue Geng,[1] Yeting Chen,[1] Wei Sun,[1] Yingmin Gu,[1] Yongjie Zhang,[1] Mei Li,[2] Jiajun Xie,[1] and Xuesong Tian[1]

[1]*Innovation Research Institute of Traditional Chinese Medicine, Center for Drug Safety Evaluation and Research, Shanghai University of Traditional Chinese Medicine, Shanghai, China*
[2]*Department of Physiology, Shanghai University of Traditional Chinese Medicine, Shanghai, China*

Correspondence should be addressed to Xuesong Tian; xuesong.tian@shutcm.edu.cn

Received 16 November 2019; Accepted 17 February 2020; Published 16 March 2020

Guest Editor: Tae Jin lee

The beneficial effects of electroacupuncture (EA) at Shuigou (GV26) and Neiguan (PC6) on poststroke rehabilitation are critically related to the activation of the delta-opioid receptor (DOR). The underlying anti-inflammatory mechanisms in DOR activation and EA-mediated neuroprotection in cerebral ischemia/reperfusion (I/R) injury were investigated in the current study. Cell proliferation and apoptosis were detected by morphological changes, cell counting kit-8 (CCK-8) assay, lactate dehydrogenase (LDH) release, and TUNEL staining. The mRNA levels were evaluated by using real-time quantitative polymerase chain reaction (RT-qPCR), and the protein expression was measured by western blot or enzyme-linked immunosorbent assay (ELISA) *in vitro*. Infarct volume was examined by cresyl violet (CV) staining, neurologic recovery was assessed by neurological deficit scores, and pro- and anti-inflammatory cytokines were determined by immunofluorescence *in vivo*. DOR activation greatly ameliorated morphological injury, reduced LDH leakage and apoptosis, and increased cell viability. It reversed the oxygen-glucose deprivation/reoxygenation- (OGD/R-) induced downregulation of DOR mRNA and protein, as well as BDNF protein. DOR activation also reduced proinflammatory cytokine gene expression, including TNF-α, IL-1β, and IL-6, and at the same time, increased anti-inflammatory cytokines IL-4 and IL-10 in OGD/R challenged PC12 cells. EA significantly reduced middle cerebral artery occlusion/reperfusion- (MCAO/R-) induced infarct volume and attenuated neurologic deficit scores. It markedly increased the expression of IL-10 and decreased IL-1β, while sham EA did not have any protective effect in MCAO/R-injured rats. DOR activation plays an important role in neuroprotection against OGD/R injury by inhibiting inflammation via the brain-derived neurotrophic factor/tropomyosin-related kinase B (BDNF/TrkB) pathway. The neuroprotective efficacy of EA at Shuigou (GV26) and Neiguan (PC6) on cerebral I/R injury may be also related to the inhibition of inflammatory response through the DOR-BDNF/TrkB pathway.

1. Introduction

Stroke is the third leading cause of mortality in most western countries, preceded only by coronary heart disease and malignant tumor. However, it has been the leading cause of death in China in recent years, threatening people's health and affecting their quality of life [1]. Among various types of stroke, ischemic accounts for about 87% of all strokes [2].

Reported scientific findings have highlighted that inflammatory response plays a crucial role in cerebral ischemia/reperfusion (I/R) injury and aggravates ischemic and anoxic injury, worsening patient prognosis [3]. Thus, inhibiting inflammation after cerebral I/R injury has far-reaching clinical implications. As an effective therapy and complementary medicine, acupuncture has been used in China for centuries. Recently, increasingly clinical and experimental studies have demonstrated that electroacupuncture (EA), an extended technique based on traditional acupuncture and combined with modern electrotherapy, has been proved to be an effective therapeutic method for cerebral ischemia and is related to the anti-inflammatory response [4–7].

δ-opioid receptor (DOR) is an oxygen-sensitive protein, which is sensitive to ischemia and hypoxia. The activation of DOR is neuroprotective against cerebral I/R injury through various mechanisms, including maintaining ionic homeostasis against excitotoxic and antioxidative stress [8, 9]. Recently, a large amount of research suggests that the alleviation of inflammatory response, such as downregulation of the expression of proinflammatory mediators TNF-α, IL-6, and IL-1β and upregulation of anti-inflammatory factors IL-4 and IL-10 [10–12], is also involved in the neuroprotection after cerebral I/R. The binding of brain-derived neurotrophic factor (BDNF) to its high affinity receptor tropomyosin-related kinase B (TrkB) has been recognized as one of the anti-inflammatory pathways [13, 14]. Interestingly, recent evidence also shows that BDNF is probably regulated by DOR in cerebral I/R injury [15–17]. Therefore, it remains to be verified whether or not DOR can regulate the BDNF/TrkB pathway and then alleviate cerebral I/R inflammatory response to protect against the cerebral I/R injury.

Reports suggest that one of the mechanisms of EA protection in cerebral I/R injury appears to be regulating the expression of BDNF and its receptor TrkB [18, 19]. Over the years, studies have shown that the treatment of EA has relieved the symptoms for analgesia and other diseases with activation of the endogenous opioid system in the brain [20–22]. Particularly, recent studies show that EA at Shuigou (GV26) and Neiguan (PC6) has obvious effects for cerebral I/R injury among the many acupuncture points available for treatment, and its therapeutic mechanism may be associated with the activation of DOR, one of the three classic opioid receptor subtypes [23, 24]. Nonetheless, it is unclear whether the DOR-BDNF/TrkB signaling pathway-mediated anti-inflammatory effect is involved in the therapeutic efficacy of EA at Shuigou (GV26) and Neiguan (PC6) on cerebral I/R injury.

Hence, this investigation is primarily aimed to address the following two fundamental issues using a combination of cell oxygen-glucose deprivation/reoxygenation (OGD/R) and rat middle cerebral artery occlusion/reperfusion (MCAO/R) models: (1) activation of DOR attenuates OGD/R-induced inflammation through the BDNF-TrkB signaling pathway; and (2) DOR-BDNF/TrkB signaling pathway is involved in the anti-inflammatory mechanisms of EA at Shuigou (GV26) and Neiguan (PC6) in cerebral I/R injury.

2. Materials and Methods

2.1. Chemicals and Reagents. Tan67 and Naltrindole (NTI) were purchased from Tocris bioscience (Cat: 0921, 0740). Cresyl violet (CV) was purchased from Sigma-Aldrich (Cat: C5402). Hoechst 33258, BCA assay kit (BSA standard solution) and the protein extraction kit were purchased from Beyotime Biotechnology (Cat: C1017, P0010, and P0013B). Mouse monoclonal anti-IL-10 (A-2) antibody was purchased from Santa Cruz Biotechnology (Cat: SC-365858). Rabbit polyclonal anti-IL-1β antibody was obtained from Abcam Inc (Cat: ab9722). Rabbit polyclonal anti-DOR antibody was obtained from Millipore Sigma (Cat: AB1560). Mouse monoclonal anti-β-actin antibody was obtained from Sigma-Aldrich (Cat: A5441). Alexa Fluor 647-conjugated Affinipure Donkey Anti-Rabbit IgG (H + L), Alexa Fluor 488-conjugated Affinipure Donkey Anti-Mouse IgG (H + L), Peroxidase AffiniPure Goat Anti-Rabbit IgG (H + L), and Peroxidase AffiniPure Goat Anti-Mouse IgG (H + L) are Jackson Immuno Research products (Cat: 711-605-152, 715-545-150, 111-035-003, and 115-035-003). Laemmli sample buffer is from Bio-rad (Cat: 1610747).

2.2. Cell Culture. PC12 cells were purchased from Cell Bank of Type Culture Collection of the Chinese Academy of Science (Shanghai, China) and then cultured in the full culture medium, RPMI-1640 (Gibco, Carlsbad, CA, USA), containing 10% heat-inactivated fetal bovine serum (Gibco) and 1% penicillin/streptomycin (Gibco), in a humidified incubator (5% CO_2, 95% air) at 37°C. Cells were fed with fresh medium every other day, and the cells of passages 4–6 were used for experiments.

2.3. Oxygen-Glucose Deprivation/Reoxygenation and Cell Culture Treatment. Cells of the same passage were randomly divided into 5 groups: (1) control group; (2) OGD/R group; (3) agonist group (OGD/R + Tan67); (4) antagonist group (OGD/R + NTI); (5) coadministration group (OGD/R + NTI + Tan67). The OGD/R in PC12 cells was performed as reported before [25, 26]. In brief, PC12 cells were washed with phosphate-buffered saline (PBS) twice and cultured in glucose-free RPMI-1640 culture media and then placed in a hypoxia chamber (95% N_2 and 5% CO_2) for 6 h at 37°C. The cells were then fed back with full culture medium and cultured under normal conditions for additional 24 h. Control cells were incubated in the regular cell culture incubator under normoxic conditions for the same duration. DOR agonist Tan67 or antagonist NTI was dissolved with PBS (pH 7.2) and then filtered (0.22 μm) to obtain stock solutions (25 mM). Immediately before use, the stock solution was diluted in the cell culture medium to 10 μM. In the agonist and antagonist groups, PC12 cells were pretreated with Tan67 or NTI alone for 30 min, while in the coadministration group, NTI incubation starts 30 min before adding Tan67, following by 6 h of OGD and 24 h of reperfusion. The same amount of dissolvent was added into control and OGD/R cultures to guarantee all groups under the same experimental procedure.

2.4. Animals. Healthy adult male Sprague-Dawley rats (230 ± 10 g of body weight) were obtained from Shanghai Laboratory Animal Center and maintained under specific pathogen-free conditions in Shanghai University of Traditional Chinese Medicine. Rats were housed in cages under a 12-hour light/dark cycle, 60%–70% relative humidity, and a temperature of 22°C ± 2°C, with free access to water and food. Animals were allowed one week to acclimate prior to experimentation. All procedures were performed in accordance with the Provision and General Recommendation of Chinese Experimental Animals Administration Legislation and approved by the Experimental Animal Ethics Committee

of Shanghai University of Traditional Chinese Medicine (PZSHUTCM18121401).

2.5. Experimental Groups and Lateral Ventricle Injection. Forty rats were randomly assigned into the following five groups: (1) sham group (Sham), (2) MCAO group (MCAO), (3) sham EA group (MCAO + S + EA), (4) EA group (MCAO + EA), and (5) EA + DOR antagonist group (MCAO + NTI + EA). NTI was freshly dissolved in saline to a final concentration of 100 nM and then filtered (0.22 μm). Ten microliters of NTI (100 nmol) was stereotaxically injected into the right lateral ventricle 30 min before MCAO started (Shanghai Alcott Biotechnology Co., Ltd). Ten μl Hamilton syringe (10 μl, 1701 N) was used to inject at the rate of 1 μl/min. After the injection, the needle was left in place for a few minutes before being retracted slowly and the wound was cleaned and sutured. The rat in the other group received the corresponding volume of saline. The coordinates of the injection site were 0.2 mm posterior to the bregma, 1.4 mm lateral, and 4 mm below the skull surface, with a flat skull position.

2.6. MCAO/R Model. The MCAO/R model is the most widely used animal model to mimic the cerebral I/R injury [27]. The MCAO/R (90 min/24 h) procedure was performed according to the methods of Longa with minor modifications [28]. In brief, the rats were anesthetized with pentobarbital (50 mg/kg, i.p.), and the right common carotid artery (CCA), external carotid artery (ECA), and internal carotid artery (ICA) were gently exposed through a ventral midline incision. A 3-0 monofilament nylon suture (Dermaron, Davis-Geck, USA) with a rounded tip was inserted into the right ICA though the ECA, with a depth of approximately 18 ± 2 mm. The suture was carefully removed 90 min after the ischemia for 24 h of reperfusion. Sham-operated rats were subjected to the same procedures described above without suture insertion. The rectal temperature was monitored and maintained at 37 ± 0.5°C throughout the experiment.

2.7. EA Treatments. At 30 minutes of ischemia, rats in the MCAO + EA and MCAO + NTI + EA group underwent EA stimulation for 90 min at Shuigou (GV26) and the left side of Neiguan (PC6). Acupoints of Shuigou (GV26) and Neiguan (PC6) were selected according to the "animal acupuncture points map" reported by the Experimental Acupuncture–Moxibustion Research Association of China (Academy of Acupuncture–Moxibustion). The acupoints were stimulated with an intensity of 1-2 mA and a disperse-dense frequency of 5/20 Hz (adjusted to the muscle twitch threshold) by using the EA instrument (SDZ-V EA, Suzhou, China). In the sham EA group, acupuncture needles were inserted superficially into the same acupoints without electrical stimulation [24].

2.8. Cell Morphology and Viability. To evaluate changes in cell morphology, the PC12 cells were grown in 6-well plates and treated as described above, and cell morphology was observed under an inverted microscope (Nikon, Japan).

2.8.1. Cell Viability. Cell viability was determined by the cell counting kit-8 (CCK-8) assay and lactate dehydrogenase (LDH) release. CCK-8 assay was performed according to the manufacturer's instructions (Beyotime Biotechnology, Shanghai, China) and similar to our previous study [29]. In brief, PC12 cells were seeded in 96-well plate at 1×10^5 cells/mL and allowed to adhere properly for 24 h. After OGD/R insult, 10 μl of the CCK-8 solution was added to each well and was incubated for another 1.5 h under the same incubator conditions. Subsequently, the optical density (OD) value of each well at the absorbance 450 nm was determined using a multiwell microplate reader (Synergy HT, BioTek). The mean OD of all wells in the indicated groups was used to calculate the percentage of cell viability as follows: percentage of cell viability = $(A_{\text{treatment}} - A_{\text{blank}})/(A_{\text{control}} - A_{\text{blank}}) \times 100\%$ (where$A$ = absorbance). LDH release was evaluated using a commercially available kit (A020-2-2, Jiancheng, Nanjing, China). In brief, after removal of the culture supernatants from each well, 1% Triton X-100 lysis solution was added to the wells. Cells were placed in the lysis buffer for 30 min at 37°C. Then, the collected cell culture supernatants and lysates were centrifuged at 3000g for 15 min, respectively. Subsequently, the centrifuged supernatant was transferred to a new 96-well plate for LDH activity analysis according to manufacturer's instructions. The absorbance was determined at 450 nm with a microplate reader (Synergy HT, BioTek). Background absorbance from the cell-free buffer solution was subtracted from all absorbance measurements. The percentage of LDH released to cell culture medium in total LDH was calculated: LDH leakage = LDH in cell culture supernatant/(LDH in cell culture supernatant + LDH in cell lysate) × 100%.

2.8.2. TUNEL Staining. The apoptotic cells were stained with TUNEL reagents according to the manufacturer's instructions (Roche Applied Science, Rotkreuz, Switzerland). After OGD/R, the cells were washed with PBS three times and then fixed in 4% paraformaldehyde at 37°C for 20 min. The cells were then rinsed with PBS three times and incubated in a permeabilizing solution (0.1% Triton X-100 in sodium citrate) for 3 minutes. After rinsing in PBS, the cells were incubated in TUNEL with an enzyme-to-label ratio of 1 : 9 at 37°C for 1 h and nuclei staining with Hoechst 33258 working solution (5 mg/mL) for 10 min at room temperature in the dark. After washed with PBS three times, the immunofluorescent images were observed by using a Laser Scanning Confocal Microscope (TCS SP8, Leica, Germany). TUNEL positive PC12 cells were counted in 5 randomly selected high-power fields (HPF, 400x magnification) per culture dish, respectively, and expressed as the number of apoptotic cells in each HPF.

2.9. RNA Isolation, cDNA Synthesis, and Polymerase Chain Reaction. The mRNA levels of DOR, TNF-α, IL-1β, IL-6, IL-4, and IL-10, in PC12 cells were measured by real-time

quantitative polymerase chain reaction (RT-qPCR). The total RNA was isolated using Trizol reagent (Invitrogen, Paisley, UK). Subsequently, 800 ng RNA was reversely transcribed into cDNA at 37°C for 15 min followed by 85°C for 5 sec using TB Green™ Premix Ex Taq™ (Takara, Shiga, Japan). RT-qPCR was performed with the ABI 7500 PCR system (ABI, USA). The PCR cycling conditions were 40 amplification cycles of denaturation at 95°C for 30 s, followed by 94°C for 5 sec and 60°C for 34 sec. The quantified value of each sample was normalized to β-actin expression in the same sample, which was amplified simultaneously with the target genes. The relative gene expression was quantified using the $2^{-\Delta\Delta t}$ method. Each sample was tested in triplicate. Primers for DOR, TNF-α, IL-1β, IL-6, IL-4, and IL-10 were synthesized by Kingsray Biotechnology (Nanjing, China). The sequences of the primers used in this study are listed in Table 1.

2.10. Western Blot. Western blot was used to determine DOR protein expression as previously described [30]. In short, following OGD/R, the cells were rinsed twice with ice-cold PBS and total protein was extracted using RIPA buffer (P0013B, Beyotime). Protein concentration was then measured by BCA protein assay (P0010, Beyotime). Equal amount of protein samples (20 μg/10 μL) were boiled at 100°C in Laemmli sample buffer (Bio-Rad Laboratories, Inc., USA) for 5 min and then loaded and electrophoresed on 10% SDS-polyacrylamide gel (product information). Proteins were transferred from gel to 0.22 μm nitrocellulose (NC) membrane (Millipore, Billerica, MA, USA) using a wet transfer system (Bio-Rad). The membranes were blocked with 5% nonfat milk in TBS containing 0.1% Tween-20 for 1 h at room temperature and then incubated with primary antibodies (1 : 3000 rabbit anti-DOR, and 1 : 10,000 mouse β-actin antibody) at 4°C overnight. The membranes were washed three times for 10 min each with TBS containing 0.1% Tween-20 and incubated with the corresponding horseradish peroxide-conjugated secondary antibodies (1 : 5000 goat anti-rabbit IgG and 1 : 5000 goat anti-mouse IgG) at room temperature for 2 h. Next, membranes were washed three times with 0.1% TBST, and the immune-reactive bands were detected using enhanced chemiluminescence reagent (Beyotime) and scanned with the ChemiDoc XRS imaging system (Bio-Rad). Gray-scale analysis was analyzed by Image-Pro Plus 6.0 analysis system (Media Cybernetics Inc., USA), and the protein expression was normalized to the expression of β-actin.

2.11. Measurement of BDNF Protein Levels. BDNF levels in the cell culture supernatants and cell lysates were measured by BDNF enzyme-linked immunosorbent assay (ELISA) (R&D Systems, DBNT00, Minneapolis, USA). In brief, the culture supernatants and cell lysate in 1% Triton X-100 lysing solution were collected and then centrifuged at 3000g for 15 min, respectively. Subsequently, BDNF content was determined in accordance with the manufacturer's instructions. Absorbance was measured at 450 nm with a microplate reader (Synergy HT, BioTek). The BDNF protein levels were calculated in comparison with the standard curve.

2.12. Scoring of Neurological Deficits. Neurologic deficit scores were evaluated at 24 h of reperfusion based on the method of Longa et al. [28]. The scores for the neurological behavioral were as follows: 0 = no deficit, 1 = failure to extend left forepaw fully, 2 = circling to the left, 3 = falling to the left, and 4 = no spontaneous walking with a depressed level of consciousness. The scores were rated double-blind.

2.13. Free Floating Coronal Section Preparation. At 24 h of reperfusion, under deep anesthesia with sodium pentobarbital (80 mg/kg, i.p.), the brains were carefully removed after transcardial perfusion with 0.9% saline solution followed by 4% ice-cold phosphate-buffered paraformaldehyde (PFA). Subsequently, the rat brains were fixed in 4% PFA for 12 h and then immersed sequentially in 20% and 30% sucrose solutions in 0.1 M phosphate buffer (pH 7.4) until they sank. Finally, brains were cut into 30 μm coronal sections from bregma 1.60 to −4.80 mm on a freezing microtome (CM1950, Leica, Germany) and stored at −20°C in cryoprotectant solution.

2.14. Infarct Volume Assessment. Sections at 1.60 to −4.80 mm from bregma were used for CV staining. The volume of the brain infarct was measured in each slice at 360 μm intervals with Image-Pro Plus 6.0 analysis system (Media Cybernetics Inc.). Data were presented as the percentage in the volume of the entire brain.

2.15. Immunofluorescence. Sections at 1.0 to 0.48 mm from bregma were used for immunofluorescence staining as previously described [15]. Free-floating sections were washed in 0.01 M PBS three times (5 min each). Sections were then incubated with 0.3% H_2O_2 for 30 min and placed in blocking buffer containing 10% donkey serum and 0.3% Triton X-100 in 0.01 M PBS for 30 min at room temperature. Subsequently, the sections were incubated with primary antibodies against rabbit polyclonal IL-1β (1 : 100) or mouse monoclonal anti-IL10 (1 : 50) overnight at 4°C, respectively. After washing with PBS, the sections were incubated with corresponding secondary antibodies (1 : 500) for 1 h at 37°C. Nuclei were counterstained with Hoechst 33258 (5 μg/mL) for 10 min in the dark. Finally, following additional three washes in PBS, these sections were mounted on glass slides and cover slipped using fluorescent mounting media. Images were captured using a confocal laser scanning microscope (TCS SP8, Leica, Germany) with 630x magnification at excitation 490 nm (Alexa Fluor 488), 640 nm (Alexa Fluor 647), and 360 nm (Hoechst 33258). Negative control sections received the identical process without primary antibodies and showed no specific staining.

Double-positive for IL-1β and Hoechst 33258 cells were counted in 10 randomly selected fields (630x magnification)

Table 1: Primers information for RT-qPCR.

Gene	Forward (5′-3′)	Reverse (5′-3′)
DOR	GGACGCTGGTGGACATCAAT	CGTAGAGAACCGGGTTGAGG
TNF-α	GGCTTTCGGAACTCACTGGA	AGGGAGGCCTGAGACATCTT
IL-1β	TCAAGCAGAGCACAGACCTG	GAAGACACGGGTTCCATGGT
IL-6	GCAAGAGACTTCCAGCCAGT	CTGGTCTGTTGTGGGTGGTA
IL-4	ACCGAGAACCCCAGACTTGTT	CAGGGTGCTTCGCAAATTTTAC
IL-10	AGGGTTACTTGGGTTGCCAA	TCAGCTTCTCTCCCAGGGAA

using an Image-Pro Plus 6.0 analysis system (Media Cybernetics Inc.), and the average percentage of double-positive cells was presented as double-positive/total cells × 100%. IL-10 positive staining was determined according to the mean and integrated optical density (IOD). In brief, 5 random HPFs (630x magnification) were selected in each immunofluorescence slice. Quantitative analysis of total of IL-10 positive area and IOD of positive staining area was performed according to the software as described above. The mean density = IOD SUM/area SUM.

2.16. Statistical Analyses. Statistical analysis was performed using the SPSS software (version 23; IBM Corp., Armonk, NY, USA). Data are presented as the mean ± standard error of mean (SEM). When equal variance was assumed, the data were analyzed using one-way analysis of variance (ANOVA) followed by Dunnett's post hoc test for multiple comparisons. When equal variance was not assumed, the data were compared using the nonparametric test. To avoid false positives caused by multiple comparisons, the Bonferroni's correction was performed to adjust the test level (0.05/n). The neurologic deficit scores were expressed as the median (range) and were analyzed with a nonparametric method (Kruskal–Wallis test) followed by the Mann–Whitney U test with Bonferroni's correction. Probability values of $P < 0.05$, $P < 0.01$, and $P < 0.001$ were considered to indicate a statistically significant difference.

3. Results

3.1. DOR Activation Reduced Cellular Injury Induced by OGD/R in PC12 Cells. The PC12 cells line, which derives from rat adrenal medulla tumor, has been widely used for cell signaling studies [31]. The positive findings of this cell line can be validated in primary neuronal cultures and could also be adapted for OGD/R research [32, 33]. To examine the neuroprotective effect of the DOR on OGD/R-induced cell injuries, the cellular morphology, cell viability, and LDH release were assessed immediately after the OGD/R by inverted microscope, CCK-8 assay, and LDH leakage assay. As shown in Figure 1(a), the morphological characteristics of the PC12 cells in the control group included large cell amount, strong refractive index, and vigorous axonal growth; moreover, the synapses were clearly interwoven into a network. The OGD/R exposure resulted in a reduction in cell number, and the morphology exhibited round, slender, and degenerated cell debris (Figure 1(a)). The number of cells increased drastically, and normal morphology was restored if PC12 was pretreated with the DOR agonist Tan67 (10 μM) before OGD/R exposure, as evidenced by observations under microscope (Figure 1(a)). However, the morphology and numbers of NTI (10 μM) and NTI + Tan67 pretreated cells were similar to that in the OGD/R group (Figure 1(a)). The results were further quantified by the CCK-8 assay, which measures cell viability, and were expressed as % cell viability of control (Figure 1(b)). The cell viability markedly decreased by OGD/R exposure ($68.3 \pm 2.2\%$, $P < 0.001$) (Figure 1(b)). A statistically significant increase in cell viability was detected in cells preincubated with the DOR agonist Tan67 ($81.7 \pm 2.6\%$, $P < 0.001$) (Figure 1(b)). However, the protective effect of Tan67 was blocked by concomitant incubation with the DOR antagonist NTI ($73.7 \pm 3.0\%$, $P > 0.05$) (Figure 1(b)), suggesting that DOR activation contributes to the protection against OGD/R-induced cell death. The application of NTI itself did not change cell viability ($68.7 \pm 1.8\%$, $P > 0.05$) in the OGD/R-treated cells (Figure 1(b)).

Next, to further confirm the effect of DOR on OGD/R-induced PC12 cell injury, LDH leakage assay was performed (Figure 1(c)). The increased release of LDH is recognized as a reliable index of neuronal injury [8]. The LDH leakage rate was significantly increased after PC12 cells were exposed to OGD/R ($254.2 \pm 8.8\%$, $P < 0.01$), comparing with the control group ($100.0 \pm 3.1\%$) (Figure 1(c)). However, activating DOR with Tan67 (10 μM) clearly attenuated the LDH leakage rate ($179.7 \pm 7.7\%$, $P < 0.01$) in comparison to the OGD/R group (Figure 1(c)), whereas, as shown in the last bar in Figure 1(c), the increase in LDH leakage in the coadministration group ($257.3 \pm 3.7\%$, $P > 0.05$) was the same as that in none drug-treated OGD/R group, indicating that the Tan67-mediated neuroprotection was abolished by the blockade on DOR activation. NTI alone did not make any difference in the LDH release ($255.4 \pm 2.7\%$, $P > 0.05$) compared with the OGD/R group (Figure 1(c)). These data indicate that DOR plays a significant role in neuroprotection against OGD/R-induced injury.

3.2. Effect of DOR Activation on Cell Apoptosis. To evaluate the effects of DOR activation on OGD/R-induced apoptosis in PC12 cells, the TUNEL assay was applied. As shown in Figure 2(a), apoptosis was identified by the nuclear staining in green. TUNEL and Hoechst 33258 double-positive cells (yellow) in each group were counted manually by two independent observers in 6 random microscopic fields, and the numbers of double-positive cells were subsequently calculated (Figure 2(b)).

There were almost no apoptotic changes noted in the nuclei in the control group (Figure 2(b)). Extensively

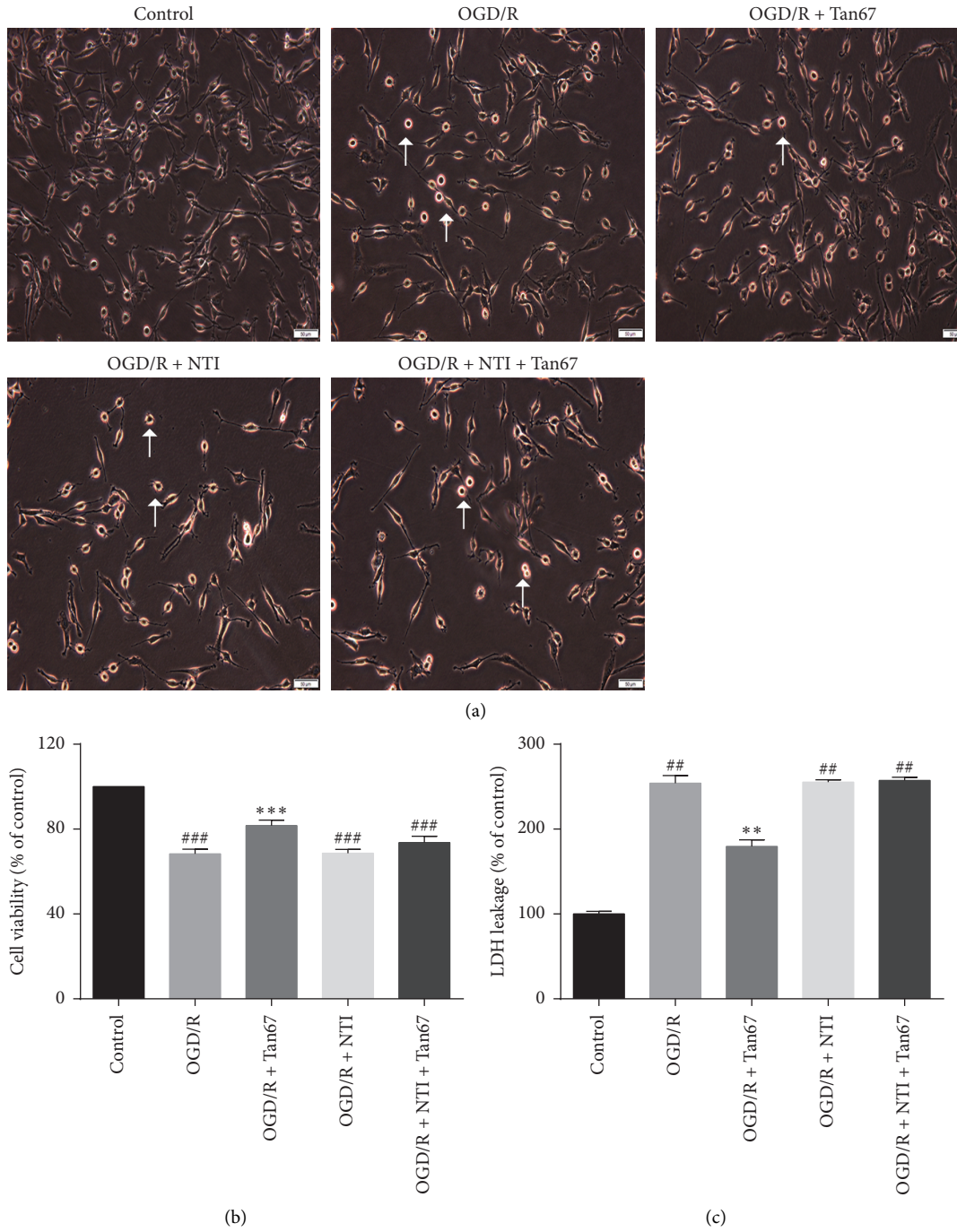

Figure 1: DOR activation increases cell viability in OGD/R-exposed PC12 cells. The cellular morphological changes, cell viability, and LDH level were evaluated after exposure to 6 h OGD followed by 24 h reperfusion (OGD/R). The DOR agonist or antagonist treatment is 30 min before OGD. In the coadministration group, antagonist NTI was added to the cell culture medium 30 min before the agonist Tan67 incubation. (a) Representative images of PC12 cells in the sham group, OGD/R group, agonist group, antagonist group, and coadministration group. Cell viability was measured by (b) CCK-8 assay and (c) LDH release. Activation of DOR attenuated the PC12 cells injury, whereas it was totally abolished by preincubation of DOR antagonist. Scale bar = 50 μm. $N = 6$ in each group. $^{###}P < 0.001$ and $^{##}P < 0.01$ vs. control group. $^{***}P < 0.001$ and $^{**}P < 0.01$ vs. OGD/R group.

TUNEL-positive apoptotic cells were observed in PC12 culture exposed to OGD/R (12.4 ± 1.6, $P < 0.001$), while pretreatment with Tan67 remarkably decreased the number of TUNEL-positive cells (8.0 ± 0.7, $P < 0.01$) (Figure 2(b)). However, pretreatment with NTI (14.6 ± 1.2, $P > 0.05$) attenuated the beneficial effect of Tan67, suggesting that DOR activation might inhibit apoptosis (Figure 2(b)). NTI alone did not exert a significant effect on OGD/R-induced apoptosis (11.4 ± 1.0, $P > 0.05$) (Figure 2(b)). This result indicates that DOR activation may inhibit apoptosis.

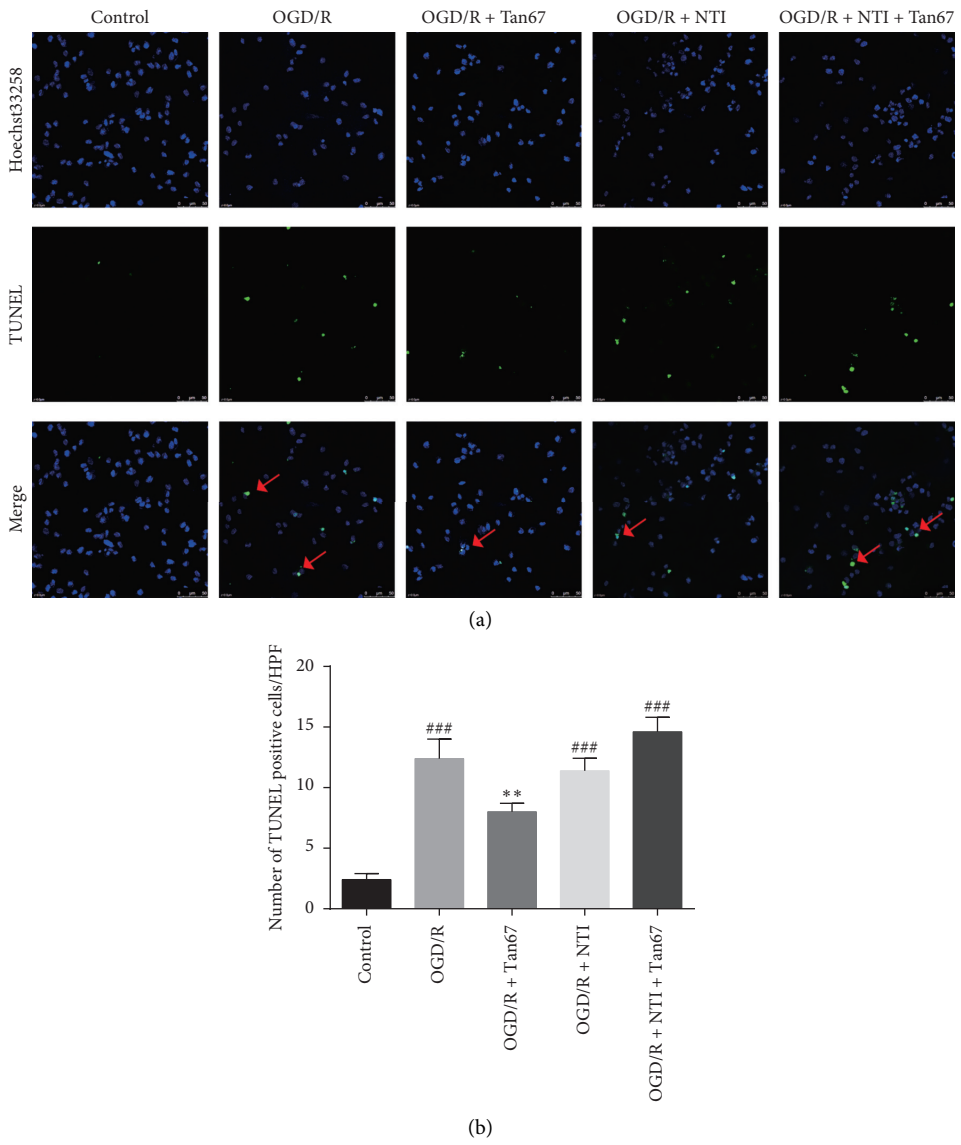

Figure 2: DOR activation protects against OGD/R-induced cell apoptosis. The apoptotic cells were evaluated after exposure to 6 h OGD followed by 24 h reperfusion (OGD/R). (a) The top panels are representative images of TUNEL staining (400x) in indicated groups. Red arrows indicate colocalization (yellow) between TUNEL-positive apoptotic cells (green) and cell nuclei (blue) in PC12 cells. Cell nuclei were visualized by Hoechst 33258 staining (blue). (b) The bottom panel is the statistical analysis of the number of apoptotic cells. DOR activation reduced cell apoptosis, and NTI blocked the effect. Scale bar = 50 μm. $N = 3$ in each group. $^{###}P < 0.001$ vs. control group and $^{**}P < 0.01$ vs. OGD/R group.

3.3. Effect of DOR Activation on the Production of Proinflammatory Cytokines (TNF-a, IL-1β, and IL-6) and Anti-Inflammatory Cytokines (IL-4 and IL-10). Inflammation response plays a pivotal role in the pathological process of cerebral I/R injury. Further to clarify the specific mechanism of DOR activation in neuroprotection, the RT-qPCR was performed to evaluate how DOR affects the expression of inflammation-related factors. The mRNA levels of TNF-α, IL-1β, and IL-6 in the OGD/R group ($800.4 \pm 60.1\%$, $192.9 \pm 9.6\%$, and $257.2 \pm 9.2\%$, $P < 0.01$ or $P < 0.05$) (Figures 3(a)–3(c)) were dramatically increased compared with the control group. In contrast, the mRNA levels of IL-4 and IL-10 were decreased after OGD/R ($63.8 \pm 2.4\%$ and $58.6 \pm 1.1\%$, $P < 0.001$) (Figures 3(d) and 3(e)). Pretreatment with Tan67 dramatically decreased TNF-α, IL-1β, and IL-6 expression ($185.0 \pm 31.9\%$, $114.3 \pm 1.8\%$, and $117.2 \pm 2.0\%$, $P < 0.01$ or $P < 0.05$) (Figures 3(a)–3(c)) and increased IL-4 and IL-10 expression ($83.4 \pm 1.5\%$, $85.1 \pm 2.8\%$, $P < 0.001$) (Figures 3(d) and 3(e)) in PC12 cells compared with the OGD/R group. However, pretreatment with NTI reversed the protective effect of Tan67, while NTI application alone had no effect on the mRNA levels, as evidenced by the expression of TNF-α, IL-1β, IL-6, IL-4, and IL-10 in the OGD/R + NTI + Tan67 group ($615.0 \pm 18.8\%$, $145.9 \pm 2.5\%$, $182.3 \pm 1.1\%$, $63.0 \pm 2.1\%$, and $58.8 \pm 3.2\%$, $P > 0.05$) and the OGD/R + NTI group ($673.5 \pm 33.8\%$, $168.5 \pm 4.2\%$, $191.2 \pm 1.7\%$, $67.7 \pm 2.8\%$, and $62.3 \pm 3.8\%$, $P > 0.05$) (Figures 3(a)–3(e)). These results demonstrate that DOR activation reduces proinflammatory cytokines

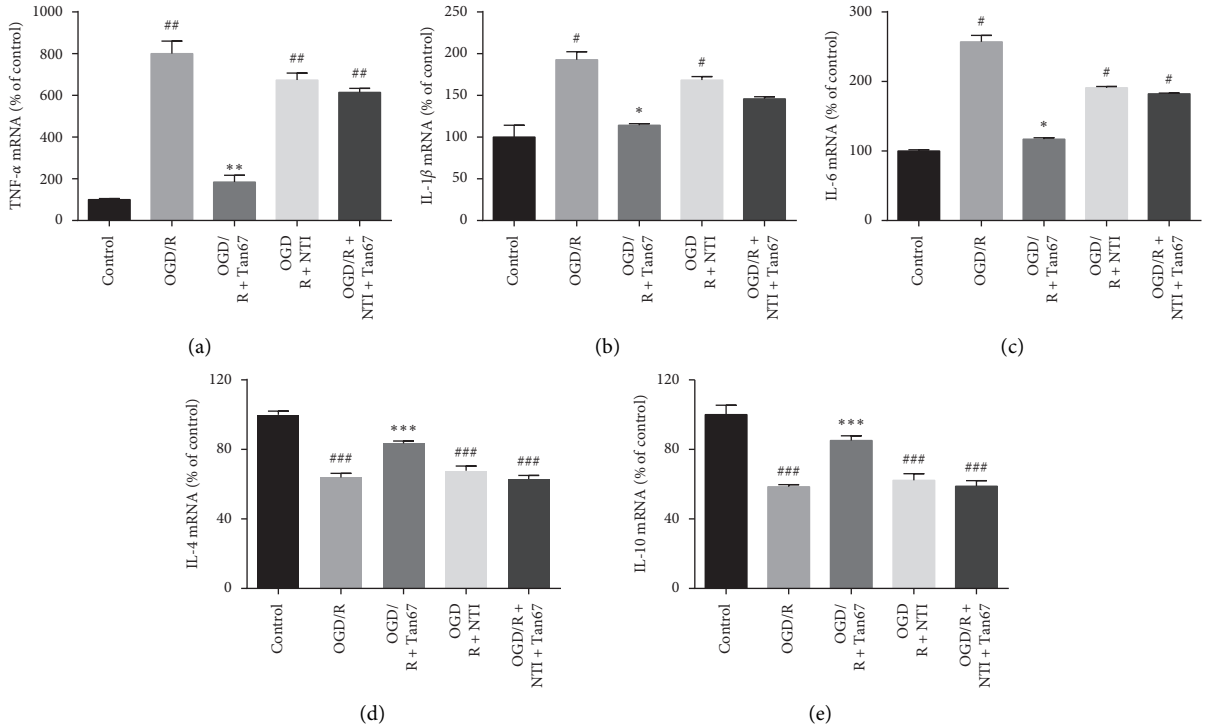

Figure 3: DOR activation reduces inflammatory response. The expression of proinflammatory cytokines (e.g., TNF-α, IL-1β, and IL-6) and anti-inflammatory cytokines (e.g., IL-4 and IL-10) was evaluated by RT-qPCR at 24 h of reperfusion following 6 h OGD. Statistical analysis of (a) TNF-α, (b) IL-1β, (c) IL-6, (d) IL-4, and (e) IL-10 mRNA expression is shown. DOR activation prevented the OGD/R-induced upregulation of proinflammatory factors (TNF-α, IL-1β, and IL-6) and downregulation of the anti-inflammatory factors (IL-4 and IL-10), and the effects were blocked by NTI treatment. $N = 3$ in each group. $^{\#}P < 0.05$ and $^{\#\#\#}P < 0.001$ vs. control group. $^{*}P < 0.05$, $^{**}P < 0.01$, and $^{***}P < 0.001$ vs. OGD/R group.

and increases anti-inflammatory cytokines gene expression, thus attenuating OGD/R injury.

3.4. Effect of DOR Activation on DOR and BDNF Expression. Next, to study how DOR activation suppresses inflammation in OGD/R exposed PC12 cells, the BDNF signaling pathway was investigated. We determined the expression of DOR and BDNF by western blot, RT-qPCR, and ELISA, respectively. Comparing with control, the expression levels of DOR mRNA ($53.8 \pm 2.1\%$, $P < 0.001$) and protein ($72.5 \pm 5.2\%$, $P < 0.01$) were significantly reduced in the OGD/R group (Figures 4(a)–4(c)). Pretreatment of PC12 with Tan67 could obviously inhibit the decline of DOR mRNA ($82.6 \pm 8.1\%$,$P < 0.01$) and protein ($90.7 \pm 5.9\%$, $P < 0.05$) expression induced by OGD/R (Figures 4(a)–4(c)). However, the effect of Tan67 was reversed by pretreatment with NTI ($53.7 \pm 4.6\%$, $P > 0.05$; $66.1 \pm 5.7\%$, $P > 0.05$) and had no significant difference compared with the OGD/R group (Figures 4(a)–4(c)). The expression levels of DOR mRNA and protein in the OGD/R + NTI group ($59.0 \pm 2.8\%$, $P > 0.05$; $72.1 \pm 3.1\%$, $P > 0.05$) have no notable difference in comparison to the OGD/R group (Figures 4(a)–4(c)) as well.

Consistent with the expression of DOR, similar results were shown on BDNF. BDNF protein level was detected in lysates (33.7 ± 1.5 pg/mL) and cell culture supernatants (36.7 ± 1.2 pg/mL) in the control group (Figures 4(d) and 4(e)). OGD/R exposure markedly reduced BDNF expression both in lysates (22.1 ± 0.5 pg/mL, $P < 0.001$) and cell culture supernatants (19.1 ± 0.7 pg/mL, $P < 0.001$) (Figures 4(d) and 4(e)), while pretreatment with Tan67 resulted in a noticeable enhancement of BDNF in cell lysates (28.0 ± 0.7 pg/mL, $P < 0.001$) and supernatant (29.8 ± 1.5 pg/mL, $P < 0.001$). The coadministration of NTI and Tan67 significantly reversed the effect of Tan67 in lysates (21.1 ± 1.8 pg/mL, $P > 0.05$) and cell culture supernatants (22.4 ± 1.4 pg/mL,$P > 0.05$) (Figures 4(d) and 4(e)). There was no significant difference in the expression of BDNF in lysates (20.1 ± 1.6 pg/mL,$P > 0.05$) and cell culture supernatants (23.2 ± 1.3 pg/mL, $P > 0.05$) in the OGD/R + NTI group compared with the OGD/R group (Figures 4(d) and 4(e)). These results further indicate that the expression of DOR and BDNF was restored by DOR activation.

3.5. DOR Antagonist Reversed EA-Induced Neuroprotective Effects in Infarct Volume and Neurologic Deficit Scores. To investigate whether DOR activation is involved in the neuroprotective effects of EA against cerebral I/R, the infarct volume and neurological deficit scores were evaluated at 24 h of reperfusion (Figure 5). No visible infarct volume and neurological deficit were observed in the sham group (Figures 5(b) and 5(c)). EA treatment at Shuigou (GV26) and Neiguan (PC6) significantly reduced the infarct volume

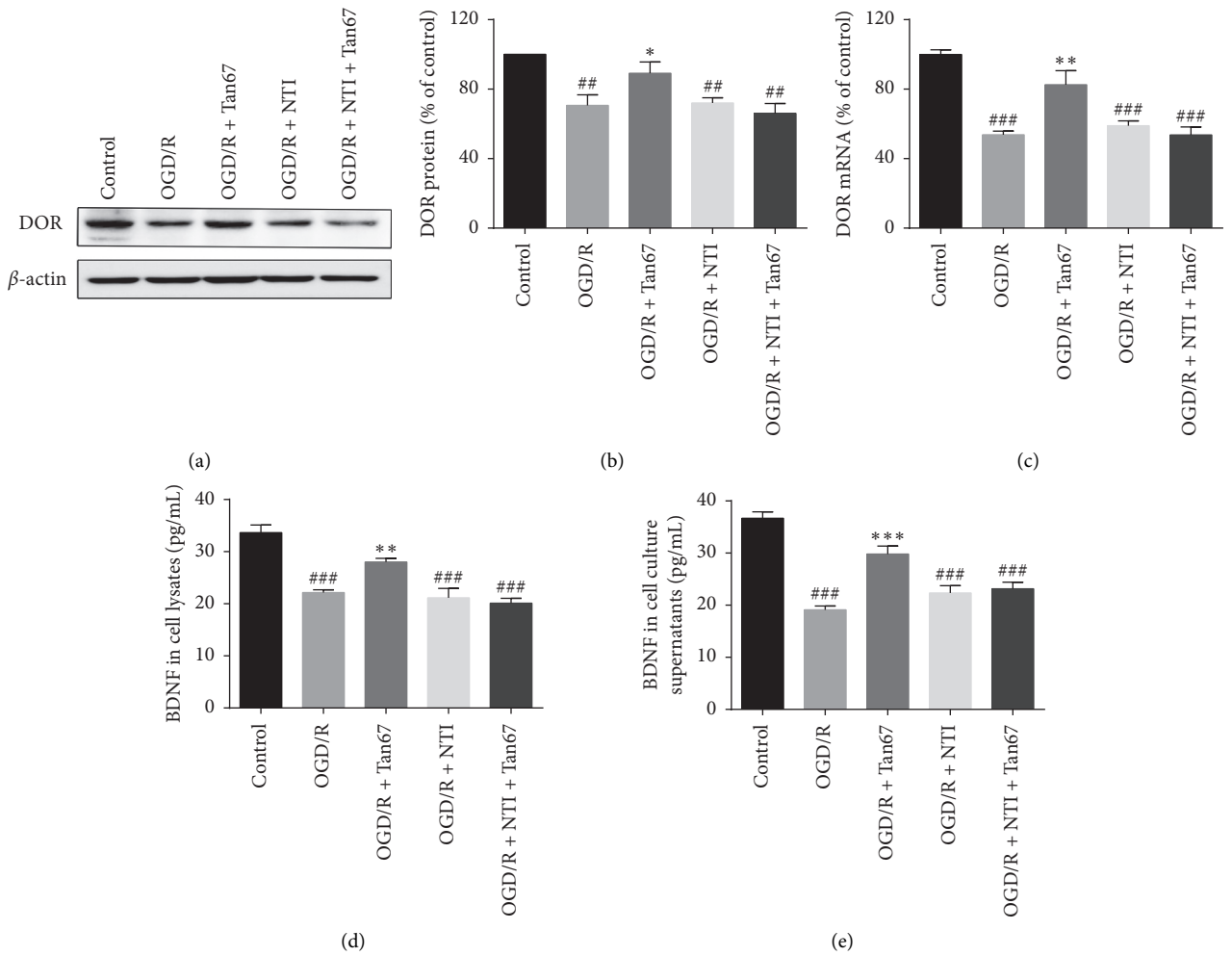

Figure 4: DOR activation elevates DOR and BDNF expression. The mRNA level of DOR was determined by RT-qPCR, and protein expression of DOR and BDNF was measured by western blot or ELISA at 24 h of reperfusion following 6 h OGD. (a) Representative western blot images of DOR expression. (b) Statistical analysis of DOR protein expression. (c) Statistical analysis of DOR mRNA expression. (d) Statistical analysis of BDNF protein expression in cell lysates. (e) Statistical analysis of BDNF protein expression in cell culture supernatants. DOR activation inhibited the OGD-induced decline of DOR mRNA, DOR protein, and BDNF protein expression in PC12 cells, while NTI blocked the effect. $N = 3$ in each group. $^{\#}P < 0.05$ and $^{\#\#\#}P < 0.001$ vs. control group. $^{*}P < 0.05$, $^{**}P < 0.01$, and $^{***}P < 0.001$ vs. OGD/R group.

($10.2 \pm 1.0\%$, $P < 0.05$) and neurologic deficit scores (2.3 ± 0.2, $P < 0.05$) compared with the MCAO group ($24.5 \pm 6.5\%$; 2.8 ± 0.2) (Figures 5(a)–5(c)). However, NTI administration before MCAO injury reversed the neuroprotective effects of EA on infarct volume ($33.7 \pm 3.7\%$, $P > 0.05$) and neurologic deficit scores (3.6 ± 0.2, $P < 0.05$) (Figures 5(a)–5(c)). Sham-operated EA showed no significant improvement compared to MCAO rats in infarct volume ($17.3 \pm 2.8\%$, $P > 0.05$) and neurologic deficit scores (2.6 ± 0.2, $P > 0.05$) (Figures 5(a)–5(c)). The results suggest that EA stimulation at Shuigou (GV26) and Neiguan (PC6) may activate DOR and therefore protects against MCAO/R-induced brain injury.

3.6. DOR Antagonist Reversed EA-Induced Neuroprotective Effects in Inflammatory Responses. Ample experimental data showed that IL-1β, one of the most extensive proinflammatory cytokines, plays a critical role in cerebral I/R injury [34]. At the same time, IL-10, a well-known anti-inflammatory cytokine, was reported to attenuate cerebral I/R injury because of its ability to suppress the production of a variety of proinflammatory cytokines, including IL-1β, IL-6, IL-8, and TNF-α [35, 36]. Therefore, the expression of IL-1β and IL-10 in the cerebral I/R region was detected by the immunofluorescence staining.

As shown in Figures 6(a) and 6(c), the number of IL-1β positive cells in the MCAO group ($34.0 \pm 2.8\%$, $P < 0.001$) was higher than that in sham group ($5.8 \pm 1.9\%$). Comparable to IL-1β, the IL-10 was significantly lower in the MCAO group (0.09 ± 0.00, $P < 0.001$) than in the sham group (0.22 ± 0.02) (Figures 6(b) and 6(d)), as calculated by IOD measurement. Treatment at Shuigou (GV26) and Neiguan (PC6) with EA decreased the number of IL-1β positive cells ($20.6 \pm 2.7\%$, $P < 0.01$), as well as increased the levels of IL-10 (0.15 ± 0.01, $P < 0.01$) in the cerebral ischemia area (Figures 6(a)–6(d)). Moreover, the lateral ventricle

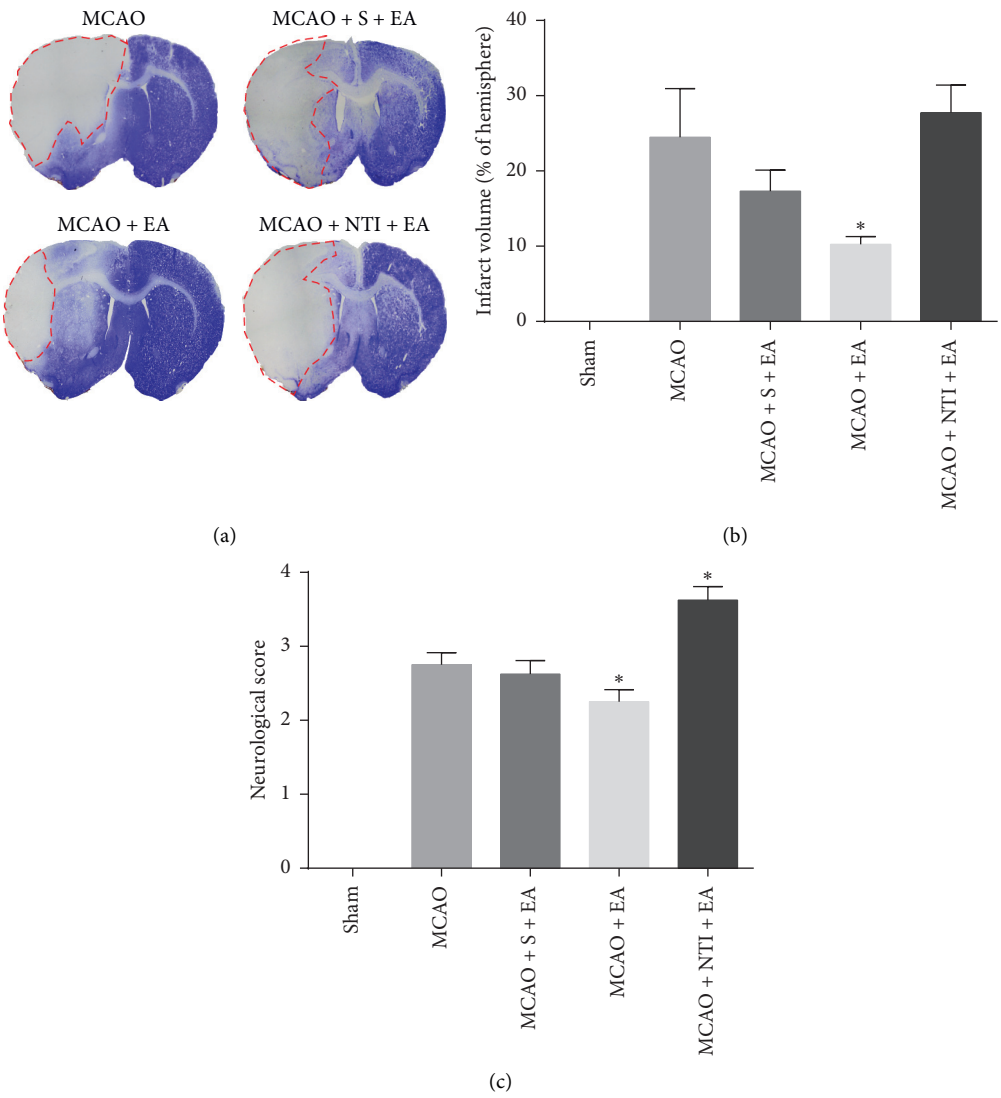

Figure 5: EA-mediated neuroprotective effects in infarct volume and neurologic deficit scores are reversed by DOR antagonist. Infarct volume and neurologic deficit scores were evaluated at 24 h of reperfusion following 90 min MCAO. (a) Representative images of brain infarct volume presented typically in the striatum and cortex indicated by CV staining. The area of pallor, which is inside the red circle, delineates the ischemic core. (b) Statistical analysis of the infarct volume in each group. (c) Statistical analysis of the neurological deficits scores in each group. DOR antagonist NTI abolished the reduction on infarct volume and neurologic deficit scores by EA stimulation at Shuigou (GV26) and Neiguan (PC6). $N = 8$ in each group. $^*P < 0.05$ vs. MCAO group.

injection of DOR antagonist NTI 30 min before MCAO prevented the changes and brought back the expression of IL-1β ($35.1 \pm 1.9\%$, $P > 0.05$) and IL-10 (0.09 ± 0.00, $P > 0.05$) to the similar levels as in the MCAO group (Figures 6(a)–6(d)). Sham-operated EA showed no significant improvement compared to MCAO rats on IL-1β ($30.4 \pm 3.0\%$, $P > 0.05$) and IL-10 (0.11 ± 0.01, $P > 0.05$) (Figures 6(a)–6(d)). These data indicate that DOR activation is likely involved in EA-mediated neuroprotection through suppressing inflammatory responses in cerebral I/R injury.

4. Discussion

The principle observations in the current study are as follows: (1) activation of DOR prevents the cell injury induced by OGD/R in PC12 cells; (2) DOR activation markedly reduces OGD/R-induced inflammation; (3) DOR activation restores the mRNA and protein expression of DOR and protein level of BDNF, which were lowered by OGD/R exposure; and (4) EA at Shuigou (GV26) and Neiguan (PC6) suppresses inflammatory responses, reduces ischemic infarct volume, and attenuates neurologic deficit scores in rats with cerebral I/R injury. Together with our previous work [15, 16, 30], we have the following conclusion that DOR-mediated anti-inflammation of BDNF/TrkB pathway plays an important role in ameliorating OGD/R-induced PC12 cells injury, and the beneficial effects of EA treatment may be related to the activation of DOR-BDNF/TrkB pathway in inhibiting the inflammatory response after cerebral I/R-induced neuronal injury.

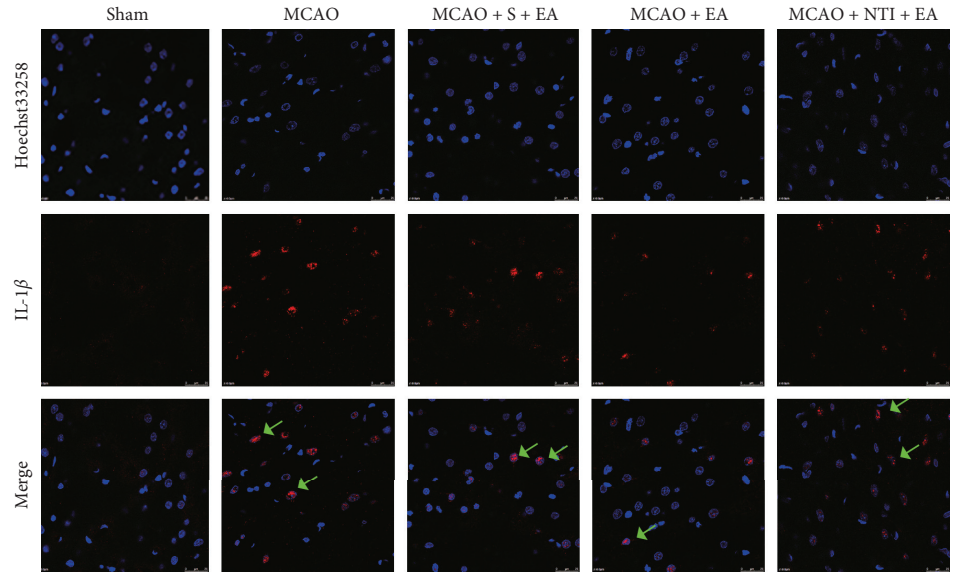

(a)

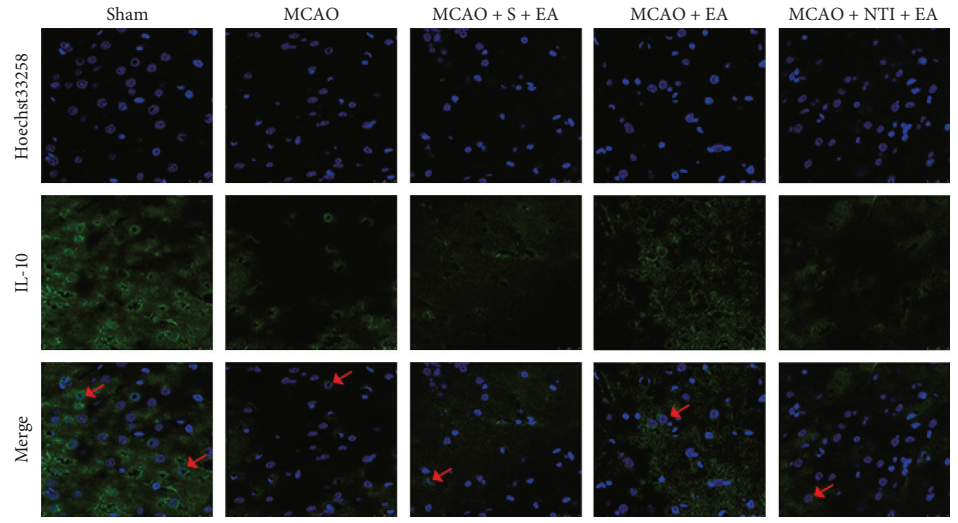

(b)

Figure 6: Continued.

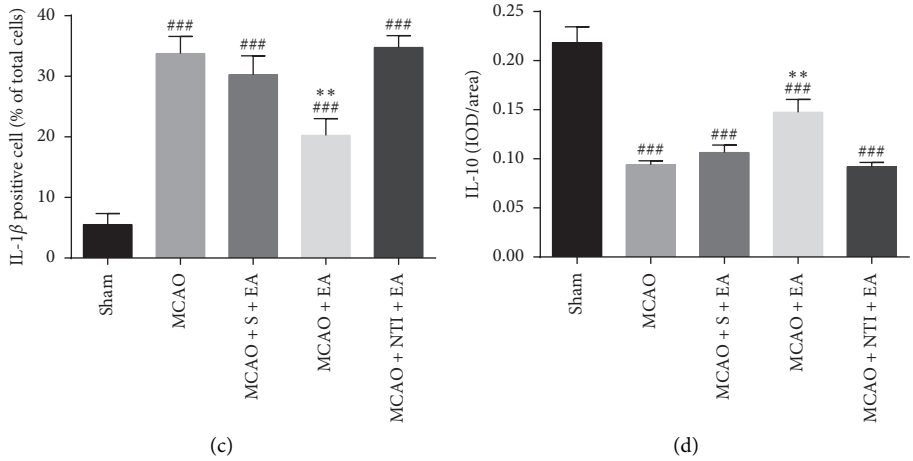

Figure 6: DOR antagonist reversed EA-induced neuroprotective effects in inflammatory responses. Proinflammatory cytokines (IL-1β) and anti-inflammatory cytokines (IL-10) were evaluated at 24 h of reperfusion following 90 min MCAO. (a) Representative immunofluorescent staining images of IL-1β positive cells in the cortex. (b) Representative images of IL-10 positive immunofluorescent staining in the cortex. (c) Statistical analysis of the percentage of IL-1β positive cells. (d) Statistical analysis of the mean density of IL-10 positive staining. Green arrows indicate colocalization (pink) between IL-1β positive cells (red) and cell nuclei (blue). Red arrows indicate that IL-10 positive staining (green) is found diffusely distributed across the cytosol and located around the nuclei (blue). Cell nuclei were visualized by Hoechst 33258 staining (blue). EA at Shuigou (GV26) and Neiguan (PC6) reduces the inflammatory factor IL-1β and increases the anti-inflammatory factor IL-10, and NTI reversed the EA effect. Scale bar = 50 μm. $N = 4$ in each group. $^{###}P < 0.001$ vs. sham group. $^{**}P < 0.01$ vs. MCAO group.

Four independent assays to detect OGD/R-induced PC12 cells injury (morphological pathology, cell viability, membrane integrity, and DNA breakdown) showed that DOR activation largely attenuated the PC12 cells injury induced by OGD/R, as indicated by reduced morphological changes, increased cell viability, as well as decreased LDH leakage and apoptosis. DOR antagonist totally abolished the DOR activation mediated protective effect, indicating a critical role of the DOR in neuronal protection. This result is supported by previous studies, which showed that DOR activation has potent neuroprotective effect on primary cultured neuron against hypoxia-induced injury [37, 38].

DOR is an oxygen-sensitive protein, and the expression depends on the duration and extent of hypoxia or ischemia. DOR expression is upregulated by short-term or mild hypoxia exposure, which is also called hypoxic preconditioning, and downregulated after prolonged and severe hypoxia/ischemia exposure [8, 30, 39]. Compared treatment with hypoxic preconditioning by exposure to 5% oxygen for 6 h, OGD 6 h followed by reperfusion 24 h is severe hypoxia. Our study showed similar results that both DOR mRNA and protein levels declined in a major way after OGD/R. The DOR agonist Tan67 reverses the downregulation of DOR mRNA and proteins normally produced by OGD/R, whereas the DOR antagonist NTI blocks such protection, suggesting that the Tan67-regulated expression of DOR mainly occurs at the transcriptional and posttranscriptional levels. However, details remain unclear and further experiments need to be carried out.

BDNF binding to its specific receptor-TrkB plays an important role in inhibiting inflammatory response and protecting neurons in both in vitro and in vivo studies. In *in vitro* and *in vivo* models of depression, BDNF was shown to improve depressive-like behavior by upregulating anti-inflammatory cytokine IL-10, IL-4, and TGF-β1 and downregulating the pro-inflammatory cytokine IL-1β, IL-17, and TNF-α [40]. Exogenous BDNF suppressed the expression of proinflammatory factors, including TNF-α, IL-1β, and IL-6, and increased the expression of the anti-inflammatory factor IL-10 [13]. Evidence from recent studies showed that the expression of BDNF is probably regulated by DOR. For instance, DOR activation significantly upregulated the mRNA expression of BDNF in the frontal cortex through a DOR-mediated mechanism because this effect was blocked by specific DOR antagonist NTI, but not by μ- or k-opioid receptor antagonists [17, 41]. Indeed, we previously found that BDNF was colocalized with DOR in DOR-rich regions in the brain [15]. Our previous studies have also demonstrated that DOR activation upregulates BDNF-TrkB signals thereby decreasing the level of TNF-α and protecting the cortex against hypoxic injury [16]. In the present study, we observed that the activation of DOR promoted the expression of BDNF in cell lysates and cell culture supernatants, reduced the mRNA levels of TNF-α, IL-1β, and IL-6, and increased IL-4 and IL-10, further confirming that DOR mediates the anti-inflammatory effect of the BDNF/TrkB pathway.

According to the theory of traditional Chinese medicine, there are many acupoints used in the treatment of stroke. The evidence from our previous studies have suggested that EA applied at two specific acupoints, Shuigou (GV26) and Neiguan (PC6), may produce significant benefits for cerebral I/R injury, in which the beneficial effects are related to DOR. For example, EA at points Shuigou (GV26) and Neiguan (PC6) could attenuate infarction size and reduce the neurological deficit score of cerebral I/R rats by increasing the expression of DOR, and the effects were specifically blocked by NTI, a DOR antagonist [23]. DOR antagonist NTI can

reverse the neuroprotective effect of cumulative EA at Shuigou (GV26) and Neiguan (PC6) on cerebral I/R as well [24]. These results together suggested that DOR activation is involved in the mechanism of the neuroprotection of EA at Shuigou (GV26) and Neiguan (PC6) against cerebral I/R injury. In addition, prior to cerebral I/R injury, cumulative EA treatments could mimic ischemic preconditioning to induce protective function to the brain, presenting reduced infarct volume and improved neuronal function in rats after cerebral ischemia, and this protection is selectively blocked by DOR antagonist NTI [42]. However, whether DOR activation-induced anti-inflammatory response is involved in the underlying mechanism of EA effects in cerebral I/R injury is of great interest to us.

EA at Neiguan (PC6) effectively attenuates the expression of proinflammatory cytokines in cerebral ischemia and improves neurological deficit score [43]. Furthermore, recent reports show that EA at Shuigou (GV26) inhibits inflammatory reactions and induces functional improvement in motor function in CNS injuries, including stroke and spinal cord injury [44, 45]. However, to our knowledge, there was no such scientific research reporting inhibition of inflammation induced by EA at Shuigou (GV26) and Neiguan (PC6) simultaneously at present. In this work, our data indicated that EA at Shuigou (GV26) and Neiguan (PC6) treatment significantly reduced the expression of proinflammatory cytokines IL-1β and increased IL-10 after I/R injury. Also, the scores of neurological deficits and the infarct volume after I/R injury were significantly reduced following EA treatment. While NTI injection was combined with EA, the NTI abolished the EA-induced neuroprotective effect in ischemic infarction and neurological deficits and also intervened on the expression of proinflammatory/anti-inflammatory cytokines, suggesting that EA at Shuigou (GV26) and Neiguan (PC6) inhibits inflammatory responses and could be mediated by DOR. In addition, EA at Shuigou (GV26) or Neiguan (PC6) could upregulate the expression of BDNF in the brain of cerebral I/R injured rats and depressed rats, thereby exerting neuroprotective effects [46, 47]. Based on our previous cell experimental work, we conclude that the neuroprotection by EA at Shuigou (GV26) and Neiguan (PC6) are very likely linked to the inhibition of inflammation via the DOR-BDNF/TrkB pathway after I/R injury.

5. Conclusion

In summary, our data shows that DOR activation is crucial to neuroprotection against cerebral I/R injury. The DOR-mediated neuroprotection might be related to inflammation suppression through the BDNF/TrkB pathway in OGD/R-induced PC12 cells injury. Moreover, the neuroprotection of EA might depend on curbing the inflammatory response through the DOR-BDNF/TrkB signaling pathway after cerebral I/R injury. The present study suggests that EA at Shuigou (GV26) and Neiguan (PC6) acupoints is a promising therapeutic tool for patients with cerebral I/R injury.

Data Availability

The data used to support the findings of this study are available from the corresponding author upon request.

Conflicts of Interest

The authors declare that they have no conflicts of interest.

Authors' Contributions

Yue Geng and Yeting Chen contributed equally to this work. Yue Geng, Yeting Chen, Wei Sun, Yingmin Gu, Yongjie Zhang, Mei Li, and Jiajun Xie performed the experiments. Xuesong Tian conceived of and designed the experimental plan, wrote the manuscript, and secured funding. All authors have read and approved the final version of the manuscript.

Acknowledgments

This work was supported by the National Natural Science Foundation of China (81574078 and 81072646).

References

[1] W. Wang, B. Jiang, H. Sun et al., "Prevalence, incidence, and mortality of stroke in China: results from a nationwide population-based survey of 480 687 adults," *Circulation*, vol. 135, no. 8, pp. 759–771, 2017.

[2] S.-H. Koh and H.-H. Park, "Neurogenesis in stroke recovery," *Translational Stroke Research*, vol. 8, no. 1, pp. 3–13, 2017.

[3] P. Wang, Y. He, D. Li et al., "Class I PI3K inhibitor ZSTK474 mediates a shift in microglial/macrophage phenotype and inhibits inflammatory response in mice with cerebral ischemia/reperfusion injury," *Journal of Neuroinflammation*, vol. 13, no. 1, p. 192, 2016.

[4] M.-H. Shen, C.-B. Zhang, J.-H. Zhang, and P.-F. Li, "Electroacupuncture attenuates cerebral ischemia and reperfusion injury in middle cerebral artery occlusion of rat via modulation of apoptosis, inflammation, oxidative stress, and excitotoxicity," *Evidence-Based Complementary and Alternative Medicine*, vol. 2016, Article ID 9438650, 15 pages, 2016.

[5] A.-J. Liu, J.-H. Li, H.-Q. Li et al., "Electroacupuncture for acute ischemic stroke: a meta-analysis of randomized controlled trials," *The American Journal of Chinese Medicine*, vol. 43, no. 8, pp. 1541–1566, 2015.

[6] L. Lan, J. Tao, A. Chen et al., "Electroacupuncture exerts anti-inflammatory effects in cerebral ischemia-reperfusion injured rats via suppression of the TLR4/NF-κB pathway," *International Journal of Molecular Medicine*, vol. 31, no. 1, pp. 75–80, 2013.

[7] J. Jiang, Y. Luo, W. Qin et al., "Electroacupuncture suppresses the NF-kappaB signaling pathway by upregulating cylindromatosis to alleviate inflammatory injury in cerebral ischemia/reperfusion rats," *Frontiers in Molecular Neuroscience*, vol. 10, p. 363, 2017.

[8] M.-C. Ma, H. Qian, F. Ghassemi, P. Zhao, and Y. Xia, "Oxygen-sensitive {delta}-opioid receptor-regulated survival and death signals: novel insights into neuronal preconditioning and protection," *Journal of Biological Chemistry*, vol. 280, no. 16, pp. 16208–16218, 2005.

[9] X. He, H. K. Sandhu, Y. Yang et al., "Neuroprotection against hypoxia/ischemia: δ-opioid receptor-mediated cellular/molecular events," *Cellular and Molecular Life Sciences*, vol. 70, no. 13, pp. 2291–2303, 2013.

[10] Y. Jiang, N. Wei, T. Lu, J. Zhu, G. Xu, and X. Liu, "Intranasal brain-derived neurotrophic factor protects brain from ischemic insult via modulating local inflammation in rats," *Neuroscience*, vol. 172, pp. 398–405, 2011.

[11] Y. Li, L. Huang, Q. Ma et al., "Repression of the glucocorticoid receptor aggravates acute ischemic brain injuries in adult mice," *International Journal of Molecular Sciences*, vol. 19, no. 8, 2018.

[12] V. N. Shishkova, T. V. Adasheva, A. Y. Remenik, V. N. Valyaeva, and V. M. Shklovsky, "Prognostic significance of clinical-anthropometric, biochemical, metabolic, vascular-inflammatory and molecular-genetic markers in the development of the first ischemic stroke," *Zhurnal Nevrologii i Psikhiatrii im. S.S. Korsakova*, vol. 118, no. 2, pp. 4–11, 2018.

[13] D. Xu, D. Lian, J. Wu et al., "Brain-derived neurotrophic factor reduces inflammation and hippocampal apoptosis in experimental Streptococcus pneumoniae meningitis," *Journal of Neuroinflammation*, vol. 14, no. 1, p. 156, 2017.

[14] J. Yang, H. Yan, S. Li, and M. Zhang, "Berberine ameliorates MCAO induced cerebral ischemia/reperfusion injury via activation of the BDNF-TrkB-PI3K/akt signaling pathway," *Neurochemical Research*, vol. 43, no. 3, pp. 702–710, 2018.

[15] X. Tian, J. Guo, M. Zhu et al., "Delta-opioid receptor activation rescues the functional TrkB receptor and protects the brain from ischemia-reperfusion injury in the rat," *PLoS One*, vol. 8, no. 7, Article ID e69252, 2013.

[16] X. Tian, F. Hua, H. Sandhu et al., "Effect of δ-opioid receptor activation on BDNF-TrkB vs. TNF-α in the mouse cortex exposed to prolonged hypoxia," *International Journal of Molecular Sciences*, vol. 14, no. 8, pp. 15959–15976, 2013.

[17] M. M. Torregrossa, C. Isgor, J. E. Folk, K. C. Rice, S. J. Watson, and J. H. Woods, "The δ-opioid receptor agonist (+) BW373U86 regulates BDNF mRNA expression in rats," *Neuropsychopharmacology*, vol. 29, no. 4, pp. 649–659, 2004.

[18] J. Wang, L. Hu, J. Xu et al., "Electroacupuncture stimulation of different acupoint or paired acupoints on expression of BDNF and TrkB proteins and genes in hippocampus in myocardial ischemic rats," *Zhen Ci Yan Jiu*, vol. 41, no. 1, pp. 40–44, 2016.

[19] M.-W. Kim, Y. C. Chung, H. C. Jung et al., "Electroacupuncture enhances motor recovery performance with brain-derived neurotrophic factor expression in rats with cerebral infarction," *Acupuncture in Medicine*, vol. 30, no. 3, pp. 222–226, 2012.

[20] D. Qi, S. Wu, Y. Zhang, and W. Li, "Electroacupuncture analgesia with different frequencies is mediated via different opioid pathways in acute visceral hyperalgesia rats," *Life Sciences*, vol. 160, pp. 64–71, 2016.

[21] Y. Jiang, X. He, X. Yin, Y. Shen, and J. Fang, "Anti-inflammatory and synovial-opioid system effects of electroacupuncture intervention on chronic pain in arthritic rats," *Zhongguo Zhen Jiu*, vol. 35, no. 9, pp. 917–921, 2015.

[22] D. Mayor, "An exploratory review of the electroacupuncture literature: clinical applications and endorphin mechanisms," *Acupuncture in Medicine*, vol. 31, no. 4, pp. 409–415, 2013.

[23] X. S. Tian, F. Zhou, R. Yang et al., "Electroacupuncture protects the brain against acute ischemic injury via up-regulation of delta-opioid receptor in rats," *Journal of Chinese Integrative Medicine*, vol. 6, no. 6, pp. 632–638, 2008.

[24] X. Tian, F. Zhou, R. Yang et al., "Role of intracerebral δ-opium receptors in protecting ischemic injury in rats by cumulative electro- acupuncture," *Shanghai Journal of Traditional Chinese Medicine*, vol. 42, no. 6, pp. 71–74, 2008.

[25] T. Tao, J.-Z. Feng, G.-H. Xu, J. Fu, X.-G. Li, and X.-Y. Qin, "Minocycline promotes neurite outgrowth of PC12 cells exposed to oxygen-glucose deprivation and reoxygenation through regulation of MLCP/MLC signaling pathways," *Cellular and Molecular Neurobiology*, vol. 37, no. 3, pp. 417–426, 2017.

[26] M. Agrawal, V. Kumar, A. K. Singh et al., "*trans*-resveratrol protects ischemic PC12 Cells by inhibiting the hypoxia associated transcription factors and increasing the levels of antioxidant defense enzymes," *ACS Chemical Neuroscience*, vol. 4, no. 2, pp. 285–294, 2013.

[27] C. J. Sommer, "Ischemic stroke: experimental models and reality," *Acta Neuropathologica*, vol. 133, no. 2, pp. 245–261, 2017.

[28] E. Z. Longa, P. R. Weinstein, S. Carlson, and R. Cummins, "Reversible middle cerebral artery occlusion without craniectomy in rats," *Stroke*, vol. 20, no. 1, pp. 84–91, 1989.

[29] Y. Gu, J. Lu, W. Sun et al., "Oxymatrine and its metabolite matrine contribute to the hepatotoxicity induced by radix *Sophorae tonkinensis* in mice," *Experimental and Therapeutic Medicine*, vol. 17, no. 4, pp. 2519–2528, 2019.

[30] X. S. Tian, F. Zhou, R. Yang et al., "Effects of intracerebroventricular injection of delta-opioid receptor agonist TAN-67 or antagonist naltrindole on acute cerebral ischemia in rat," *Sheng Li Xue Bao*, vol. 60, no. 4, pp. 475–484, 2008.

[31] J. A. Hillion, K. Takahashi, D. Maric, C. Ruetzler, J. L. Barker, and J. M. Hallenbeck, "Development of an ischemic tolerance model in a PC12 cell line," *Journal of Cerebral Blood Flow & Metabolism*, vol. 25, no. 2, pp. 154–162, 2005.

[32] L. A. Greene and A. S. Tischler, "Establishment of a noradrenergic clonal line of rat adrenal pheochromocytoma cells which respond to nerve growth factor," *Proceedings of the National Academy of Sciences*, vol. 73, no. 7, pp. 2424–2428, 1976.

[33] A. Lahiani, A. Brand-Yavin, E. Yavin, and P. Lazarovici, "Neuroprotective effects of bioactive compounds and MAPK pathway modulation in "ischemia"-Stressed PC12 pheochromocytoma cells," *Brain Sciences*, vol. 8, no. 2, p. 32, 2018.

[34] J. Huang, U. M. Upadhyay, and R. J. Tamargo, "Inflammation in stroke and focal cerebral ischemia," *Surgical Neurology*, vol. 66, no. 3, pp. 232–245, 2006.

[35] D. Frenkel, Z. Huang, R. Maron, D. N. Koldzic, M. A. Moskowitz, and H. L. Weiner, "Neuroprotection by IL-10-producing MOG CD4+ T cells following ischemic stroke," *Journal of the Neurological Sciences*, vol. 233, no. 1-2, pp. 125–132, 2005.

[36] Y. Morita, S. Takizawa, H. Kamiguchi, T. Uesugi, H. Kawada, and S. Takagi, "Administration of hematopoietic cytokines increases the expression of anti-inflammatory cytokine (IL-10) mRNA in the subacute phase after stroke," *Neuroscience Research*, vol. 58, no. 4, pp. 356–360, 2007.

[37] S.-S. Hong, G. T. Gibney, M. Esquilin, J. Yu, and Y. Xia, "Effect of protein kinases on lactate dehydrogenase activity in cortical neurons during hypoxia," *Brain Research*, vol. 1009, no. 1-2, pp. 195–202, 2004.

[38] J. Zhang, G. T. Gibney, P. Zhao, and Y. Xia, "Neuroprotective role of δ-opioid receptors in cortical neurons," *American Journal of Physiology-Cell Physiology*, vol. 282, no. 6, pp. C1225–C1234, 2002.

[39] J. Zhang, H. Qian, P. Zhao, S.-S. Hong, and Y. Xia, "Rapid hypoxia preconditioning protects cortical neurons from glutamate toxicity through δ-opioid receptor," *Stroke*, vol. 37, no. 4, pp. 1094–1099, 2006.

[40] J.-C. Zhang, W. Yao, and K. Hashimoto, "Brain-derived neurotrophic factor (BDNF)-TrkB signaling in inflammation-related depression and potential therapeutic targets," *Current Neuropharmacology*, vol. 14, no. 7, pp. 721–731, 2016.

[41] H. Zhang, M. M. Torregrossa, E. M. Jutkiewicz et al., "Endogenous opioids upregulate brain-derived neurotrophic factor mRNA through δ- and μ-opioid receptors independent of antidepressant-like effects," *European Journal of Neuroscience*, vol. 23, no. 4, pp. 984–994, 2006.

[42] L.-Z. Xiong, J. Yang, Q. Wang, and Z.-H. Lu, "Involvement ofδ-and μ-opioid receptors in the delayed cerebral ischemic tolerance induced by repeated electroacupuncture

preconditioning in rats," *Chinese Medical Journal*, vol. 120, no. 5, pp. 394–399, 2007.

[43] B. Han, Y. Lu, H. Zhao et al., "Electroacupuncture modulated the inflammatory reaction in MCAO rats via inhibiting the TLR4/NF-kappaB signaling pathway in microglia," *International Journal of Clinical and Experimental Pathology*, vol. 8, no. 9, pp. 11199–11205, 2015.

[44] D. C. Choi, J. Y. Lee, Y. J. Moon, S. W. Kim, T. H. Oh, and T. Y. Yune, "Acupuncture-mediated inhibition of inflammation facilitates significant functional recovery after spinal cord injury," *Neurobiology of Disease*, vol. 39, no. 3, pp. 272–282, 2010.

[45] X. Zhang, X. N. Fan, and S. Wang, "Dynamic physiologic and pathologic changes in brain of rat with middle cerebral artery obstruction and effects of acupuncture in different frequencies on them," *Zhongguo Zhong Xi Yi Jie He Za Zhi*, vol. 30, no. 9, pp. 970–973, 2010.

[46] Y. Chen and X. Huang, "Effect of electroacupuncture on BDNF expression at ischemia cortex and infarct volume after middle cerebral artery occlusion in rat," *Acupuncture Research*, vol. 25, no. 3, pp. 165–169, 2000.

[47] D.-Z. Mu and X. Huang, "Anti-depression effects of electroacupuncture through up-regulating serum E2 and BDNF and expression of BDNF in hippocampus in chronic depression rats," *Journal of Acupuncture and Tuina Science*, vol. 13, no. 3, pp. 141–145, 2015.